COEVOLUTIONARY IMPLICATIONS OF ENVELOPE-MEDIATED RESISTANCE TO PHAGE

By

Alita Burmeister

A DISSERTATION

Submitted to
Michigan State University
in partial fulfillment of the requirements
for the degree of

Microbiology and Molecular Genetics—Doctor of Philosophy
Ecology, Evolutionary Biology and Behavior—Dual Major

2017

PUBLIC ABSTRACT

COEVOLUTIONARY IMPLICATIONS OF ENVELOPE-MEDIATED RESISTANCE TO PHAGE

By

Alita Burmeister

In my dissertation, I study parasites, their hosts, and how they impact each other's evolution. When I began my graduate studies, biologists already understood that natural selection favors resistant hosts over hosts that are sensitive to their parasites. They had also figured out that selection favors parasites that can evade host resistance. Together, hosts and parasites impact one another's evolution, and this process – termed coevolution – is the starting point of my work.

To understand how hosts and parasites coevolve, I used a method called experimental evolution. This technique involves growing organisms in the lab for many generations. During that time, some individuals come by random mutations that happen to make them a better (or worse!) fit for their environment. For example, hosts that have mutations that make them resistant to a parasite will live longer and reproduce more than sensitive hosts, and over time, they will replace the sensitive hosts. For experimental evolution to proceed rapidly enough that an experiment can fit within the length of a Ph.D. degree, it helps to use organisms that replicate rapidly, so I used the cellular organism *Escherichia coli* ("*E. coli*") which fits well into a flask (actually we can fit over a 10 million of them in a flask) and replicates rapidly (seven generations per *day*). For the parasite, I used the Lambda ("λ") virus that infects and kills *E. coli*.

Although many people often think of natural selection as an all all-or-nothing process (e.g., organisms live or die, they go hungry or they eat, etc.), the strength of natural

selection can actually vary quite a bit from situation to situation. Selection acts on a continuum, and there are many situations where the environment may kill, say, only 4% of organisms. Therefore, to understand how selection works, we need to measure both what it does and how strong it is. In this dissertation, I present my findings from experiments that measured the strength of natural selection on experimentally evolved *E. coli* and Lambda.

My results support the basic idea that natural selection changes the genetic composition of populations over time, driving their adaptive evolution. In the case of coevolving bacteria and their predator-like viruses, as little as a *single* mutation, such as the evolution of resistance, can set the populations on a new course. While resistance might very well drive the viruses extinct, in many cases the viruses happen to get one or a few mutations that improve infectivity, and coevolution continues.

ABSTRACT

COEVOLUTIONARY IMPLICATIONS OF ENVELOPE-MEDIATED RESISTANCE TO PHAGE

By

Alita Burmeister

This dissertation concerns the coevolution of pathogens and their hosts. For my thesis, I have worked with *Escherichia coli* and phage λ using experimental evolution, molecular biology, and theory that describes general host-pathogen interactions. This work centers on three themes of broad interest to evolutionary biology and microbiology: coevolutionary origins of novelty and diversity, the role of tradeoffs in constraining evolvability, and the ecological impacts of host resistance.

In Chapter 1, I worked with a set of experimentally coevolved *E. coli*/λ communities to investigate the bacterial genes that gained mutations and whether fitness tradeoffs had constrained the evolution of those mutations. To do this, I isolated bacteria from the coevolution experiment and sequenced the genomes of the isolates. I found resistance mutations that modified the expression or sequence of proteins used by λ during infection: LamB and OmpF at the outer membrane, and ManY and ManZ at the inner membrane. To test for fitness tradeoffs, I estimated the isolates' fitness in the presence and absence of λ. Phage selection strongly favored resistance mutations, despite those mutations incurring pleiotropic costs related to resource acquisition and homeostasis.

For my second chapter, I was particularly interested in the *E. coli manY* and *manZ* mutations that allowed phage to adsorb to the outside of the cell but limited the phage's ability to eject its genome into the cytoplasm. I thought that these mutations might effectively "trap" phage in non-productive infections, thereby accelerating the rate of

phage loss from the extracellular environment. However, I found no evidence for such traps; instead, λ had evolved independence of *manY* and *manZ*. These results indicate that for each of the known resistance-conferring mutations evolved by *E. coli*, the coevolving λ populations discovered evolutionary routes to circumvent the resistance.

For Chapter 3, I shifted briefly from laboratory experiments to mathematical theory to further investigate the trap idea. Although it turned out that the *manY* and *manZ* mutations don't act as traps, I was more generally interested in host defenses on the inside of the cell, such as CRISPR-Cas defense and restriction enzymes, which exist for many bacterial species. Comparable to other studies on parasite traps in animal hosts, I used theory to predict that in the presence of trap alleles, bacteriophage densities would be lower than they otherwise would be, even if more permissive hosts were available to them.

In my final chapter, I returned to the coevolution experiment with *E. coli* and λ. Although it was known that laboratory populations of phage evolved to use OmpF, and that this function required multiple mutations in the phage *J* gene, it was unknown how those mutations accumulated. I studied how both phage *J* gene mutations and bacterial *malT* (a positive regulator of *lamB*) mutations influenced the phage's adaptive landscape. I found that bacterial evolution strongly affected selection patterns on different phage genotypes: in many cases the evolution of host resistance more strongly favored increased phage adsorption rate. Because of that, the evolutionary intermediates between the ancestral and OmpF-infecting phage were positively selected, revealing that host coevolution can increase the rate at which phage evolve to use novel host structures.

ACKNOWLEDGMENTS

"To learn to think, you need two things: large blocks of time, and as much one-on-one interaction as you can get with someone who thinks more clearly than you do."

– Steve Stearns

This book is a cairn that marks time and interaction with many people. My dissertation started not five years ago, but thirty years ago when my older siblings taught me to read and write. It grew from my teachers' encouragement and my mentors' advice, long hours of conversation with friends and colleagues, and the generous support of many others.

I thank my family: John and Dianne Burmeister and my siblings John, Athena, Sara, Megan, Suzette, Jake, Katie, Andy, Scarlet, and Michael. I grew up in a home with a library, a subscription to National Geographic, and the collective knowledge of a household of people with unique and challenging experiences. My formal education could only build upon the knowledge imparted by my family. And even then, my pursuits were possible only through the fortune of living in a time and place with free public education – I'm immensely grateful for these last few things, and I wish for them for everyone who wants to know the universe more closely.

I thank my English teachers: Ms. Scherrer, Mr. Guilding, Mr. Oberwetter, and Professor Auerbach. They demanded more than standards, sent every manuscript back for revision until it was perfect, demonstrated creativity's infinite life, and required substance over B.S. For Chapter 3, I thank Mr. Folk, who taught me calculus.

Academics are often stereotyped as single-minded, but that hasn't been my experience with those who chaperoned me through grad school. I am thankful for my committee members – Kristin Parent, Rob Abramovitch, Ian Dworkin, Ned Walker, and Chris Adami, – not only for their guidance, advice, and tough questions, but also for their advice-by-example: keep your door open, give your time to your family, get help when you need it, and know your own fortune. I thank Jim Smith, my brother Jake, and Michael and Mira Bagdasarian for their additional mentorship, encouragement, and hot tea.

I am especially thankful for my advisor, Richard Lenski, for his advice and examples of how to live well as a scientist. His advising imparted my curiosity about evolving systems, insisted on the pairing of abstract thinking with quantitative data, and forged my academic grit. His professional guidance was complemented by infallible life advice: stay home when you have a cold, write an essay about someone you admire, give little gifts during the holidays, take time off when you gain or lose someone important to you, share poetry, and buy a round of drinks. Rich's awareness lead to a dynamic group of brilliant people I consider my "lab siblings." I'm especially thankful for Justin Meyer, Luis Zaman, Caroline Turner, Mike Wiser, and Rohan Maddamsetti for creating an atmosphere of respect, teaching me to think like an evolutionary biologist, and showing me that it's *good* to argue. As Caroline described, truth is a thing with which to cultivate a relationship.

I love academia for the wonderful conversations I get to have with smart, witty, critical, curious people. I had a fortune of hours discussing ideas with Bruce Levin, Gary Mittelbach, Elena Litchman, Chris Klausmeier, Paul Turner, Dominique Schneider, and many others, including my friends in the Beagle Book Club. During the last five years, I've also learned – in large part over beers at Crunchy's – most of what I know about feminism

and social justice, including how our culture affects our science and our lives as scientists; I'm grateful to the patience and perspectives of Elizabeth Baird, Nkrumah Grant, Jay Bundy, Kayla Miller, Kyle Card, Keara Grady, and many other friends who have helped me think critically on these topics.

This dissertation would not be as heavy as it is without Rachel Sullivan, who spent kilograms of patience on research that never even made it into these pages. She conducted many of the experiments presented in Chapters 1 and 2, and I'm grateful to have worked with her for four years. And behind *every* chapter, Neerja Hajela was there, making sure the Lenski lab's cabinets were stocked and the bacteria well fed. Outside the lab, Becky Mansel, Connie James, and Betty Miller made everything else at BPS easy. I'm grateful for their many hours of often-last-minute help, from booking my first bus ticket to East Lansing (during a snowstorm) to the paperwork for this very book.

Thank you to Jory, whose humor, kindness, and love gave grad school a soundtrack that I will not forget.

I thank the families of John Hannah, Rudolph Hugh, and Gueh-Djen (Edith) Hsiung for their contributions to endowments that helped fund my research.

Finally, I have been generously supported by the people of the United States through the National Science Foundation – you have chosen to value the discovery and sharing of knowledge, and I hope my discoveries will contribute to our continued, collective enlightenment.

PREFACE

The bacteriophages, discovered 101 years ago, remain curious things. Many phage exist strictly by infecting, replicating within, and killing their bacterial hosts; others reside latently, contributing genes that boost their host's fitness as well as their own. Between these extremes, phages may sap off host resources and bud from viable cells, and others mediate host kin selection by killing only specific host cells. Phages can be parasites, but they can also be predator-like, attacking and killing their hosts in order to obtain resources. Yet unlike predators, a phage particle may get only a single chance at host attack, itself dying if unable to kill. Given their wide variety of modes of resource acquisition and effects on their hosts, I find it amazing that the phages remain grouped together under one term. Certainly not all phages fit the etymological definition of "bacteriophage," which translates roughly to "bacteria eater."

So what is it, exactly, that unifies the phage as a group? My favorite answer is that phages occupy ecological niches in which their unit of selection floats somewhat freely between the unit of the phage genome and the unit of the host genome. In the lyosgenic state, phages are selected with their hosts. In the lytic state, phage genomes evolve independently of – and indeed antagonistically with – their hosts. It's this dichotomy that makes phage (and their conceptual relatives the plasmids, gene transfer agents, and molecular parasites) so evolutionarily intriguing. In my Ph.D. research, I investigated the antagonistic end of the phage lifestyle continuum, looking for the patterns in which host genomes and phage genomes brought about selection on one another. To do this, I used experimental evolution of *Escherichia coli* and bacteriophage λ. With this system, I investigated how reciprocal selection pressures influenced the direction and timing of

coevolution, focusing on interactions between *E. coli* and λ at the outer and inner membranes of the cell.

Many of the molecular interactions of λ infection have been well described in the classic molecular biology literature. Phage λ particles uses a two-step infection process to cross the bacterial outer and inner bacterial membranes, and this series involves only a few gene products: λ tail proteins J, V, and H, and *E. coli* membrane proteins LamB, ManY, and ManZ. The λ tail initiates infection at the outer membrane of the cell, where the J protein fibers adsorb to bacterial outer membrane protein LamB. Although the second step of infection is not yet thoroughly understood, λ tail proteins V and/or H allow entry into the periplasm and interaction with the bacterial inner membrane mannose permease proteins (encoded by *manY* and *manZ*), which λ exploits for rapid genome ejection into the cell's cytoplasm. Resistance to λ can involve blocking either of these steps, with resistance mutations mapping to *lamB*, *lamB*'s positive regulator *malT*, or the mannose permease genes *manY* and *manZ.*

In addition to their model system status in molecular biology, *E. coli* and λ share a history in the field of experimental evolution, where many aspects of their genetic interactions have been illuminated from a natural selection perspective. Studied in a variety of environments, sensitive *E. coli* and lytic λ can coexist together, along with resistant *E. coli* mutants, in both continuous and batch cultures. Analysis of mutations in these systems suggest a coevolutionary dynamic in which *E. coli* first gains *malT* mutations that reduce *lamB* expression, resulting in phage resistance, and the phage regains infectivity through phage *J* mutations that increased adsorption rate and fitness. In some, but not all, batch culture experiments, specific sets of *J* mutations cumulatively allow novel exploitation of

a second *E. coli* outer membrane protein, OmpF, catalyzing further evolutionary change and evolution of modified *ompF* alleles. Many of these changes are repeatable, but the evolution of resistance and its downstream effects depends on the carbon source available to the bacteria. The fitness of λ also depends on contribution of the phage *stf* allele to adsorption rate and the phage *S* allele to lysis time. Despite so much being known about the molecular biology of *E. coli* and λ's interactions at the molecular level, little was known about the fitness consequences of resistance and host range evolution, and that's where my research picks up.

In addition to characterizing evolutionary and ecological phenomena specific to *E. coli* and λ, during the last five years I have gained appreciation for an idea that shapes much of biology, which is that we can look for general patterns using specific study systems. As biochemist Jacques Monod put it, "Anything found to be true of *E. coli* must also be true of elephants." While I would not empirically attempt to transfer 10 million elephants into a 50 cubic centimeter flask, Monod's idea does apply to the general patterns I've sought to understand with *E. coli*: the coevolutionary origins of novelty and diversity, the role of tradeoffs in constraining evolvability, and the ecological impacts of host resistance.

TABLE OF CONTENTS

LIST OF TABLES

LIST OF FIGURES

CHAPTER 1:

FITNESS COSTS AND BENEFITS OF RESISTANCE TO PHAGE LAMBDA IN EXPERIMENTALLY EVOLVED *ESCHERICHIA COLI*

Authors: Alita R. Burmeister, Rachel M. Sullivan, and Richard E. Lenski

Abstract

Fitness tradeoffs play important roles in the evolution of microbial communities. One such tradeoff often occurs when bacteria become resistant to phage at the cost of reduced competitiveness for resources. Quantifying the cost of phage resistance has frequently relied on measuring specific traits of interest to industrial applications. In an evolutionary context, however, fitness encompasses the effects of all traits relevant to an organism's survival and reproductive success in a particular environment. Therefore, measurements of the net reproduction and survival of alternative genotypes offer greater power for predicting the fate of different genotypes in complex and dynamic communities. In this study, we measured the fitness of experimentally evolved, λ-resistant *Escherichia coli* isolates relative to their sensitive progenitor in both the absence and presence of phage. We also characterized certain phage-related phenotypes and obtained complete genome sequences of the bacteria. All of the evolved bacteria exhibited a tradeoff, such that they were more fit than the ancestor in the presence of phage, but less fit than the ancestor in the absence of phage. The fitness benefit of evolved resistance in the presence of phage was generally much larger than the cost, and these effects appear to be driven by only a few resistance mutations. This asymmetrical benefit-to-cost relation is consistent with the observation that sensitive cells did not persist in the experimental communities.

Quantifying fitness effects in both the presence and absence of phage may thus provide a useful approach for predicting evolutionary outcomes in natural and applied microbial communities.

Importance

Bacteria and the viruses that infect them coexist widely in the natural world and applied systems. The bacteria often face a tradeoff, however, between resistance to infection and competitiveness for resources. Such tradeoffs may mediate coexistence of resistant and sensitive hosts, thereby also allowing the virus to persist even after resistance evolves. Therefore, knowing whether, when, and why virus resistance is costly improves our understanding of how diversity is maintained in microbial ecosystems, potentially improving microbial engineering and approaches for treating unhealthy microbiomes. In this study of Lambda viruses and *Escherichia coli* bacteria, we examined the tradeoffs faced by evolved resistant bacteria. We found that the evolved bacteria experienced tradeoffs, although the fitness benefit of resistance in the presence of viruses was much greater than its cost in the absence of viruses.

Introduction

The grim reaper looms large for microbes, which face frequent and intense selection by phages and other antagonists. Bacteria often pay the ultimate penalty – death – for sensitivity to phage, but despite this cost, resistant and sensitive bacteria typically coexist in natural ecosystems, including the ocean (1) and phyllosphere (2), as well as in engineered systems, including wastewater treatment facilities (3) and laboratory

microcosms (4, 5). One hypothesis to explain this coexistence is that bacteria pay a cost for resistance, one that is incurred whether or not phages are present. Such costs are typically manifest as a loss of competitiveness for resources, for example caused by the modification or loss of sugar-transport proteins (6). As consequences of the tradeoff, resistant and sensitive host populations may coexist in the presence of phage (provided that the dynamics equilibrate such that neither host type has an overall fitness advantage (5)), and independently coevolving populations may diverge from one another (7, 8).

Resistance costs have been reported in many phage-bacteria systems (5, 9-23). However, not all evolved resistance traits incur costs (10, 15, 22), costs may depend on the environmental context and mechanism of resistance (13, 21, 24), and in some cases phage may even increase bacterial fitness (25, 26). Gaining more knowledge of whether, when, and why resistance is costly will improve understanding of the role of phage-bacteria interactions in maintaining diversity in microbial ecosystems. Such knowledge may also eventually aid in the preservation of natural communities, the maintenance of industrial fermentations, and the engineering of synthetic ecosystems.

In addition to its interest to the fields of ecology and evolutionary biology, the study of resistance tradeoffs has a rich history rooted in applied biology, where the cost of phage resistance often has implications for strain performance. Early studies sought to characterize trait-specific costs, such as the rate of acid production and bacterial doubling time. This focus on functional traits influenced later studies, including those in ecology and evolutionary biology. Therefore, we will first briefly review the history of tradeoffs in applied microbiology and its implications. We will then discuss evolutionary-based

approaches that aim to encompass all aspects of bacterial fitness, which may offer greater potential for understanding and managing natural and applied microbial communities.

Attempts to obtain high-performing but phage-resistant bacterial strains date to the 1930s, when Whitehead and Cox allowed *Lactococcus lactis* ("*Str. cremoris*" at the time) to grow for two days in the presence of phage and then screened for isolates that rapidly produced lactic acid (27). This approach was refined throughout the 20th century, including strain modifications generated by conjugation and transformation of resistance plasmids (28) in attempts to obtain low-cost resistance. The emergence of theoretically motivated studies of microbial ecology and experimental evolution in the 1960s and 1970s led to experimental analyses of resistance tradeoffs for their own sake. Continuous culture systems allowed for the study of host-phage community dynamics over extended periods, including the coexistence of sensitive bacteria, resistant bacteria, and phage (29-31). Levin *et al.* added dynamical population modeling to these studies, demonstrating that the stable coexistence of phage with both sensitive and resistant bacteria depended on resistance tradeoffs (5). Other recent studies have examined phage resistance and its costs to bacterial hosts in natural systems of applied importance including the plant pathogen *Pseudomonas syringae* (21) and the human pathogen *Pseudomonas aeruginosa* (18).

These studies have often focused on various fitness components, such as the bacteria's growth rate and the rate of phage attack. For example, Levin *et al.* measured the maximum growth rate of *E. coli* in the absence of phage T2 along with the adsorption rate of T2 to resistant and sensitive hosts (5). Such fitness-component (i.e., trait-specific) approaches have proven to be useful for parameterizing mathematical models of phage-host interactions, similar in that respect to models of parasites and long-lived animal and plant

hosts (32). Measuring specific fitness components is also important when the costs of phage resistance affect specific bacterial traits of interest, such as virulence determinants (9, 18, 19) and the ability to use various carbon sources (33). Although these approaches have clearly demonstrated tradeoffs associated with phage resistance, much remains to be learned about the *net* effect of resistance mutations on host fitness.

Most bacteria and phage have short generation times, and therefore the relative fitness of mutants and their progenitors can be readily determined by measuring their differential survival and reproduction across multiple generations. This approach captures the costs and benefits associated with all life stages including lag, exponential, stationary, and death phases for bacteria, as well as adsorption, intracellular replication, lysis, and extracellular survival for phage. It also accounts for the different selection pressures that may exist in a given environment over time, such as those caused by nutrient depletion, the accumulation of cell debris, pH changes, and the like. Therefore, multi-generation assays offer a powerful and general method for quantifying evolutionary fitness. Such assays been used extensively in the field of experimental evolution for bacteria (11, 14, 34) and phage (35, 36), and we employ them here to quantify the impact of phage resistance on bacterial fitness.

We isolated bacterial clones from seven *E. coli* populations that were serially passaged and coevolved with phage λ, including two clones from one population and one from each of six others. For these isolates and their ancestor, we obtained certain qualitative phage-related phenotypes, complete genome sequences, and quantitative fitness measurements in both the presence and absence of phage. These integrated data provide new insights into the benefits, costs, genetics, and mechanisms of bacterial resistance to phage.

Materials and Methods

Experimental evolution: All of the resistant strains used in this study are experimentally evolved descendants of *E. coli* B strain REL606. Replicate populations founded with REL606 previously coevolved with phage λ strain cI26 for 20 rounds of serial transfers, with each community archived by freezing samples on a daily basis (37). The cI26 strain is obligately lytic and uses the host's outer membrane protein LamB (maltose transport porin) as a receptor. In this study, we isolated several individual bacterial clones from the day 19 frozen samples of seven of the experimentally evolved communities. We chose communities based on two criteria: (i) the final communities had phage present; and (ii) at least some of the phage present had evolved the ability to infect the bacteria through a second outer membrane protein, OmpF, as previously reported (37). We also isolated and used the experimentally evolved phage λ G9-15b, which can use OmpF, from a frozen sample of one of the evolved communities.

Growth conditions and phenotypic assays: All bacterial fitness assays were conducted in the same medium and other conditions as the original evolution experiment, except that phage were present or absent as described below. Specifically, bacteria and phage (when added) were propagated in modified M9 (mM9) medium (M9 salts with 1 g/L magnesium sulfate, 1 g/L glucose, and 0.02% LB), as used previously (37). We assessed phage sensitivity by plating a lawn of the bacterial strain in a soft-agar overlay on an LB base agar and spotting 10 μl of a concentrated phage stock on the lawn. If a plaque formed, then we scored the bacterial strain as sensitive to the phage. Resistance to phage λ is associated with the partial or complete loss of the ability to grow on maltose, mannose, or both, because wild type λ requires the LamB maltose transporter for initial attachment (38, 39)

and the ManXYZ mannose permease for its DNA to enter the host cell (6, 40, 41). Therefore, we used colony phenotypes on tetrazolium-maltose and tetrazolium-mannose indicator media to characterize resistance-associated diversity among evolved isolates. Bacteria that are deficient in growth on a given sugar will typically produce red colonies on the corresponding indicator agar, although we saw some exceptions that will be discussed later. In cases where we saw the same phenotypic pattern for multiple isolates from the same community, we selected a representative clone for additional phenotypic characterization, genome sequencing, and reporting.

Genome sequencing: We isolated genomic DNA from ten of the evolved bacterial clones (four from population A8 and one from each of the other populations) using the Qiagen Genomic-tip 100/G kit (Cat. No. 10243). Short-read sequences were generated by the Michigan State University Research Technology Support Facility on an Illumina MiSeq platform. We aligned the sequences and compared them to the annotated sequence of the ancestral strain REL606 using the *breseq* pipeline (42).

Fitness assays: We estimated the fitness of each bacterial clone by performing competition assays similar to those described previously (34). During the competitions, the evolved phage-resistant descendents of REL606 (ara^-) compete for resources with REL607, which is a genetically marked ara^+ derivative of REL606. REL606 and its descendents form red colonies on tetrazolium-arabinose agar plates, whereas REL607 forms pink colonies, allowing the abundance of each competitor to be quantified. We confirmed that REL606 and REL607 have equal fitness in mM9 medium in both the presence and absence of phage λ (Appendix, Fig. A1.1). To initiate the fitness assays, we revived the bacterial strains from the –80°C stocks by streaking for isolated colonies on LB agar plates. To precondition the

cultures, we picked individual colonies into 10 ml of mM9 medium and incubated them at 37°C and 120 rpm overnight. We began each replicate fitness assay with a unique colony of the evolved competitor and another of the reference competitor REL607; this approach ensures independence with respect to any mutations that might arise and affect fitness, such as ones that confer phage resistance. We sampled the bacteria by plating on tetrazolium-arabinose plates from all of the fitness assays at 0, 4, 8, and 24 h. We also sampled the assays performed without phage after three and six days, with 1:100 dilutions into fresh mM9 medium each day. The final fitness measurements reported in the main text were determined using colony counts obtained at 24 h with phage present and after six days without phage (except for strain AB113, where we used the three-day counts). These times were constrained by the speed with which one competitor excluded the other, which prevents enumeration of the rarer competitor on the indicator plates. For the fitness assays conducted in the presence of phage, we added 10^5 pfu/ml of the ancestral phage strain cI26 immediately after sampling the initial bacterial composition; the initial phage density corresponds to a MOI of ~0.01. We added an equivalent volume (100 μl) of mM9 for assays performed without phage.

Statistical analysis: We tested the following predictions about the fitness of the bacteria: (i) the evolved isolates are more fit than their ancestor in the presence of phage, and (ii) the evolved isolates are less fit than the ancestor in the absence of phage. To test these directional predictions, we used one-tailed *t*-tests. To account for multiple tests, we used sequential Bonferroni corrections (43) for each environment. We tested for differences in the variance of fitness measurements between the two environments for each bacterial

strain using two-tailed *F*-tests based on the competition data obtained at 24 h. All data were analyzed using custom R scripts (44).

Results

Phenotypic properties of the evolved bacteria: The bacterial isolates varied phenotypically in terms of their phage resistance and sugar use (Table 1.1, Fig. 1.1). All isolates were resistant to the ancestral λ phage, and clones from population A8 were also resistant to the evolved λ strain that can infect through the outer membrane protein OmpF. Resistance to λ is typically caused by the reduced expression or loss of the LamB porin and the ManXYZ permease that allow the cell to import maltose and mannose across the outer and inner membranes, respectively (6, 37, 39, 40). Therefore, we examined the ability of the bacteria to use these sugars when growing on tetrazolium indicator agar (Fig. 1.1). In our experience, mutations that eliminate the ability to use a sugar result in red colonies on tetrazolium agar, whereas strains that can grow on that sugar form white or pink colonies. The ancestral host, REL606, is both Mal^+ and Man^+, forming pink colonies on the tetrazolium maltose and tetrazolium mannose agar, respectively (Fig. 1.1). All of the evolved isolates formed darker colonies on tetrazolium maltose agar, indicating either complete or partial loss of growth on maltose. Some of the isolates (AB114, AB125) also formed darker colonies on tetrazolium mannose agar, but most (AB113, AB117, AB124, AB128, and AB131) retained the ancestral coloration. Isolate AB121 formed colonies with a magenta hue on both indicator media. AB113 colonies were typically smaller than the ancestor, while AB121 colonies were typically as large as or larger than the ancestor.

Table 1.1. Phenotypic properties of evolved, phage-resistant bacterial isolates. Isolates that metabolize a specific sugar form pink colonies on tetrazolium agar containing the sugar; those that lack the ability form red colonies. Fig. 1.1 shows representative colonies.

Isolate	Population	λ_{LamB}	λ_{OmpF}	Tetrazolium maltose colony morphology	Tetrazolium mannose colony morphology
AB113	A8	R	R	Small red	Small Pink
AB114	A8	R	R	Red	Red
AB117	C3	R	S	Red	Pink
AB121	C4	R	S	Large magenta	Large magenta
AB124	D4	R	S	Red	Reddish-pink
AB125	D7	R	S	Red	Red
AB128	F6	R	S	Red	Pink
AB131	H2	R	S	Red	Pink

Population: Population from which the isolate was obtained; λ_{LamB}: Plaque spot test for ancestral phage that uses the LamB porin as its receptor; λ_{OmpF}: Plaque spot test for an evolved phage that can also use the OmpF porin as its receptor. S: Sensitive; R: Resistant.

Table 1.2. Mutations in sequenced genomes of evolved λ-resistant isolates of *E. coli*. Resistance Associated Mutations: Mutations in genes known from previous studies to confer resistance to phage λ. Other Mutations: Mutations at other loci not known to confer resistance to phage λ. Asterisks (*) indicate stop codons, plus signs (+) indicate insertions, and triangles (Δ) indicate deletions. Table A1.1 provides further details on all of the mutations.

Isolate (Population)	Resistance Associated Mutations			Other Mutations
	malT	***manY, manZ***	***ompF, ompR***	
AB113 (A8)[1]	T47P (ACC→CCC)	none	Δ1 bp (805/1089 nt) in *ompF*	*ampH*
AB114 (A8)[2]	25-bp duplication	Δ*manXYZ*	Y26* (TAT→TAG) in *ompF*	*ybaK-ybaP* intergenic region, Δ*rbs* operon
AB117 (C3)	+A (435/2706 nt)	none	+A (237/720 nt) in *ompR*	Δ*ecb_00726-00739,* Δ*rbs* operon
AB121 (C4)	T154P (ACC→CCC)	G21* (GGA→TGA) *manY*	none	Δ*rbs* operon
AB124 (D4)	Δ89 bp	none	none	none
AB125 (D7)	W334* (TGG→TAG)	IS3 (–) +4 bp :: +TC coding (543-546/861 nt) *manZ*	none	*ecb_01992,* Δ*rbs* operon
AB128 (F6)	25 bp duplication	none	none	*ecb_01992, ecb_02825,* Δ*rbs* operon
AB131 (H2)	Δ4 bp	none	none	*ecb_02825,* Δ*rbs* operon

1: Isolate AB116 had the identical genome sequence to AB113. 2: Isolate AB115 had the identical genome sequence to AB114.

Figure 1.1. Bacterial phenotypes associated with sugar use on two types of tetrazolium indicator agar. The ancestral strain, REL606, is *mal*$^{+}$ and *man*$^{+}$ and forms pink colonies on both types. The evolved isolates produce more deeply pigmented colonies on one or both agar types, which indicates that their ability to use maltose, mannose, or both was diminished or lost during evolution.

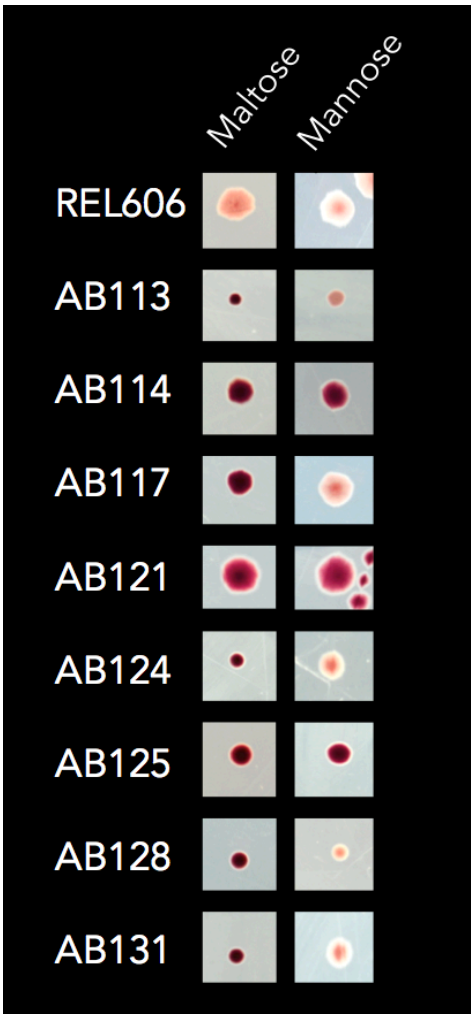

Genomic signatures of phage resistance: We sequenced the genomes of the ten evolved bacterial clones and compared them to the ancestral strain REL606 (Table 1.2, Table A1.1). We observed several instances of parallel evolution at the gene level. All sequenced isolates contained a *malT* mutation, and those from populations A8 (AB114), C4 (AB121), and D7 (AB125) had a mutation in or deletion of *manY, manZ*, or both. Isolates from two populations (AB113 and AB114 from A8 and AB117 from C3) had mutations of either

ompF or *ompR*, which is a positive regulator of *ompF* (45). Population A8 harbors two genotypes (AB113 and AB114) that share no mutations, indicating that they represent lineages that arose independently and early during the coevolution experiment. Two additional isolates from A8 had exactly the same genomic sequences as AB113 and AB114 (see footnotes to Table 1.3).

Bacterial fitness in the presence and absence of phage: We ran multi-generation competition assays to estimate the fitness of the evolved bacteria relative to their ancestor in both the presence and absence of phage. In all cases, the mean fitness of the evolved clone was higher than the ancestor in the presence of phage and lower in the absence of phage (Fig. 1.2), indicating an evolutionary tradeoff between phage resistance and competitiveness. After performing sequential Bonferroni corrections to account for the multiple statistical comparisons, this pattern was significant in most cases (Table 1.3). The fitness estimates were significantly much more variable in the presence of phages than in their absence (Table 1.3); we consider the explanation for this difference in the Discussion section.

An important feature of the competition assays run in the presence of phage is that the phage replicate during the experiment, thus subjecting their hosts to dynamic changes in the strength of selection. We therefore expected that selection for the evolved resistant bacteria would increase over the course of the assays. To test this prediction, we counted the ancestral and evolved competitors after 4, 8, and 24 h during the first day of the assays. All of the genotypes, including the sensitive ancestor, had net positive growth over the full 24 h period, even in the presence of λ (Fig. 1.3A-B). However, between 8 and 24 h, the resistant bacteria increased (Fig. 1.3A) while their sensitive ancestor declined in density

(Fig. 1.3B), consistent with the expected increase in the phage density over time. In the absence of phage, both the ancestor and evolved bacteria populations increased throughout the growth cycle (Fig. 1.4A-B).

Table 1.3. Fitness costs and benefits of the evolved resistant isolates. In most cases, the evolved isolates were more fit than the progenitor (selection rate > 0) in the presence of phage and less fit (selection rate < 0) in the absence of phage. Most values were significantly different from the null hypothesis (selection rate = 0) even after performing sequential Bonferroni corrections for multiple tests of the same hypothesis; however, one test was non-significant even before the corrections (indicated in bold), and three others were non-significant after the corrections (indicated in italics). In all cases, the variance associated with measuring the selection rate after one day was significantly greater in the presence than in the absence of phage.

	Fitness expressed as selection rate (day^{-1})							
	Without Phage			With Phage			Measurement Variance	
Isolate	*N*	Mean	*p*-value	*N*	Mean	*p*-value	*F*	*p*-value
AB113	7	-1.018	<0.0001	8	2.139	*0.0210*	18.4	0.0010
AB114	8	-0.550	<0.0001	7	2.452	*0.0280*	52.0	<0.0001
AB117	8	-0.404	<0.0001	7	1.487	0.0100	11.2	0.0054
AB121	8	-0.038	**0.1860**	8	1.785	0.0002	7.1	0.0191
AB124	7	-0.196	0.0001	8	2.366	0.0007	29.8	0.0002
AB125	8	-0.143	0.0027	7	1.959	0.0010	21.4	0.0017
AB128	8	-0.155	<0.0001	8	1.709	0.0053	38.9	<0.0001
AB131	8	-0.151	*0.0150*	8	2.278	0.0008	6.5	0.0249

To calculate the changes in relative fitness over the course of the competition assays, we subtracted the net growth of the ancestor from the net growth of the evolved bacteria at each time point, yielding the difference shown in Fig. 1.3C and Fig. 1.4C. As in Figure 1.2, when the resulting difference is *greater* than zero, the evolved competitor has the fitness advantage, whereas a value *below* zero means the ancestor has the advantage. In all cases, the evolved resistant strain had the advantage after 24 h in the presence of phages (Fig. 1.3C), and in all cases the ancestral sensitive strain had the 24-h advantage in the absence of phages (Fig. 1.4C). To express these data in terms of the selection rate shown in Figure 1.2, the difference in net growth was divided by the duration of the assay in days. Thus, the 24-h data in Fig. 1.3C divided by time (here, 1 day) yields precisely the selection rates

shown by the filled circles in Figure 1.2. However, the selection-rate values in the absence of phage, shown as open circles in Figure 1.2, were computed from the differences between the competitors' growth rates over longer periods than shown in Figures 1.3 and 1.4, in order to increase the resolution of the much smaller differences in net growth observed in that environment (see Materials and Methods). As expected, in the presence of phage, the growth-rate differential between the evolved and ancestral bacteria increased as the phage replicated over the 24-h period (Fig. 1.3C).

Figure 1.2. Tradeoff in fitness of evolved resistant bacteria in the presence and absence of phage λ. Selection rates greater or less than 0 indicate that the evolved bacteria are more or less fit, respectively, relative to their sensitive ancestor. Error bars are 95% CIs, based on the number of replicates shown in Table 1.3.

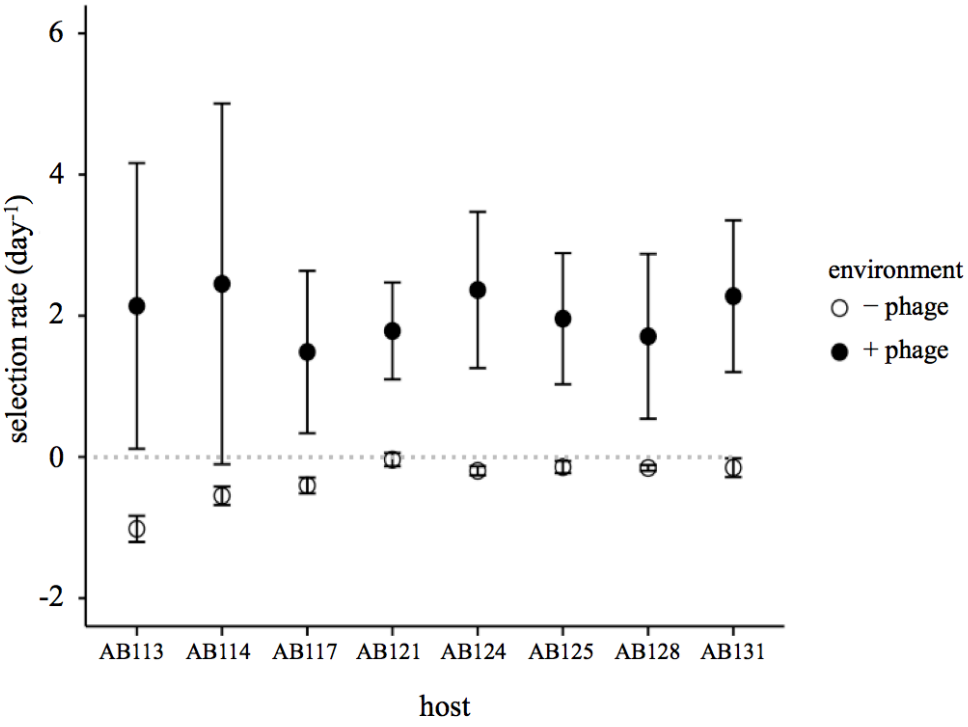

Figure 1.3. Growth of evolved resistant and ancestral sensitive bacteria during competition over a 24-h cycle in the presence of phage λ. A) Net growth of each of the eight evolved isolates (gray) and their grand mean (black). B) Net growth of the ancestral strain during the eight sets of competitions with the evolved isolates (gray) shown in A, and the ancestor's grand mean (black). C) The difference in net growth between the evolved and ancestral competitors shown in panels A and B. All time points have been systematically shifted and arranged in order of the isolate numbers, with AB113 furthest to the left and AB131 furthest to the right; the actual time points at which all data were collected are 0, 4, 8, and 24 h. Error bars are 95% CIs, based on the number of replicates shown in Table 1.3.

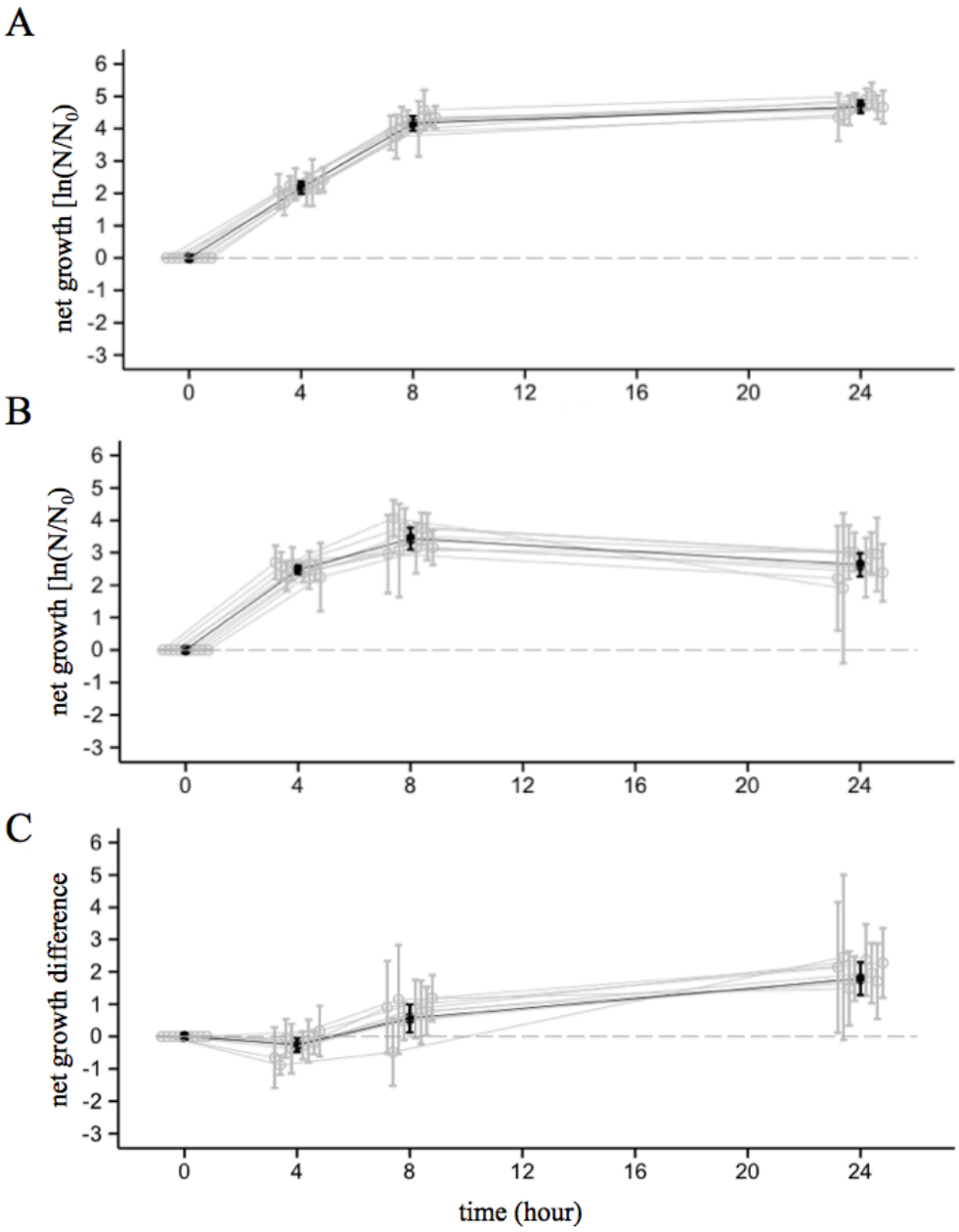

Figure 1.4. Growth of evolved resistant and ancestral sensitive bacteria during competition over a 24-h cycle in the absence of phage. See Fig. 1.3 for panel descriptions and details. Note that AB113 is the evolved isolate that showed the decline in density between 8 and 24 h (panel A), as discussed in the text.

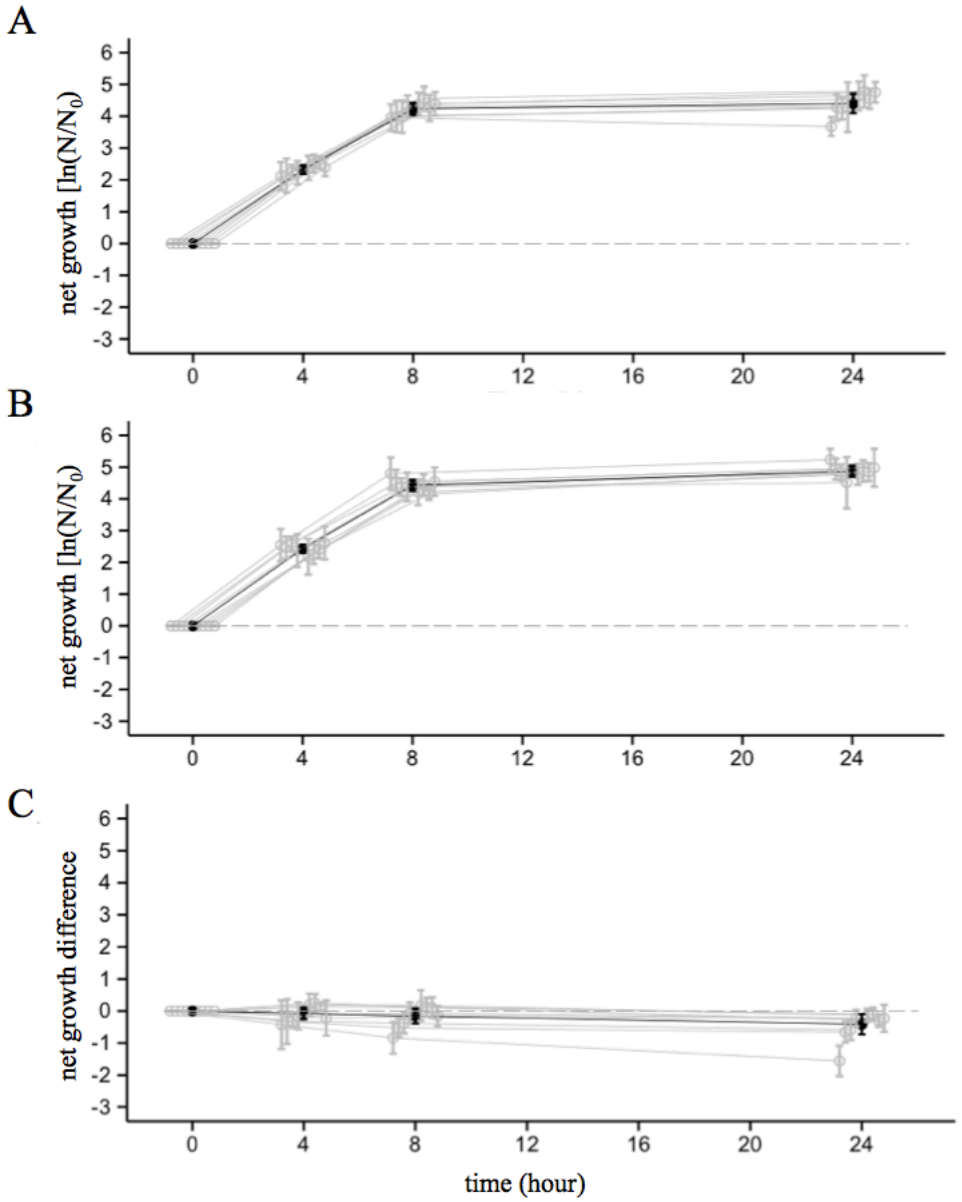

Discussion

Tradeoffs play a major role in the evolution and maintenance of diversity, allowing for the coexistence of community members with diverse traits by constraining how well each member can perform. To examine tradeoffs in a microbial community, we characterized the genotypes, phenotypes and fitness patterns of a set of experimentally evolved phage-resistant *E. coli* isolates along with their ancestor.

We observed a variety of phenotypes and genotypes among the evolved isolates (Tables 1.1 and 1.2). Several of the derived alleles had mutations in the *malT*, *manY*, *manZ*, *ompF*, and *ompR* genes. These mutations likely underlie phage resistance, as these genes affect the expression or structure of known phage receptors involved in λ's adsorption to the cell's outer membrane or the entry of λ's DNA across the inner membrane (6, 31, 36-41, 45). Other mutations in the bacteria (Table 1.1, Table A1.1) have no obvious relationship to phage resistance; they might be neutral mutations or confer benefits unrelated to the phage. For example, deletions of ribose genes (*rbs*) also arose, albeit more slowly, in an evolution experiment without phage (46), and *malT* mutations (which reduce *lamB* expression) also conferred a benefit in that experiment (47).

Within population A8, genotypes AB113 and AB114 share no mutations, indicating that at least two lineages arose independently from the ancestral strain and that this population had not undergone any hard selective sweeps that would result in mutations achieving fixation (48). Two processes could, in principle, explain this coexistence. First, clonal interference might have prevented either lineage from fixing (49). Alternatively, the two lineages might have been maintained by negative frequency-dependent selection caused by phage specialization or other ecological feedbacks. We saw no evidence for

phage specialization between these isolates (Table 1.1), although we did not characterize enough phage or analyze their properties in enough detail to exclude this hypothesis.

More generally, our finding of a fitness tradeoff when the ancestral and evolved bacteria compete in the presence and absence of phages (Table 1.3, Fig. 1.2) is consistent with their resistance phenotypes (Table 1.1) and genotypes (Table 1.2), as well as with many previous studies (5, 9-23). Bacterial fitness has multiple components, including competitiveness for limiting resources as well as survival. Many phages exploit bacterial transporters for sugars and other resources in order to initiate infections, and resistance to λ can occur through the loss, reduced expression, or modification of such structures (6, 37, 39, 40). The effects of the resistance-conferring mutations on such transporters (Table 1.1, Fig. 1.1) likely reduce competitiveness for glucose, which is the main fitness component in the absence of phage.

Some of the evolved bacteria may also face a tradeoff between resistance and osmotic regulation. In *E. coli* K12, OmpF and OmpC, regulated by the EnvZ/OmpR two-component system (50), allow glucose and electrolyte to flow across the cell envelope. However, the ancestral strain, REL606, is a derivative of *E. coli* B and has a truncated *ompC* gene (coding 935/1101 base pairs), leaving the task of osmoregulation to OmpF (51, 52). Changes to OmpF or its expression may therefore adversely affect the ability to regulate osmotic stress, thereby reducing growth rate and perhaps even increasing rates of cell death. Indeed, evolved isolates AB113, AB114, and AB117 have mutations in either *ompF* or *ompR*, and they have the highest fitness costs in the absence of phage (Table 1.2, Fig. 1.2). The most severe of these, AB113, has a 1-bp deletion in *ompF* that causes a premature stop codon and truncated protein; this isolate has the lowest fitness of all those

tested (Fig. 1.2), it produces small colonies (Fig. 1.1), and it shows signs of an early onset of death phase between 8 and 24 h (Fig. 1.4A).

The fitness benefits of the evolved resistant bacteria in the presence of phage λ were many times the magnitude of their fitness costs in the absence of phage (Fig. 1.2). In another study, experimentally evolved *Pseudomonas aeruginosa* isolates with resistance to phage PP7 showed a similar fitness asymmetry (14). It is not surprising that resistant bacteria should at least initially outperform their sensitive ancestors when phage are present (5, 10), although the subsequent dynamics may be complex. In our experiments, the phage population began at 10^5 pfu/ml, but its density would have increased owing to infections of the sensitive bacteria. In chemostat culture, the resistant bacteria, sensitive bacteria, and phage can often coexist in a dynamic equilibrium if the bacteria experience a tradeoff between resistance and competiveness for the limiting resources (5, 10, 12). In serial batch culture, such as used in our experiments, the outcome is more uncertain and complex. For example, if the phage density rises too high during its initial growth, then it might drive the sensitive bacteria extinct; and if the phage cannot evolve to overcome the resistant population's defenses, then the phage might also go extinct. In any case, the management of bacterial strains for industrial applications often requires finding or designing resistant strains that are also strong performers in terms of their growth and production of desired products (28). The existence of tradeoffs between resistance and other desired traits makes strain development both more important and more challenging.

Conversely, some applications may benefit when the costs of resistance outweigh the benefits. For example, the use of antibiotics and phage to treat pathogens selects for drug- and phage-resistant bacteria. If the resistant bacteria pay a sufficiently high fitness cost,

then they might be unable to outcompete their sensitive ancestor, thereby slowing or halting the evolution of resistance (9, 23). Therefore, therapies for which resistance tradeoffs are more severe could provide longer-term benefits than therapies for which those tradeoffs are weak. As in our experiment, the magnitude of tradeoffs in applications will depend on the bacterial genotype as well as the phage density (or drug concentration in the case of an antibiotic), so using relevant phage densities (or drug concentrations) to quantify tradeoffs should yield more accurate predictions.

We also observed that estimates of fitness were much more variable in the presence than the absence of phage (Table 1.3). One possible explanation for the unequal variance is the spontaneous occurrence of resistance mutations in the sensitive ancestral population during the preconditioning step of the fitness assays. The presence, timing, number, and genotype of such resistance mutations will randomly vary from replicate to replicate (53). When selection is strong, as it is in the presence of phage, such mutations can meaningfully affect the subsequent dynamics (36). Conversely, in the absence of phage, selection is weaker and new mutations would have less impact on any given fitness assay and hence on the variation across the replicate assays.

In summary, *E. coli* isolates that coevolved with phage λ had improved fitness in the presence of phage and reduced fitness in the absence of phage relative to their sensitive ancestor, providing clear evidence of a tradeoff. In the glucose-limited minimal medium used in this study, and at the initial phage density employed, the fitness gain in the presence of phage was much greater than the cost of resistance in the absence of phage. Whole-genome sequencing of the bacteria also revealed parallel evolution across the resistant isolates affecting several loci including *malT*, *manYZ*, *ompF*, and *ompR*. These mutations

caused additional tradeoffs including reduced abilities to grow on maltose and mannose. Future studies might investigate how these tradeoffs in bacterial performance are affected by changes in the density and genetic composition of the coevolving phage population over time.

Acknowledgments

We thank Justin Meyer for sharing strains and discussions, and Neerja Hajela for assistance in the laboratory. We thank Caroline Turner, Mike Wiser, Rohan Maddamsetti and Kayla Miller for feedback that improved this manuscript. This paper is based upon work supported by the National Science Foundation Graduate Research Fellowship (DGE-1424871) to A.R.B., the BEACON Center for the Study of Evolution in Action (NSF Cooperative Agreement DBI-0939454), and the John Hannah endowment from Michigan State University. Any opinions, findings, and conclusions or recommendations expressed in this paper are those of the authors and do not necessarily reflect the views of the National Science Foundation.

APPENDIX

Marker neutrality experiments. Before conducting the fitness assays on the evolved isolates, we conducted three experiments to test whether the arabinose utilization marker used to distinguish bacterial competitors is neutral in the presence and absence of phage. In Experiment 1, we competed the Ara^- ancestral bacterial strain, REL606, against its Ara^+ derivative, REL607, measuring fitness after one and six days in the absence of phage (Fig. A1.1, Exp. 1). In Experiment 2, we competed the same Ara^- and Ara^+ strains in the presence of 10^5 pfu/ml of phage cI26 using a single "preconditioning culture" for each strain to begin all of the replicate competitions. Experiment 2 suggested that the Ara marker might not be neutral, and so we performed Experiment 3 using separately preconditioned cultures for each replicate competition. By separately growing each of the cultures used to start the competitions, we limit the influence of resistance mutations that arose at random before the start of the competition. Indeed, by doing so the apparent fitness effect of the marker disappeared (Fig. A1.1, Exp. 3). To further ensure neutrality, we conducted tests of the marker's fitness effect alongside the competitions (reported in the main text) performed to assess the fitness of the evolved resistant bacteria relative to their sensitive progenitor (Fig. A1.1, Exp. 4). For each experiment, we tested for neutrality using a two-tailed, one-sample *t*-test against the null hypothesis ($r = 0$).

Figure A1.1. Tests of Ara marker neutrality (Ara^- relative to Ara^+) in mM9 medium with and without phage λ. +P, with phage; –P, without phage; 1-d, one-day competition; 6-d, six-day competition; Sep, separate preconditioning step. Error bars depict 95% confidence intervals.
Experiment 1: REL606 (Ara^-) vs. REL607 (Ara^+) competed in the absence of phage for one ($p = 0.0646$, $N = 7$) and six days ($p = 0.1543$, $N = 7$).
Experiment 2: REL606 vs. REL607 competed in the presence of phage using common bacterial preconditioning cultures ($p = < 0.0001$, $N = 8$).
Experiment 3: REL606 vs. REL607 competed in the presence of phage using separate bacterial preconditioning cultures for each replicate ($p = 0.0690$, $N = 8$).
Experiment 4: REL606 vs. REL607 competed in the presence of phage ($p = 0.2537$, $N = 8$) and absence of phage ($p = 0.9646$, $N = 7$) using separate bacterial preconditioning cultures and performed alongside the competitions reported in Fig. 1.2 of the main text.

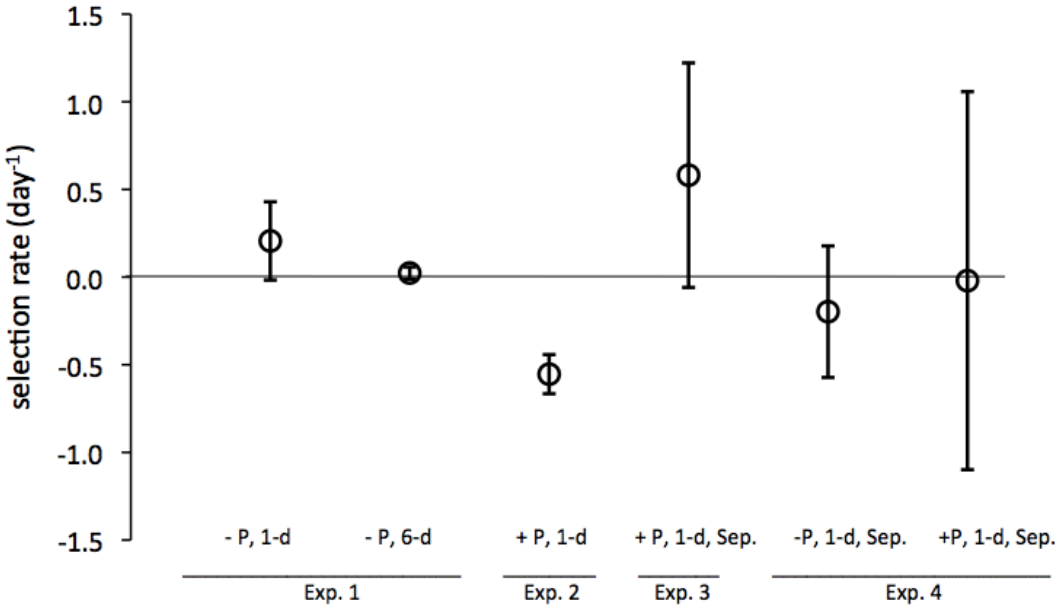

Table A1.1. Mutations in sequenced genomes of evolved λ-resistant isolates of *E. coli*. Asterisks (*) indicate stop codons, plus signs (+) indicate insertions, and triangles (Δ) indicate deletions. IS*150*-mediated, for example, indicates that an IS*150* insertion sequence caused the mutation. The Description column lists the gene product annotation or, in the case of multi-gene deletions, shows the set of deleted genes. Brackets denote partial deletions of the named gene.

Isolate	Genome Position	Mutation	Protein Change	Gene	Description
AB113	363,781	C→T	M51I (ATG→ATA)	*ampH*	beta-lactamase/D-alanine carboxypeptidase
	1,003,270	Δ1 bp	coding (805/1089 nt)	*ompF*	outer membrane porin 1a (Ia;b;F)
	3,481,823	A→C	T47P (ACC→CCC)	*malT*	transcriptional regulator MalT
AB114	479,323	IS*1* (–) +9 bp	intergenic (-174/+22)	*ybaK* ← / ← *ybaP*	hypothetical protein/hypothetical protein
	1,003,997	A→C	Y26* (TAT→TAG)	*ompF*	outer membrane porin 1a (Ia;b;F)
	1,879,350	Δ5,451 bp		*[yoaE]–[yebN]*	*[yoaE], manX, manY, manZ, yobD, [yebN]*
	3,482,676	25 bp duplication		*malT*	transcriptional regulator MalT
	3,894,997	Δ3,773 bp, IS*150*-mediated		*rbsD–[rbsB]*	*rbsD, rbsA, rbsC, [rbsB]*
AB115	479,323	IS*1* (–) +9 bp	intergenic (-174/+22)	*ybaK* ← / ← *ybaP*	hypothetical protein/hypothetical protein
	1,003,997	A→C	Y26* (TAT→TAG)	*ompF*	outer membrane porin 1a (Ia;b;F)
	1,879,350	Δ5,451 bp		*[yoaE]–[yebN]*	*[yoaE], manX, manY, manZ, yobD, [yebN]*
	3,482,676	25 bp duplication		*malT*	transcriptional regulator MalT
	3,894,997	Δ3,773 bp, IS*150*-mediated		*rbsD–[rbsB]*	*rbsD, rbsA, rbsC, [rbsB]*
AB116	363,781	C→T	M51I (ATG→ATA)	*ampH*	beta-lactamase/D-alanine carboxypeptidase
	1,003,270	Δ1 bp	coding (805/1089 nt)	*ompF*	outer membrane porin 1a (Ia;b;F)
	3,481,823	A→C	T47P (ACC→CCC)	*malT*	transcriptional regulator MalT
AB117	787,879	Δ12,090 bp		*ECB_00726–ECB_00739*	14 unannotated hypothetical genes
	3,465,032	+A	coding (237/720 nt)	*ompR*	osmolarity response regulator
	3,482,119	+A	coding (435/2706 nt)	*malT*	transcriptional regulator MalT
	3,894,997	Δ653 bp	IS*150*-mediated	*rbsD–[rbsA]*	*rbsD, [rbsA]*
AB121	1,881,721	G→T	G21* (GGA→TGA)	*manY*	mannose-specific enzyme IIC component of PTS
	3,482,144	A→C	T154P (ACC→CCC)	*malT*	transcriptional regulator MalT
	3,894,997	Δ3,773 bp, IS*150*-mediated		*rbsD–[rbsB]*	*rbsD, rbsA, rbsC, [rbsB]*
AB124	3,481,852	Δ89 bp	coding (168-256/2706 nt)	*malT*	transcriptional regulator MalT
AB125	1,883,007	IS*3* (–) +4 bp :: +TC[a]	coding (543-546/861 nt)	*manZ*	mannose-specific enzyme IID component of PTS
	2,103,887	+CAGCCAGC	coding (154/216 nt)	*ECB_01992*	hypothetical protein, in posible regulatory region of *ECB_01993* hypothetical gene
	3,482,685	G→A	W334* (TGG→TAG)	*malT*	transcriptional regulator MalT
	3,894,997	Δ3,773 bp, IS*150*-mediated		*rbsD–[rbsB]*	*rbsD, rbsA, rbsC, [rbsB]*
AB128	2,103,888	Δ4 bp	coding (155-158/216 nt)	*ECB_01992*	hypothetical protein, in posible regulatory region of *ECB_01993* hypothetical gene
	3,023,945	Δ777 bp		*insB-22–[ECB_02825]*	*insB-22, insA-22, [ECB_02825]*
	3,482,676	25 bp x 2	duplication	*malT*	transcriptional regulator MalT
	3,894,997	Δ4,631 bp, IS*150*-mediated		*rbsD–[rbsK]*	*rbsD, rbsA, rbsC, rbsB, [rbsK]*
AB131	3,023,945	Δ777 bp		*insB-22–[ECB_02825]*	*insB-22, insA-22, [ECB_02825]*
	3,481,938	Δ4 bp	coding (254-257/2706 nt)	*malT*	transcriptional regulator MalT
	3,894,997	Δ6,796 bp, IS*150*-mediated		*rbsD–[yieO]*	*rbsD, rbsA, rbsC, rbsB, rbsK, rbsR, [yieO]*

[a]Genome AB125 contained an IS*3*-mediated disruption of *manZ* with an additional two base pairs (TC) inserted directly after the IS*3* element.

REFERENCES

REFERENCES

1. **Waterbury JB**, **Valois FW**. 1993. Resistance to co-occurring phages enables marine *Synechococcus* communities to coexist with cyanophages abundant in seawater. Appl and Environ Microbiol **59**:3393–3399.

2. **Koskella B**, **Lin DM**, **Buckling A**, **Thompson JN**. 2015. The evolution of bacterial resistance against bacteriophages in the horse chestnut phyllosphere is general across both space and time. Philos Trans R Soc Lond B Biol Sci **370**:1896–1903.

3. **Hantula J**, **Kurki A**, **Vuoriranta P**, **Bamford DH**. 1991. Ecology of bacteriophages infecting activated sludge bacteria. Appl Environ Microbiol **57**:2147–2151.

4. **Gratia A**. 1921. Studies on the d'Hérelle phenomenon. J Exp Med **34**:115–126.

5. **Levin BR**, **Stewart FM**, **Chao L**. 1977. Resource-limited growth, competition, and Am Nat **111**:3–24.

6. **Elliott J**, **Arber W**. 1978. *E. coli* K-12 *pel* mutants, which block phage λ DNA injection, coincide with *ptsM*, which determines a component of a sugar transport system. Mol Gen Genet **161**:1–8.

7. **Paterson S**, **Vogwill T**, **Buckling A**, **Benmayor R**, **Spiers AJ**, **Thomson NR**, **Quail M**, **Smith F**, **Walker D**, **Ben Libberton**, **Fenton A**, **Hall N**, **Brockhurst MA**. 2010. Antagonistic coevolution accelerates molecular evolution. Nature **464**:275–278.

8. **Scanlan PD**, **Hall AR**, **Blackshields G**, **Friman V-P**, **Davis MR**, **Goldberg JB**, **Buckling A**. 2015. Coevolution with bacteriophages drives genome-wide host evolution and constrains the acquisition of abiotic-beneficial mutations. Mol Biol Evol **32**:1425–1435.

9. **Smith HW**, **Huggins MB**. 1982. Successful treatment of experimental *Escherichia coli* infections in mice using phage: Its general superiority over antibiotics. J Gen Microbiol **128**:307–318.

10. **Lenski RE**, **Levin BR**. 1985. Constraints on the coevolution of bacteria and virulent phage: A model, some experiments, and predictions for natural communities. Am Nat **125**:585–602.

11. **Lenski RE**. 1988. Experimental studies of pleiotropy and epistasis in *Escherichia coli.* I. Variation in competitive fitness among mutants resistant to virus T4. Evolution **42**:425–432.

12. **Bohannan B**, **Lenski RE**. 1999. Effect of prey heterogeneity on the response of a model food chain to resource enrichment. Am Nat **153**:73-82.

13. **Bohannan BJM**, **Kerr B**, **Jessup CM**, **Hughes JB**, **Sandvik G**. 2002. Trade-offs and coexistence in microbial microcosms. Antonie Van Leeuwenhoek **81**:107–115.

14. **Brockhurst MA**, **Buckling A**, **Rainey PB**. 2005. The effect of a bacteriophage on diversification of the opportunistic bacterial pathogen, *Pseudomonas aeruginosa*. Proc R Soc Lond B Biol Sci **272**:1385–1391.

15. **Lennon JT**, **Khatana SAM**, **Marston MF**, **Martiny JBH**. 2007. Is there a cost of virus resistance in marine cyanobacteria? ISME J **1**:300–312.

16. **Quance MA**, **Travisano M**. 2009. Effects of temperature on the fitness cost of resistance to bacteriophage T4 in *Escherichia coli.* Evolution **63**:1406–1416.

17. **Koskella B**, **Lin DM**, **Buckling A**, **Thompson JN**. 2012. The costs of evolving resistance in heterogeneous parasite environments. Proc R Soc Lond B Biol Sci **279**:1896–1903.

18. **Hosseinidoust Z**, **Tufenkji N**, **van de Ven TGM**. 2013. Predation in homogeneous and heterogeneous phage environments affects virulence determinants of *Pseudomonas aeruginosa*. Appl Environ Microbiol **79**:2862–2871.

19. **Hosseinidoust Z**, **van de Ven TGM**, **Tufenkji N**. 2013. Evolution of *Pseudomonas aeruginosa* virulence as a result of phage predation. Appl Environ Microbiol **79**:6110–6116.

20. **Koskella B**, **Brockhurst MA**. 2014. Bacteria–phage coevolution as a driver of ecological and evolutionary processes in microbial communities. FEMS Microbiol Rev **38**:916–931.

21. **Meaden S**, **Paszkiewicz K**, **Koskella B**. 2015. The cost of phage resistance in a plant pathogenic bacterium is context-dependent. Evolution **69**:1321–1328.

22. **Vale PF**, **Lafforgue G**, **Gatchitch F**, **Gardan R**, **Moineau S**, **Gandon S**. 2015. Costs of CRISPR-Cas-mediated resistance in *Streptococcus thermophilus*. Proc R Soc Lond B Biol Sci **282**:20151270.

23. **Chan BK**, **Sistrom M**, **Wertz JE**, **Kortright KE**, **Narayan D**, **Turner PE**. 2016. Phage selection restores antibiotic sensitivity in MDR *Pseudomonas aeruginosa.* Scientific Reports **6**:26717.

24. **Buckling A**, **Wei Y**, **Massey RC**, **Brockhurst MA**, **Hochberg ME**. 2006. Antagonistic coevolution with parasites increases the cost of host deleterious mutations. Proc R Soc Lond B Biol Sci **273**:45–49.

25. **Rice SA**, **Tan CH**, **Mikkelsen PJ**, **Kung V**, **Woo J**, **Tay M**, **Hauser A**, **McDougald D**, **Webb JS**, **Kjelleberg S**. 2008. The biofilm life cycle and virulence of *Pseudomonas aeruginosa* are dependent on a filamentous prophage. ISME J **3**:271–282.

26. **Meyer JR**, **Agrawal AA**, **Quick RT**, **Dobias DT**, **Schneider D**, **Lenski RE**. 2010. Parallel changes in host resistance to viral infection during 45,000 generations of relaxed selection. Evolution **64**:3024–3034.

27. **Whitehead HR**, **Cox GA**. 1936. Bacteriophage phenomena in cultures of lactic *Streptococci*. Journal of Dairy Research **7**:55–62.

28. **Moineau S**. 1999. Applications of phage resistance in lactic acid bacteria. Antonie Van Leeuwenhoek **76**:377–382.

29. **Paynter MJB**, **Bungay HR III**. 1969. Dynamics of coliphage cp 6 infections, pp. 323–335. *In* Perlmen, D (ed.), Fermentation Advances. Academic Press, New York.

30. **Horne MT**. 1970. Coevolution of *Escherichia coli* and bacteriophages in chemostat culture. Science **168**:992–993.

31. **Spanakis E**, **Horne MT**. 1987. Co-adaptation of *Escherichia coli* and coliphage λvir in continuous culture. J Gen Microbiol **133**:353–360.

32. **May RM**, **Anderson RM**. 1983. Epidemiology and genetics in the coevolution of parasites and hosts. Proc R Soc Lond B Biol Sci **219**:281–313.

33. **Middelboe M**, **Holmfeldt K**, **Riemann L**, **Nybroe O**, **Haaber J**. 2009. Bacteriophages drive strain diversification in a marine *Flavobacterium*: Implications for phage resistance and physiological properties. Environ Microbiol **11**:1971–1982.

34. **Wiser MJ**, **Ribeck N**, **Lenski RE**. 2013. Long-term dynamics of adaptation in asexual populations. Science **342**:1364–1367.

35. **Shao Y**, **Wang IN**. 2008. Bacteriophage adsorption rate and optimal lysis time. Genetics **180**:471–482.

36. **Burmeister AR**, **Lenski RE**, **Meyer JR**. Host coevolution alters the adaptive landscape of a virus. Proc R Soc Lond B Biol Sci **283**:20161528.

37. **Meyer JR**, **Dobias DT**, **Weitz JS**, **Barrick JE**, **Quick RT**, **Lenski RE**. 2012. Repeatability and contingency in the evolution of a key innovation in phage Lambda. Science **335**:428–432.

38. **Thirion JP**, **Hofnung M**. 1972. On some genetic aspects of phage λ resistance in *E. coli* K12. Genetics **71**:207–216.

39. **Hofnung M**, **Jezierska A**, **Braun-Breton C**. 1976. *lamB* mutations in *E. coli* K12: Growth of λ host range mutants and effect of nonsense suppressors. Mol Gen Genet **145**:207–213.

40. **Scandella D**, **Arber W**. 1974. An *Escherichia coli* mutant which inhibits the

injection of phage λ DNA. Virology **58**:504–513.

41. **Erni B**, **Zanolari B**, **Kocher HP**. 1987. The mannose permease of *Escherichia coli* consists of three different proteins: Amino acid sequence and function in sugar transport, sugar phosphorylation, and penetration of phage λ DNA. J Biol Chem **262**:5238–5247.

42. **Barrick JE**, **Colburn G**, **Deatherage DE**, **Traverse CC**, **Strand MD**, **Borges JJ**, **Knoester DB**, **Reba A**, **Meyer AG**. 2014. Identifying structural variation in haploid microbial genomes from short-read resequencing data using *breseq*. BMC Genomics **15**:1039.

43. **Holm S**. 1979. A simple sequentially rejective multiple test procedure. Scan J Stat **6**:65–70.

44. **R Development Core Team**. 2011. R: A language and environment for statistical computing. R Foundation for Statistical Computing, Vienna, Austria.

45. **Kato M**, **Aiba H**, **Tate S**, **Nishimura Y**, **Mizuno T**. 1989. Location of phosphorylation site and DNA-binding site of a positive regulator, OmpR, involved in activation of the osmoregulatory genes of *Escherichia coli*. FEBS Lett **249**:168–172.

46. **Cooper VS**, **Schneider D**, **Blot M**, **Lenski RE**. 2001. Mechanisms causing rapid and parallel losses of ribose catabolism in evolving populations of *Escherichia coli* B. J Bacteriol **183**:2834–2841.

47. **Pelosi L**, **Kühn L**, **Guetta D**, **Garin J**, **Geiselmann J**, **Lenski RE**, **Schneider D**. 2006. Parallel changes in global protein profiles during long-term experimental evolution in *Escherichia coli*. Genetics **173**:1851–1869.

48. **Messer PW**, **Petrov DA**. 2013. Population genomics of rapid adaptation by soft selective sweeps. Trends Ecol Evol **28**:659–669.

49. **Gerrish PJ**, **Lenski RE**. 1998. The fate of competing beneficial mutations in an asexual population. Genetica **102-103**:127–144.

50. **Russo FD**, **Silhavy TJ**. 1991. EnvZ controls the concentration of phosphorylated OmpR to mediate osmoregulation of the porin genes. J Mol Biol **222**:567–580.

51. **Studier FW**, **Daegelen P**, **Lenski RE**, **Maslov S**, **Kim JF**. 2009. Understanding the differences between genome sequences of *Escherichia coli* B strains REL606 and BL21(DE3) and comparison of the *E. coli* B and K-12 genomes. J Mol Biol **394**:653–680.

52. **Crozat E**, **Hindré T**, **Kühn L**, **Garin J**, **Lenski RE**, **Schneider D**. 2011. Altered regulation of the OmpF porin by Fis in *Escherichia coli* during an evolution experiment and between B and K-12 strains. J Bacteriol **193**:429–440.

53. **Luria SE**, **Delbrück M**. 1943. Mutations of bacteria from virus sensitivity to virus resistance. Genetics **28**:491–511.

CHAPTER 2:

COEVOLVING POPULATIONS OF PHAGE LAMBDA BECOME INDEPENDENT OF THE *ESCHERICHIA COLI* MANNOSE PERMEASE

Authors: Alita R. Burmeister, Rachel M. Sullivan, and Richard E. Lenski

Abstract

The structure of genetic interaction networks underlies host-pathogen coevolution. In bacteria and phage, these networks are often structured such that resistance arises via the loss of a function, while phage infectivity is gained by exploiting other functions. We investigated such an interaction at the inner membrane of *Escherichia coli*, where λ exploits the mannose permease proteins for the entry of its genome into the cytoplasm, and where *E. coli* evolves mutations in the *manY* and *manZ* genes that impair λ's ability to infect the cell. We measured the growth of ancestral and experimentally evolved λ on wild-type bacteria and strains with *manY* or *manZ* deletions. The deletions severely reduced the growth of the ancestral λ, but evolved isolates grew well on the deletion mutants, indicating that λ regained infectivity by evolving the ability to inject its genome into the cytoplasm independently of the mannose permease. Data from the evolution experiments showed that *man* mutants arose during the same coevolutionary arms race involving genes that govern the interaction of *E. coli* and λ at the outer membrane. Taken together, coevolution of the interactions at the outer and inner membranes reveals a three-locus inverse-gene-for-gene infection network.

Introduction

Pathogens and their hosts share genetic networks in which host alleles affect selection on pathogen phenotypes and pathogen alleles influence selection on host phenotypes. These interactions include the classic gene-for-gene (GFG) model, the matching-alleles (MA) model, and various related models (1). These models make different predictions about host-range patterns (2, 3), and so understanding the structure of the genetic interaction network is important for understanding historical coevolution as well as predicting future coevolutionary changes.

Bacteria and their phage often share a specific type of network in which phage infectivity depends on the exploitation of specific bacterial features, and resistance to phage involves the elimination of the exploited features. This form of interaction network has been called the inverse-gene-for-gene (IGFG) model (2, 4). Unlike the classic gene-for-gene (GFG) model originally proposed for plants and their pathogens, host defense in the IGFG model does not require pathogen recognition by the host, and the pathogen's evasion of host resistance does not require the loss of a defense elicitor. The IGFG model provides a useful framework for representing genetic changes in coevolving communities of bacteria and phage. For example, if phage cannot evolve to exploit new features after bacteria evolve resistance, then phage populations may be evolutionarily static (5, 6). Conversely, if phage exploit essential features of the bacteria that cannot be eliminated, then the host's evolution is constrained and phage infectivity may remain elevated (7, 8).

Experimental evolution with model organisms allows one to determine the structure of coevolutionary infection networks, especially when the molecular genetics of a system are reasonably well understood, as they are for *Escherichia coli* and phage λ. Phage λ uses a

two-step infection process to cross the outer and inner bacterial membranes, and this process is thought to involve only a few gene products: in λ the tail proteins J, V, and H; and in *E. coli* the membrane proteins LamB, ManY, and ManZ. The λ tail initiates infection at the outer membrane of the cell, where the J protein fibers adsorb to the bacterial protein LamB (9, 10). The tail proteins V and H allow λ to enter the periplasm and thereby interact with the mannose permease proteins (encoded by *manY* and *manZ*) on the inner membrane, which enables λ to eject its genome into the cell's cytoplasm (11-14). Resistance to λ can involve blocking either of these steps, with resistance mutations mapping to *lamB*, *lamB*'s positive regulator *malT* (9, 10), or the mannose permease genes (11-13).

In addition to serving as a model system in molecular biology, *E. coli* and λ share a history in the field of experimental evolution, where certain aspects of their interactions have been studied from the perspective of natural selection and coevolutionary dynamics. It has been shown that sensitive *E. coli* and lytic λ can coexist, along with resistant *E. coli* mutants, in both continuous (15) and batch culture regimes (16). Genetic analysis of these systems suggests IGFG dynamics: *E. coli* first evolves *malT* mutations that reduce LamB expression, resulting in resistance to λ (15-17), and the phage regains infectivity through mutations in the *J* gene that increase its adsorption rate and fitness (15, 18). In some, but not all, experiments, specific sets of *J* mutations allow the novel exploitation of a second outer membrane protein, OmpF, catalyzing further evolution including mutations in the *ompF* gene (16, 19). Depending on the particular strain of λ used and the selection regime, the phage's evolution may also depend on the contribution of its *stf* gene to its adsorption rate and its *S* gene to its lysis time (20, 21).

Despite extensive knowledge about the evolution of the initial (adsorption) and final (lysis) steps of λ infection of *E. coli*, much less is known about the evolution of the genetic networks during other stages of infection, including λ's passage through the periplasmic space and the ejection of its DNA into the host cytoplasm. Meyer *et al.* (16) found that *E. coli* coevolving with λ often acquired mutations that impacted their ability to grow on mannose, which presumably were favored because they disrupted the phage's genome entry via the mannose permease. In this study, we focus on two populations from that previous coevolution experiment. We examine the evolution of the bacterial *manY* and *manZ* mutations including their effects on various λ genotypes as well as when these mutations arose relative to other coevolutionary events.

Results and Discussion

To examine whether and how the coevolution experiment affected λ's dependence on the ManY and ManZ proteins, we measured the population growth of the ancestral and coevolved phage isolates on bacteria with and without the *manY* and *manZ* genes. Both the ancestral and evolved phage grew well on bacteria with intact *manY* and *manZ* genes, including both the ancestral *E. coli* B strain, REL606, used in the coevolution experiment and the K12 genetic background in which the Keio collection was made (Fig. 2.1, Table 2.1). Deletion of either the *manY* or *manZ* gene in either background severely reduced the ancestral phage's population growth. In two cases (REL606 Δ*manZ* and Keio Δ*manY*), we saw no increase whatsoever in the phage population after 24 hours; in the other case (Keio Δ*manZ*), the ancestral phage population increased ~10-fold, but that was several orders of magnitude less than the increase on the same background with the permease gene present.

In striking contrast to the ancestral phage, the phage isolates from both coevolved populations showed substantial growth on all three bacterial strains that lacked either the *manY* or *manZ* gene (Fig. 2.1). These results indicate an inverse-gene-for-gene coevolutionary interaction at the inner membrane; that is, the bacteria modified or lost the ability to transport mannose across the inner membrane, and the phage countered by evolving independence of that bacterial function.

Figure 2.1. Phage λ population growth on wild type, Δ*manY,* and Δ*manZ* bacteria. Whether the phage could grow was assessed by performing one-tailed *t*-tests on the $\log_{10}$-transformed ratio of phage population densities at the start and end of a one-day cycle, with the null hypothesis of zero growth (***, $p < 0.001$; ** $0.001 < p < 0.01$; ns, not significant, $p > 0.05$). Each test was based on 5 or 6 replicate assays. Phage isolates D9 and G9 evolved in a batch-culture regime with 100-fold dilution each day, and so 100-fold growth would be required for persistence; this break-even level is indicated by the dashed line.

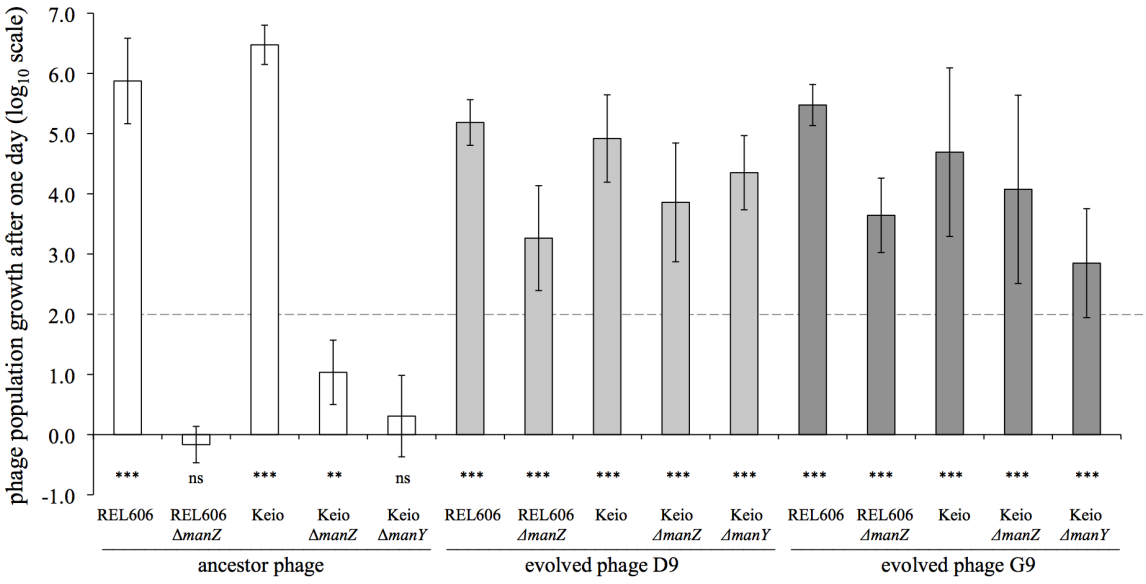

To determine when the mutant mannose permease (*man*) alleles arose in the two *E. coli* populations studied here, we plated frozen samples of the coevolution experiments on tetrazolium mannose indicator agar. We were particularly interested in the timing of the appearance of the *man* mutants with respect to two other key steps in the coevolutionary

arms race that were previously characterized: (i) the evolution of *malT*$^{-}$ mutations that reduced the bacteria's expression of LamB and thus the adsorption of the ancestral phage λ (18); and (ii) λ's evolution of the new ability to use OmpF as an outer membrane receptor (16). The phage growth data demonstrate that *manY* and *manZ* deletions confer substantial resistance even to the ancestral phage, which can use only the LamB surface receptor (Fig. 2.1). That result suggested the possibility that the *man* mutants might have arisen early in the coevolution experiments, perhaps alongside the *malT* mutations that provided resistance at the outer membrane. However, time-course data show that the *man* alleles reached high frequencies after the fixation of the *malT* mutations, which occurred by day 8 in both of the populations studied here (16) (Fig. 2.2, Appendix).

These temporal data also show that the mutant *man* alleles had nearly fixed in both populations (frequencies >95% on day 10 in D9 and on day 12 in G9), but then the mutants sharply declined over the next day, suggesting they were killed by phages that had evolved independence of the mannose permease. This result is consistent with previous data showing that mutant *man* alleles rarely fixed in the bacterial populations (16). In population D9, variation in colony morphology further suggested that different *man* alleles were present before and after the sudden decline in the frequency of *man* mutants on day 11 (Fig. A2.1). The initial boom and bust of the mutant *man* alleles in both populations also took place before the phage had evolved to use OmpF (Fig. 2.2, asterisks). Whether phage λ gained independence from the mannose permease by exploiting another inner membrane protein, and whether *E. coli* did (or could) respond by eliminating such a structure are interesting questions for future work.

Figure 2.2. Temporal dynamics of *man* mutants in *E. coli* populations D9 (panel A) and G9 (panel B). Mutant *malT* alleles had already reached fixation in both populations by day 8. Bacteria with *man* mutations, which confer resistance to phage λ, rose to high frequencies and then declined sharply in abundance in both populations after day 8, but before λ had evolved to use OmpF (timing indicated by *). These data imply that *man* mutations evolved on *malT* mutant backgrounds, and that λ evolved independence of the mannose permease—causing the precipitous decline in the frequency of *man* mutants—before it evolved the ability to use OmpF. The shaded regions indicate the maximum and minimum frequencies based on analyzing two samples per population each day (mean N = 90 colonies tested per sample). The gray dashed line shows the approximate limit of resolution.

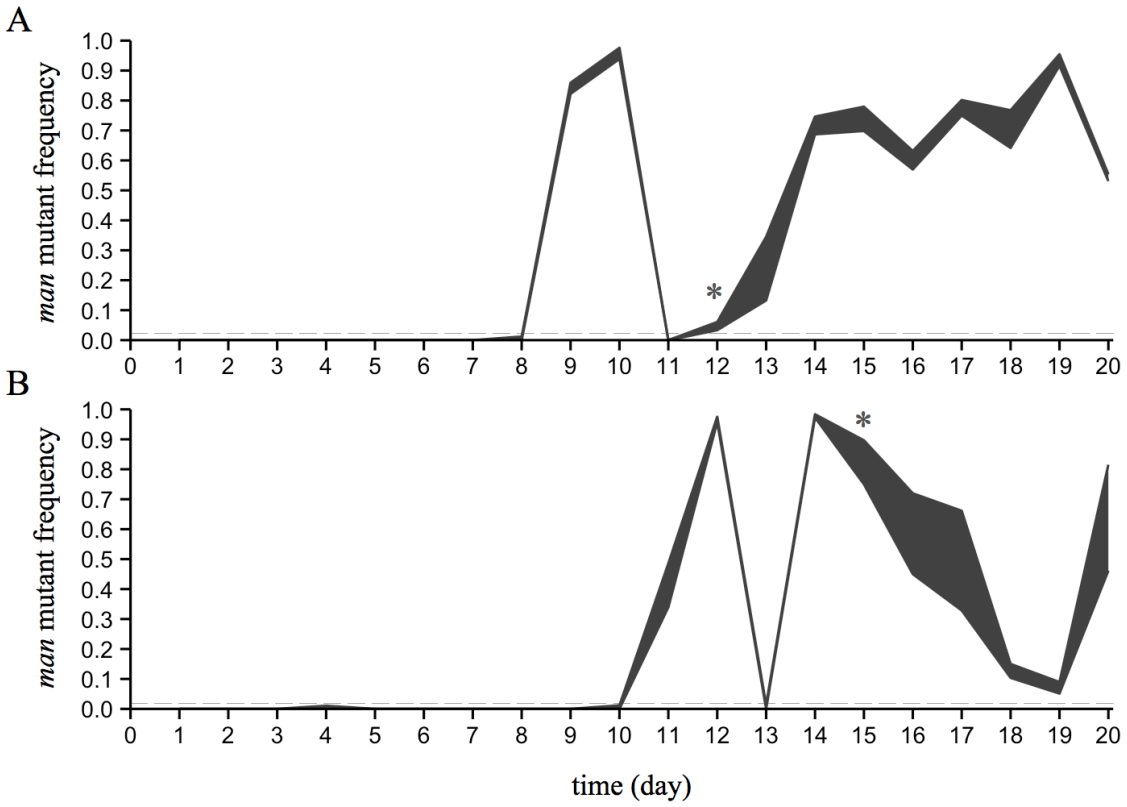

Our results are consistent with genetic and molecular biology studies of λ host-range mutations. Scandella and Arber (11) isolated *E. coli* mutants that allowed phage adsorption to the cell envelope but interfered with ejection of the phage genome, thereby reducing infection success to a small fraction of that observed on wild-type cells. The responsible mutations were mapped to the mannose permease operon (12, 22), and λ mutants that could infect these mutant bacteria had mutations in phage genes *V* or *H* (23). Williams *et al*. (22)

found that, for *E. coli* strain K12, *manZ* is not strictly required for wild-type λ to eject its genome, and our results accord with that finding (Fig. 2.1, Keio background). However, our results suggest that λ cI26 does require *manZ* when infecting the *E. coli* B background, at least in the culture conditions that we used (Fig. 2.1, REL606 background).

Alternatively, λ cI26 might occasionally infect and replicate without *manZ*, but at a rate that is offset by the spontaneous decay or inactivation of free virus particles under these conditions (16, 18). In either case, the net population growth of the ancestral phage on either the Δ*manY* or Δ*manZ* bacteria is insufficient to offset the 100-fold daily dilutions (Fig. 2.1, dashed line) that took place during the coevolution experiment (16).

Taken together, our results imply that *E. coli* and λ coevolved in an inverse gene-for-gene manner (2) that involves two infection steps (crossing first the outer and then the inner membrane) and at least three and probably four exploitable host features (Fig. 2.3). *E. coli* evolved resistance to phage λ through the loss or alteration of maltose transport across the outer membrane (via mutations in *malT*) and mannose transport across the inner membrane (via mutations in *manY* or *manZ*), while λ evolved to exploit other *E. coli* features including another outer membrane protein OmpF and, presumably, some as yet unidentified alternative inner membrane protein (encoded by a hypothetical *imx* gene in Fig. 2.3).

Figure 2.3. An inverse-gene-for-gene model showing the structure of the genetic network for coevolving *E. coli* and λ populations. Columns indicate bacterial genotypes with four exploitable features, and rows indicate λ genotypes that exploit those features: *mal*, maltose transport across the outer membrane; *man*, mannose transport across the inner membrane; *ompF*, glucose and electrolyte transport across the outer membrane; *imx*, a hypothetical inner membrane feature that is exploited by phage λ that have evolved independence of the mannose permease. Asterisks (*) indicate infectivity for each host-phage pair, with more asterisks indicating greater potential infectivity. Adaptive changes through the network proceed by two types of moves: *E. coli* resistance (to the right across rows) and increased λ infectivity (down across columns). The coevolving communities were founded by host genotype a and phage genotype vi (shown by the black circle). The communities analyzed in this study appear to have moved through the shaded nodes in five steps, as indicated by the arrows.

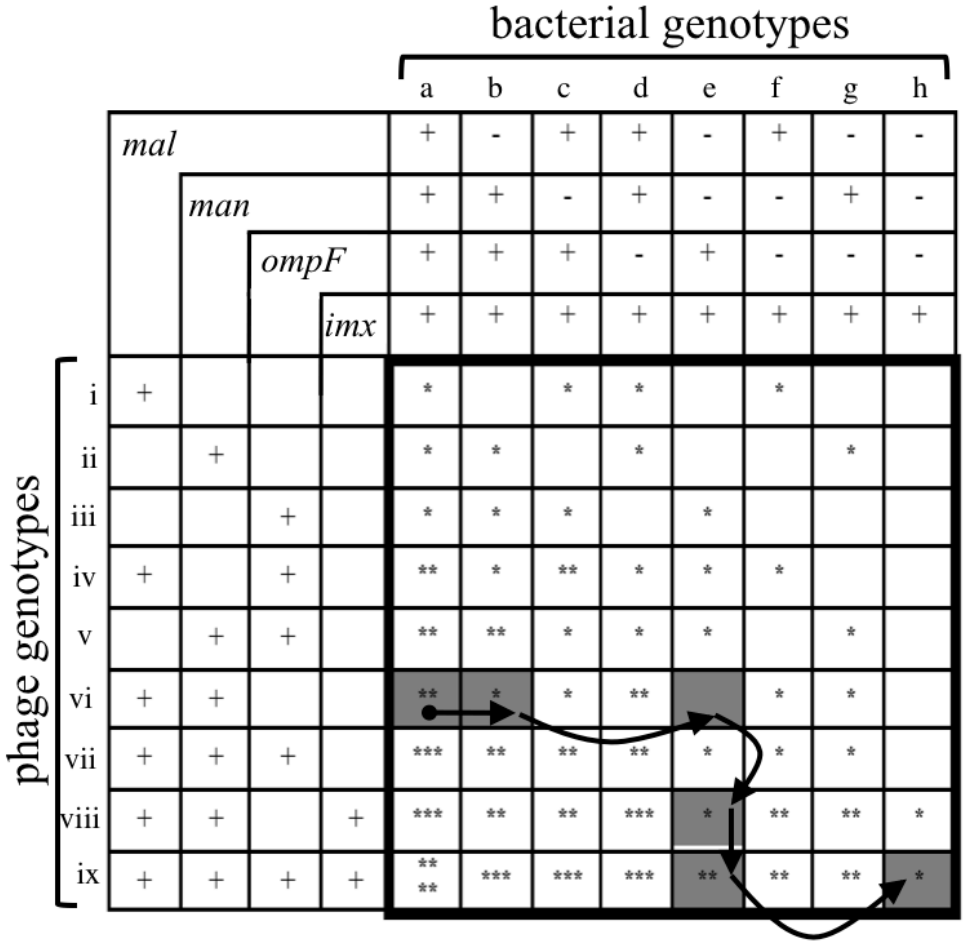

There are many potential coevolutionary paths through an inverse-gene-for-gene network that has four features subject to host defenses and parasite counter-defenses (Fig. 2.3). This multiplicity of potential paths suggests that mutation and selection might drive

replicate communities to different regions of the coevolutionary landscape, raising other interesting questions. How might different first-step resistance mutations affect the subsequent host-range evolution of the phage and further evolution of host resistance? Do communities tend to show increasing divergence with each evolutionary step as the coevolving populations follow different paths through the IGFG network? Will some communities get stuck at different endpoints, or might they eventually converge on the same phenotypic states after a period of divergence? How important are evolutionary innovations in opening new paths, relative to pleiotropic tradeoffs that may close off certain paths? In future work, we hope to investigate these and other questions about the coevolution of bacteria and phage and the structure of their genetic interaction networks.

Materials and Methods

Bacteria and phage strains: Meyer *et al.* (16) founded 96 replicate cultures with *E. coli* B strain REL606 and lytic phage λ cI26, serially passaged the communities for 20 days, and froze mixed-community samples daily. Some of the phage populations evolved the ability to use the outer membrane protein OmpF as a receptor, some of the bacteria populations evolved mutations that affected mannose metabolism, and some communities changed in both respects. We obtained phage isolates from two of the communities (D9 and G9) that changed in both respects; in each case, however, the isolates were taken four days before the source phage populations evolved the ability to use OmpF (Table 2.1, Appendix). We received *E. coli* B strain AB111 from Jenna Gallie, and *E. coli* K12 strains KJC9, JW1807, and JW1808 are from the Keio collection (24).

Table 2.1. *E. coli* and phage λ strains used in Chapter 2.

Strain	Description	Relevant Characteristics
Bacteria		
REL606	*E. coli* B ancestor of coevolution experiment	*malT*$^+$, *ompR*$^+$, *manY*$^+$, *manZ*$^+$
AB111	*manZ* deletion, derived from REL606[a]	Δ*manZ*
KJC9	*E. coli* K12 parental strain of Keio collection	*malT*$^+$, *ompR*$^+$, *manY*$^+$, *manZ*$^+$
JW1807	*manY* deletion in Keio collection	Δ*manY*
JW1808	*manZ* deletion in Keio collection	Δ*manZ*
DH5α	Strain used for λ plaque-based enumeration	*malT*$^+$, *ompR*$^+$, *manY*$^+$, *manZ*$^+$
Phage		
cI26	Lytic λ ancestor of coevolution experiment	Requires *E. coli* LamB
D9	Population D9, day 8, isolate #4	Requires *E. coli* LamB
G9	Population G9, day 11, isolate #3	Requires *E. coli* LamB

[a]AB111 also has three other mutations that have no known relevance to interactions with phage λ (Appendix).

Phage growth assays: We measured the population growth of the ancestral and evolved phages under the same culture conditions as those in which the communities evolved (16) (Appendix). The initial density of the bacteria was ~9 x 10^6 cells per ml in all cases. We calculate the phage's net population growth as the $\log_{10}$-transformed ratio of its final density after one day to its initial density. We enumerated the initial and final phage populations using dilution plating and soft-agar overlays (Appendix). We performed 5 or 6 replicate assays for each phage-host combination shown in Figure 1.

Frequency of mutants with altered mannose phenotypes: We estimated the frequency of bacteria with mutations affecting the mannose permease by plating from the time-series of frozen samples taken from populations D9 and G9 on tetrazolium mannose agar, as done previously (16). Mutants with reduced ability to metabolize mannose form more deeply pigmented colonies that can be readily distinguished from those of the ancestral strain REL606, which forms light pink colonies on that medium.

Acknowledgments

We thank Neerja Hajela for assistance in the lab, Justin Meyer for advice on experimental methods and scientific discussions, and Rohan Maddamsetti, Caroline Turner, and Mike Wiser for comments on the manuscript. This paper is based upon work supported by the National Science Foundation Graduate Research Fellowship (DGE-1424871) to A.R.B., the BEACON Center for the Study of Evolution in Action (NSF Cooperative Agreement DBI-0939454), and the John Hannah endowment from Michigan State University. Any opinions, findings, and conclusions or recommendations expressed in this paper are those of the authors and do not necessarily reflect the views of the National Science Foundation.

APPENDIX

Supplemental Methods

Phage isolation from experimentally evolved communities: We plated frozen samples taken from experimentally evolved communities to obtain isolated plaques of phages D9-8.4 and G9-11.3 on lawns of *lamB*$^{+}$ *E. coli* cells (Table 2.1). We confirmed that both of them require outer membrane protein LamB for infection by observing that neither produces plaques on *lamB*$^{-}$ *E. coli* lawns.

Phage growth assays: We measured phage growth in 10 ml of modified M9 (mM9) medium (M9 salts with 1 g/L magnesium sulfate, 1 g/L glucose, and 0.02% LB) in 50-ml glass flasks shaken at 120 rpm and 37°C. To ensure independence of the replicate assays, the bacterial stocks for each replicate were each grown from a separate bacterial colony, as done in Chapter 1. We enumerated initial phage densities before adding cells and final phage densities without removing the cells, which allowed us to quantify the final total density of viable phage including both infected hosts as well as free phage particles.

Phage enumeration: We estimated phage densities using dilution plating with soft-agar overlays. We mixed 100 µl of a diluted phage sampled with 100 µl of a stationary-phase culture of DH5α cells grown in LB (~2 x 10^8 cells) and 4 ml of reduced soft agar (rSA, 10 g/L tryptone, 1 g/L yeast extract, 8 g/L NaCl, 0.1% glucose, 2 mM of $CaCl_2$, and 1.75 g/L agar). We then poured this mixture on top of a base plate of Luria-Bertani agar (25). Note that this soft-agar formulation contains only 25% of the typical concentration of agar, which we find helps improve plaque visibility and numbers for the experimentally evolved phage λ isolates.

Genome sequencing: To sequence *E. coli* strain AB111, we isolated genomic DNA using the Qiagen Genomic-tip 100/G kit (Cat. No. 10243). The sequencing library was prepared

and sequence reads were generated by the Michigan State University Research Technology Support Facility on an Illumina MiSeq sequencer. We used the *breseq* pipeline (26) to align the sequence reads to an annotated reference genome of *E. coli* strain REL606, which is the progenitor of AB111.

Supplemental Results and Discussion

Timing of man *mutations:* Meyer *et al.* (16) reported that *malT* mutations had fixed in all of the bacterial populations by day 8 of their coevolution experiment, whereas mutations in *man* became common at later time points. We therefore expected that most or all of the *manYZ* mutations found in our study would be present on *mal* mutant backgrounds. To examine this issue, we tested two clonal isolates from each population at each day on minimal maltose, minimal mannose, and permissive tetrazolium arabinose agar plates. The *man* mutants were typically deficient in growth on the minimal maltose medium, indicating that they also carried *malT* mutations (data not shown).

Mutations in man *do not completely eliminate growth on mannose:* The isolates with mutations in *man* produced colonies that were, to varying degrees, red on tetrazolium mannose agar, which is indicative of diminished capacity to use mannose. Nonetheless, all of these isolates produced at least faint patches when spotted onto minimal mannose agar. This result indicates that the *man* mutations did not completely eliminate the ability to grow on mannose as a sole carbon source. In fact, the richly pigmented *man* isolates from population G9, as well as those from population D9 before day 12, grew robustly on minimal mannose, whereas the population D9 isolates from day 12 and later had severely reduced growth on minimal mannose.

These patch phenotypes on minimal mannose agar correlate with colony phenotypes on tetrazolium mannose plates as follows. The isolates that grew robustly on minimal mannose agar formed large magenta colonies on tetrazolium mannose plates; by contrast, those isolates with severely reduced growth on minimal mannose agar formed small red colonies on tetrazolium mannose plates (Fig. A2.1). This result implies that some *man* mutations impair the mannose permease, and possibly also the entry of phage DNA, to a greater extent than do others.

Mutations in the AB111 genome: Sequencing the AB111 genome revealed the *manZ* gene deletion (Δ853 bp starting at genome position 1,882,466) and three other mutations in genes not known to affect phage λ: (i) a 12,090-bp deletion beginning at genome position 787,879 that impacts an *E. coli* B-specific island of genes of unknown function including *ECB_00726* through *ECB_00739*; (ii) an IS-mediated insertion at genome position 3,656,171 in the intergenic region between *ECB_03412* and *yiaH*; and (iii) an IS-mediated deletion of 7,281 bp starting at position 3,894,997 that removes the ribose operon including genes *rbsD, rbsA, rbsC, rbsB, rbsK,* and *rbsR* along with part of the *yieO* gene.

Figure A2.1. Whole-population samples from day 20 of the coevolution experiment were plated on tetrazolium mannose indicator agar. Bacteria with the ancestral *man*$^{+}$ genotype form pink colonies. Panel A: Population G9 mutants make large magenta colonies. Panel B: Population D9 mutants from day 12 and later make small red colonies; earlier mutants from D9 resemble those shown in Panel A.

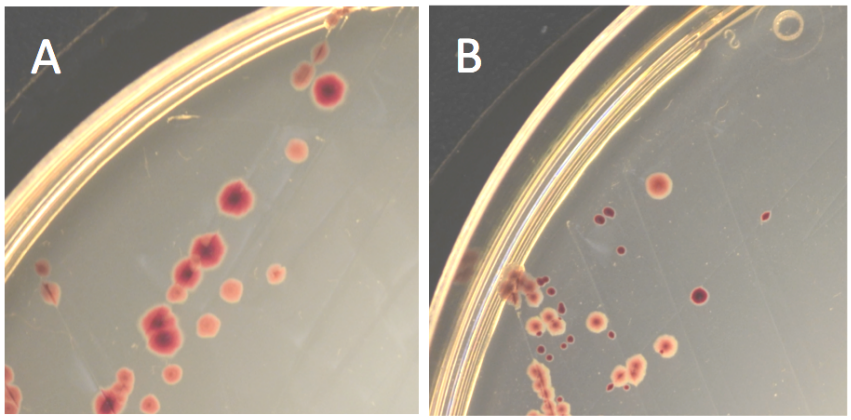

REFERENCES

REFERENCES

1. **Agrawal A**, **Lively CM**. 2002. Infection genetics: Gene-for-gene versus matching-alleles models and all points in between. Evol Ecol Res **2002**:79–90.

2. **Fenton A**, **Antonovics J**, **Brockhurst MA**. 2009. Inverse-gene-for-gene infection genetics and coevolutionary dynamics. Am Nat **174**:E230–42.

3. **Sieber M**, **Robb M**, **Forde SE**, **Gudelj I**. 2014. Dispersal network structure and infection mechanism shape diversity in a coevolutionary bacteria-phage system. ISME J **8**:504–514.

4. **Fenton A**, **Antonovics J**, **Brockhurst MA**. 2012. Two-step infection processes can lead to coevolution between functionally independent infection and resistance pathways. Evolution **66**:2030–2041.

5. **Dennehy JJ**. 2012. What can phages tell us about host-pathogen coevolution? Int J Evol Biol **2012**:1–12.

6. **Koskella B**, **Brockhurst MA**. 2014. Bacteria–phage coevolution as a driver of ecological and evolutionary processes in microbial communities. FEMS Microbiol Rev **38**:916–931.

7. **Smith HW**, **Huggins MB**. 1982. Successful treatment of experimental *Escherichia coli* infections in mice using phage: Its general superiority over antibiotics. J Gen Microbiol **128**:307–318.

8. **Chan BK**, **Sistrom M**, **Wertz JE**, **Kortright KE**, **Narayan D**, **Turner PE**. 2016. Phage selection restores antibiotic sensitivity in MDR *Pseudomonas aeruginosa.* Scientific Reports **6**:26717.

9. **Thirion JP**, **Hofnung M**. 1972. On some genetic aspects of phage λ resistance in *E. coli* K12. Genetics **71**:207–216.

10. **Hofnung M**, **Jezierska A**, **Braun-Breton C**. 1976. *lamB* mutations in *E. coli* K12: Growth of λ host range mutants and effect of nonsense suppressors. Mol Gen Genet **145**:207–213.

11. **Scandella D**, **Arber W**. 1974. An *Escherichia coli* mutant which inhibits the injection of phage λ DNA. Virology **58**:504–513.

12. **Elliott J**, **Arber W**. 1978. *E. coli* K-12 *pel* mutants, which block phage λ DNA injection, coincide with *ptsM*, which determines a component of a sugar transport system. Mol Gen Genet **161**:1–8.

13. **Erni B**, **Zanolari B**, **Kocher HP**. 1987. The mannose permease of *Escherichia coli* consists of three different proteins: Amino acid sequence and function in sugar

transport, sugar phosphorylation, and penetration of phage λ DNA. J Biol Chem **262**:5238–5247.

14. **Esquinas-Rychen M**, **Erni B**. 2001. Facilitation of bacteriophage lambda DNA injection by inner membrane proteins of the bacterial phosphoenol-pyruvate: carbohydrate phosphotransferase system (PTS). J Mol Microbiol Biotechnol **3**:361–370.

15. **Spanakis E**, **Horne MT**. 1987. Co-adaptation of *Escherichia coli* and coliphage λvir in continuous culture. J Gen Microbiol **133**:353–360.

16. **Meyer JR**, **Dobias DT**, **Weitz JS**, **Barrick JE**, **Quick RT**, **Lenski RE**. 2012. Repeatability and contingency in the evolution of a key innovation in phage Lambda. Science **335**:428–432.

17. **Meyer JR**, **Agrawal AA**, **Quick RT**, **Dobias DT**, **Schneider D**, **Lenski RE**. 2010. Parallel changes in host resistance to viral infection during 45,000 generations of relaxed selection. Evolution **64**:3024–3034.

18. **Burmeister AR**, **Lenski RE**, **Meyer JR**. 2016. Host coevolution alters the adaptive landscape of a virus. Proc R Soc Lond B Biol Sci **283**:20161528.

19. **Meyer JR**, **flores CO**, **Weitz JS**, **Lenski RE**. 2008. Key innovation in a virus catalyzes a coevolutionary arms race. A-Life Proceedings 13 **13**:532–533.

20. **Wang N**, **Dykhuizen DE**, **Slobodkin LB**. 1996. The evolution of phage lysis timing. Evol Ecol **10**:545–558.

21. **Shao Y**, **Wang IN**. 2008. Bacteriophage adsorption rate and optimal lysis time. Genetics **180**:471–482.

22. **Williams N**, **Fox DK**, **Shea C**, **Roseman S**. 1986. Pel, the protein that permits lambda DNA penetration of *Escherichia coli*, is encoded by a gene in *ptsM* and is required for mannose utilization by the phosphotransferase system. Proc Natl Acad Sci USA **83**:8934–8938.

23. **Scandella D**, **Arber W**. 1976. Phage λ DNA injection into *Escherichia* coli *pel*¯ mutants is restored by mutations in phage genes *V* or *H*. Virology **69**:206–215.

24. **Baba T**, **Ara T**, **Hasegawa M**, **Takai Y**, **Okumura Y**, **Baba M**, **Datsenko KA**, **Tomita M**, **Wanner BL**, **Mori H**. 2006. Construction of *Escherichia coli* K-12 in-frame, single-gene knockout mutants: The Keio collection. Mol Syst Biol **2**:2006.0008.

25. **Sambrook J**, **Russell DW**. 2001. Molecular Cloning: A Laboratory Manual, 3rd ed. Cold Spring Harbor Laboratory.

26. **Barrick JE**, **Colburn G**, **Deatherage DE**, **Traverse CC**, **Strand MD**, **Borges JJ**,

Knoester DB, **Reba A**, **Meyer AG**. 2014. Identifying structural variation in haploid microbial genomes from short-read resequencing data using *breseq*. BMC Genomics **15**:1039.

CHAPTER 3:

EFFECTS OF FORM AND STRENGTH OF PHAGE RESISTANCE ON MICROBIAL COMMUNITY DYNAMICS AND STRUCTURE

Authors: Alita R. Burmeister, Christopher Klausmeier, Richard E. Lenski

Abstract

Bacteriophages are found in nearly all environments, they often outnumber their hosts, and they have high replication capacities with rapid infection rates and large burst sizes. How do bacterial populations deal with this onslaught of parasites? One idea from the field of ecology is that host diversity may reduce pathogen load when there are non-productive infections on resistant hosts, thereby "trapping" pathogens and removing them from the environment. To investigate the role of phage resistance on sensitive host populations and overall community structure, we modeled the interactions among phage, sensitive bacteria, and resistant bacteria. We compared the effects of two types of resistance. In the case of "envelope" resistance, the resistant bacteria are simply infected at a lower rate than sensitive cells. In the case of "cytoplasmic" resistance, resistant cells are infected at the same rate, but some of the infections are non-productive. We show that cytoplasmic resistance provides indirect protection for susceptible hosts by reducing the phage density and that such resistance can stabilize communities. The strength of resistance also strongly influences community structure. We discuss ecological and evolutionary implications of the model for natural communities, where the potential for trap effects appears to be widespread.

Introduction

Most natural communities of microbes comprise multi-trophic-level networks in which bacteria compete for resources while facing potentially intense selection by phage (1). Given the typical excess of phages relative to bacterial cells and the often-lethal consequence of phage infection, it is a wonder that bacteria can persist at all. Models and experiments have shown, however, that sensitive bacteria and lytic phages can coexist dynamically in a manner similar to that predicted by Lotka-Volterra models of predator-prey interactions (2-5). Moreover, persistence is enhanced by the evolution of bacteria that are resistant to infections, provided that resistance trades off with resource competitiveness, in which case sensitive and resistant bacteria and phage may all stably coexist (4-6).

Bacteria have evolved a variety of mechanisms to resist phage infections. These mechanisms can be broadly divided into two classes, "envelope" and "cytoplasmic" resistance. Bacteria with envelope resistance have reduced rates of phage attachment, a trait conferred by the modification or loss of phage receptors on the surface of the cell. Envelope resistance is commonly observed in coevolution experiments with phage (7-11), including the *malT* and *ompF* resistance mutations described in Chapters 1 and 2. Cytoplasmic resistance occurs when a phage adsorbs to a cell and initiates infection but is then blocked from replicating inside the cell. Many examples of this mode of resistance, including restriction-modification and CRISPR-Cas systems, are found in nature (12, 13). The *manYZ* resistance discussed in chapter 2, whereby the successful injection of phage DNA into the cell is blocked after adsorption, represents a similar mechanism of resistance.

The mode of defense has important implications not only for the fate of individual phage but also for phage populations and thus the resulting community dynamics and

structure. A phage that encounters a cell with complete envelope resistance will be negligibly affected – it will not adsorb to the host, so it is free to diffuse away and find a cell with the required surface receptor. In contrast, a phage that encounters a cell with cytoplasmic resistance will adsorb to the cell and initiate infection. At this point, the infecting phage is trapped inside the cell; its fitness is determined by whether it can successfully complete its life cycle and produce progeny phage. If the infected cell's cytoplasmic resistance is successful – for example, the phage DNA is digested by restriction or Cas enzymes – then the phage will die without reproducing. As a consequence, sensitive cells will never encounter that trapped phage. They may thus benefit from the presence of cells with cytoplasmic resistance, even though they also compete with the resistant cells for resources. Therefore, whether resistance occurs at the cell envelope or within the cytoplasm might have important effects on the dynamics of bacteria and phage populations and the resulting community structure. To investigate the role of the resistance mode and strength of resistance on these dynamics and structure, we analyze the coupled differential equations that describe bacteria and phage population dynamics under these different scenarios.

The Base Model

Our base model is derived from Levin, Stewart, and Chao's (4) model of the interaction between *E. coli* and phage T2. The model has three trophic levels: a resource, a population of bacterial cells (n) that consume the resource, and a population of lytic phage (p) that exploit the cells, which transiently become infected cells before they are killed (m). Phage bind irreversibly to sensitive cells at an adsorption rate (γ); after adsorption, a phage spends

a fixed latent period (l) inside the infected cell before lysing it and releasing β phage progeny. The resource flows into the environment at rate ρ from a reservoir with concentration C, while the resource concentration in the environment is r. Bacterial growth is described by a maximum rate of resource uptake (P) and the resource concentration at which the resource is consumed at half the maximum rate (Q); the consumption of e_i resource units results in the production of a new cell. Infected cells do not consume resources or reproduce, and they do not adsorb additional phage. Uninfected bacteria, infected cells, free phage, and resources are all removed from the environment at the flow rate ρ. All parameters are defined in Table 3.1.

Table 3.1. Model variables and parameters used in Chapter 3. Values used in the simulations are indicated in figure legends.

General and Environmental Parameters	
t	Time
C	Resource concentration in the reservoir (μg ml^{-1})
r	Resource concentration in the environment (μg ml^{-1})
ρ	System flow rate (h^{-1})
e	The number (base of natural logarithm) when no subscript is present
Host Variables and Parameters	
n_1, n_2	Uninfected bacteria concentrations of ecotypes 1 and 2 (ml^{-1})
m_1, m_2	Infected bacteria concentrations of ecotypes 1 and 2 (ml^{-1})
P_1, P_2	Maximum rate of resource uptake of ecotypes 1 and 2 (μg h^{-1})
Q_1, Q_2	Concentration of glucose that supports growth at half the maximum rate for ecotypes 1 and 2 (μg ml^{-1})
e_1 , e_2	Resource required per new cell produced for ecotypes 1 and 2 (μg)
Phage Variables and Parameters	
p	Concentration of free phage (ml^{-1})
l	Latent period (h)
b	Burst size
γ_1, γ_2	Adsorption rate (ml h^{-1}) of phage to bacterial ecotypes 1 and 2
α	Degree of cytoplasmic susceptibility; if $\alpha = 1$, the host is fully sensitive; if $\alpha = 0$, the host is completely resistant

One-Host Model

In the simplest case, there is a single bacterial ecotype that is sensitive to the phage. The community comprises, per unit volume, n_1 uninfected cells, m_1 infected cells, p free viruses, and r units of resource. The interactions are shown conceptually in Fig. 3.1, and the resulting dynamics are described by the following coupled equations:

$$\frac{dr}{dt} = \rho(c - r) - \frac{P_1 r}{Q_1 + r}(n_1 + m_1) \quad (1\text{-}1)$$

$$\frac{dn_1}{dt} = n_1 \frac{P_1 r}{Q_1 + r}/e_1 - \rho n_1 - \gamma_1 n_1 p \quad (1\text{-}2)$$

$$\frac{dm_1}{dt} = \gamma_1 n_1 p - \rho m_1 - e^{-\rho l}\gamma_1 n_1' p' \quad (1\text{-}3)$$

$$\frac{dp}{dt} = b_1 e^{-\rho l}\gamma_1 n_1' p' - \rho p - \gamma_1(n_1 + m_1)p \quad (1\text{-}4)$$

The model is similar to the Lotka-Volterra predator-prey model, except that host resource use is described explicitly and the phage's latent period, l, adds a time lag to equations 1-3 and 1-4 (where the variables marked by apostrophes are evaluated at time $t - l$).

In this one-host model, an increase in the phage's adsorption rate to the uninfected cells causes the equilibrium density of the bacteria to decline (Fig. 3.2A). At very high adsorption rates, the predator-prey cycles are unstable (Fig. 3.2D).

Figure 3.1. Conceptual models of communities that include a single resource that may limit the growth of bacteria, populations of one or two bacterial ecotypes, and one virus population. One-host models: A single host ecotype consumes the resource and is susceptible to the virus. Two-host models: In addition to the sensitive host type, a second host type is either partially or fully resistant to the virus, and that resistance imposes a cost that reduces its competitiveness for and consumption of the limiting resource. The effects of the second host type on the phage ($*_1$), and of the phage on the second host type ($*_2$), depend on the form and effectiveness of resistance.

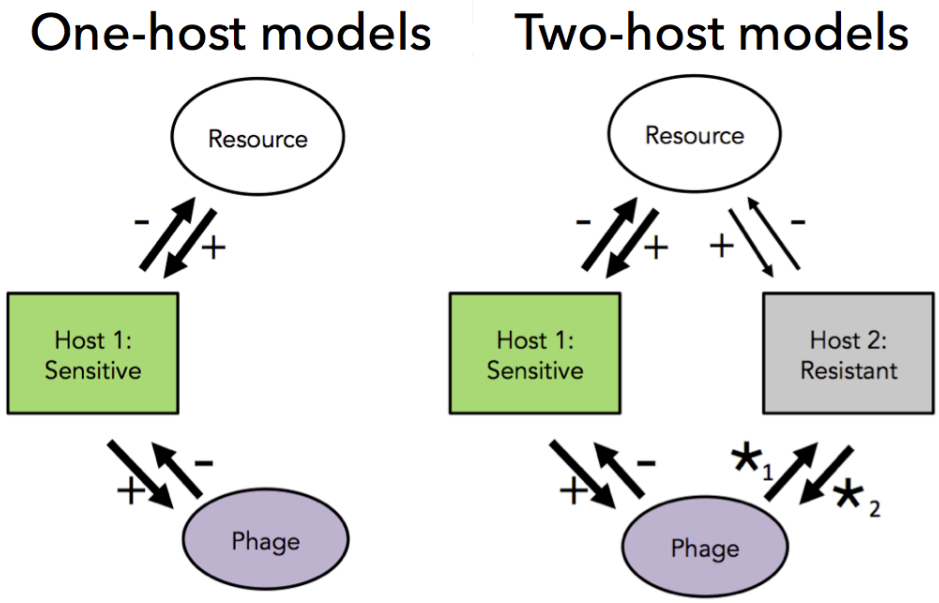

Two-Host Models

The two-host ecosystem contains two bacterial ecotypes, where the second ecotype is either partially or completely resistant to the phage (Fig. 3.1, two-host model). There is some metabolic cost of resistance, such that the resistant ecotype is less competitive for the primary resource (e.g., $P_2 < P_1$ or $Q_2 > Q_1$). In the two-host model, resistance to phage may occur in various combinations of form and strength. Cells may be partially resistant or completely resistant. They may have envelope resistance that reduces or prevents phage adsorption; or they may have cytoplasmic resistance, in which case an adsorbed phage

initiates infection, is removed from the phage population, but then has a reduced or zero probability of successfully completing the infection (Table 3.2).

Table 3.2. Combinations of form and strength of phage resistance. Resistance can occur either by preventing adsorption to the cell surface (envelope resistance) or after adsorption (cytoplasmic resistance). Resistance may be either complete (no successful infections that kill the host cell and release progeny phage) or partial (some proportion of infections are successful, resulting in host death and phage replication).

Form	Resistance Efficacy	
	Complete	**Partial**
None	Fig. 3.2 (One-host)	
Cytoplasmic	Fig. 3.3	Fig. 3.5
Envelope	Fig. 3.4	Fig. 3.4

Complete cytoplasmic resistance: We now consider the case where the second bacterial ecotype has complete cytoplasmic resistance, and there is no difference in the phage's adsorption rate to sensitive and resistant cells (i.e., $\gamma_1 = \gamma_2$). The following set of equations describes the community dynamics:

$$\frac{dr}{dt} = \rho(c - r) - \frac{P_1 r}{Q_1 + r}(n_1 + m_1) - \frac{P_2 r}{Q_2 + r}(n_2 + m_2) \quad (2\text{-}1)$$

$$\frac{dn_1}{dt} = n_1\left(\frac{P_1 r}{Q_1 + r}/e_1\right) - \rho n_1 - \gamma_1 n_1 p \quad (2\text{-}2)$$

$$\frac{dn_2}{dt} = n_2\left(\frac{P_2 r}{Q_2 + r}/e_2\right) - \rho n_2 - \gamma_2 n_2 p + m_2 \frac{P_2 r}{Q_2 + r}/e_2 \quad (2\text{-}2b)$$

$$\frac{dm_1}{dt} = \gamma_1 n_1 p - \rho m_1 - e^{-\rho l}\gamma_1 n_1' p' \quad (2\text{-}3)$$

$$\frac{dm_2}{dt} = \gamma_1 n_2 p - \rho m_2 \quad (2\text{-}3b)$$

$$\frac{dp}{dt} = b_1 e^{-\rho l}\gamma_1 n_1' p' - \rho p - \gamma_1(n_1 + m_1)p - \gamma_2(n_2 + m_2)p \quad (2\text{-}4)$$

Similar to the one-host model (Fig. 3.2A), as the phage's adsorption rate increases, the density of the sensitive bacteria decreases (Fig. 3.3A). As the density of the sensitive bacteria declines, the resource concentration increases, and thereby so does the density of the resistant bacteria (Fig. 3.3A). The presence of resistant bacteria stabilizes the

community (Fig. 3.2D vs. Fig. 3.3D) in two ways: (i) by lowering the concentration of resources, the predator-prey cycles involving the sensitive cells and phage are dampened; and (ii) by "trapping" the phage in non-productive infections, the intensity of phage attacks on the sensitive population is diminished.

Figure 3.2. Outcomes and dynamics of one-host model. Panel A: The x-axis shows the adsorption rate of the phage to the bacteria. The shaded regions depict the maximum and minimum densities for each population determined between 9800 and 10,000 hours of numerical simulations at different adsorption rates. Panels B, C, and D show dynamics at illustrative low, medium, and high adsorption rates (B: $\gamma = 0.64 \times 10^{-7}$ ml h^{-1}; C: $\gamma = 1.24 \times 10^{-7}$ ml h^{-1}; D: $\gamma = 1.84 \times 10^{-7}$ ml h^{-1}). Green: sensitive bacteria (ecotype 1); purple: phage. Parameter values: $\rho = 0.55$ h^{-1}, $C = 16$ µg ml^{-1}, $P_1 = 9.96 \times 10^{-6}$ µg h^{-1}, $e_1 = 1.35 \times 10^{-5}$ µg, $Q_1 = 4$ µg ml^{-1}, $l = 0.5$ h, $b = 98$.

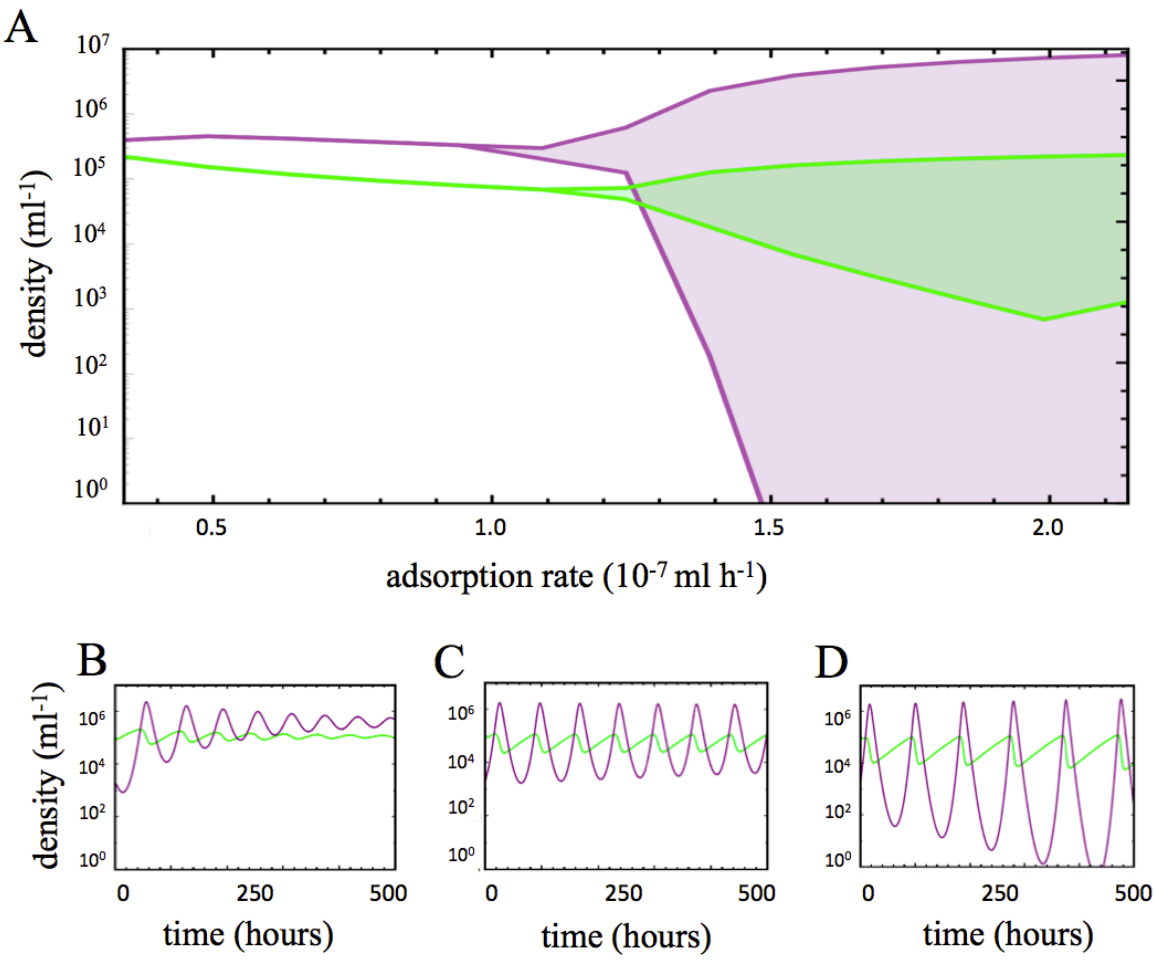

Figure 3.3. Outcomes and dynamics of two-host model with complete cytoplasmic resistance. Panel A: The x-axis shows the adsorption rate of the phage to both the sensitive (ecotype 1) and resistant bacteria (ecotype 2). The lines depict the maximum and minimum densities for each population determined between 9800 and 10,000 hours of numerical simulations at different adsorption rates. Panels B, C, and D show dynamics at illustrative low, medium, and high adsorption rates (B: $\gamma_1 = \gamma_2 = 0.64 \times 10^{-7}$ ml h^{-1}; C: $\gamma_1 = \gamma_2 = 1.24 \times 10^{-7}$ ml h^{-1}; D: $\gamma_1 = \gamma_2 = 1.84 \times 10^{-7}$ ml h^{-1}). Green: ecotype 1; purple: phage; gray: ecotype 2. Parameter values: $P_2 = 9.76 \times 10^{-6}$ µg h^{-1}, $e_2 = 1.35 \times 10^{-5}$ µg, $Q_2 = 4$ µg ml^{-1}. All other values are the same as in Fig. 3.2.

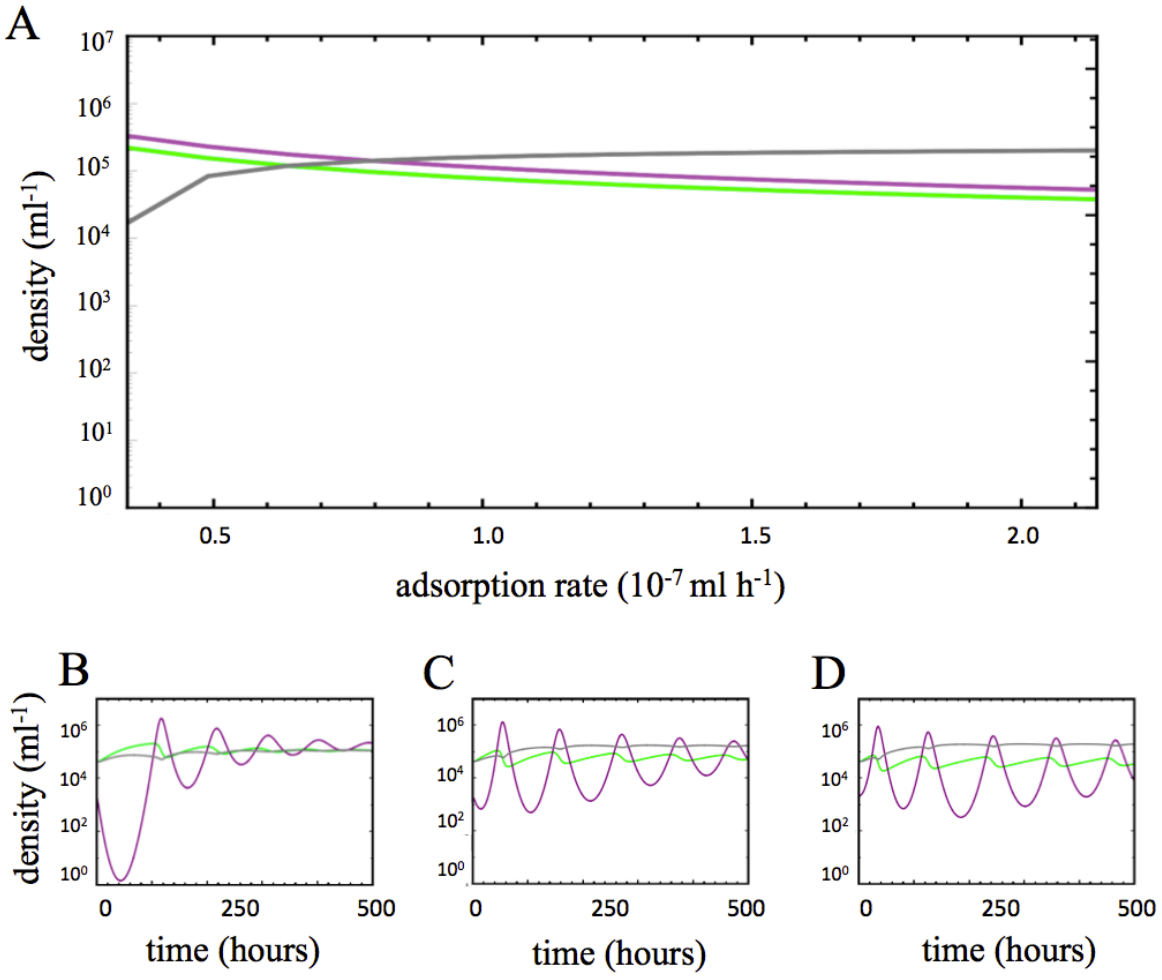

Complete and Partial Envelope Resistance: Levin *et al.* (4) investigated investigated the effects of envelope resistance on bacteria and phage population dynamics. An ecosystem with one susceptible bacterial ecotype and another with envelope resistance is described by the following set of equations:

$$\frac{dr}{dt} = \rho(c - r) - \frac{P_1 r}{Q_1 + r}(n_1 + m_1) - \frac{P_2 r}{Q_2 + r}(n_2 + m_2) \quad (3\text{-}1)$$

$$\frac{dn_1}{dt} = n_1\left(\frac{P_1 r}{Q_1 + r}/e_1\right) - \rho n_1 - \gamma_1 n_1 p \quad (3\text{-}2)$$

$$\frac{dn_2}{dt} = n_2\left(\frac{P_2 r}{Q_2 + r}/e_2\right) - \rho n_2 - \gamma_2 n_2 p \quad (3\text{-}2b)$$

$$\frac{dm_1}{dt} = \gamma_1 n_1 p - \rho m_1 - e^{-\rho l}\gamma_1 n_1' p' \quad (3\text{-}3)$$

$$\frac{dm_2}{dt} = \gamma_2 n_2 p - \rho m_2 - e^{-\rho l}\gamma_2 n_2' p' \quad (3\text{-}3b)$$

$$\frac{dp}{dt} = b_1 e^{-\rho l}\gamma_1 n_1' p' - \rho p - \gamma_1(n_1 + m_1)p - \gamma_2(n_2 + m_2)p + b_2 e^{-\rho l}\gamma_2 n_2' p' \quad (3\text{-}4)$$

If the envelope resistance prevents phage adsorption with 100% efficacy (i.e., $\gamma_2 = 0$), then we term that resistance "complete"; in that case, there are no infected bacteria of the second type and equation (3-3b) drops out of the model. On the other hand, if envelope resistance only reduces the rate of phage adsorption but does not prevent it entirely (i.e., $1 > \gamma_2 / \gamma_1 > 0$), then we term that resistance "partial".

As the efficacy of envelope resistance increases (Fig. 3.4A), the ecosystem outcomes change qualitatively across three different regimes. At low levels of envelope resistance, the resistant bacteria go extinct (Fig. 3.4A, efficacy < ~0.32; Fig. 3.4B) because the benefit of resisting phage is too small to offset their reduced competitiveness for resources. At intermediate levels of resistance (Fig. 3.4A, efficacy between ~0.32 and ~0.72; Fig. 3.4C), the resistant host population becomes established while also sustaining phage replication. In fact, the resulting phage density is sufficiently high that it drives the sensitive host to extinction. Thus, at intermediate levels of envelope resistance, the resistant bacteria act as

phage amplifiers, not as traps. This effect—whereby a host or prey species that is less competitive but better defended drives a more competitive but less defended species extinct—is sometimes called "apparent competition" (14). At high levels of resistance efficacy (Fig. 3.4A, efficacy > ~0.72; Fig. 3.4D), the resistant population again persists. In this case, however, the viruses do not reach sufficient numbers to drive the sensitive bacteria extinct. Instead, the viruses mediate the stable coexistence of the two bacterial types by disproportionately killing the superior competitor for the resources.

Figure 3.4. Outcomes and dynamics of two-host model with partial or complete envelope resistance. Panel A: The x-axis shows the resistance efficacy of bacterial ecotype 2, where 0 is as sensitive as ecotype 1 and 1 is completely resistant. The shaded regions depict the maximum and minimum densities for each population between 9800 and 10,000 hours of numerical simulation. Panels B, C, and D show dynamics at illustrative low, medium, and high resistance efficacies (B: 0.1, C: 0.5, and D: 0.9). Green: ecotype 1; gray: ecotype 2; purple: phage. Parameter values are the same as in Fig. 3.3 except $\gamma_1 = 1.24 \times 10^{-7}$.

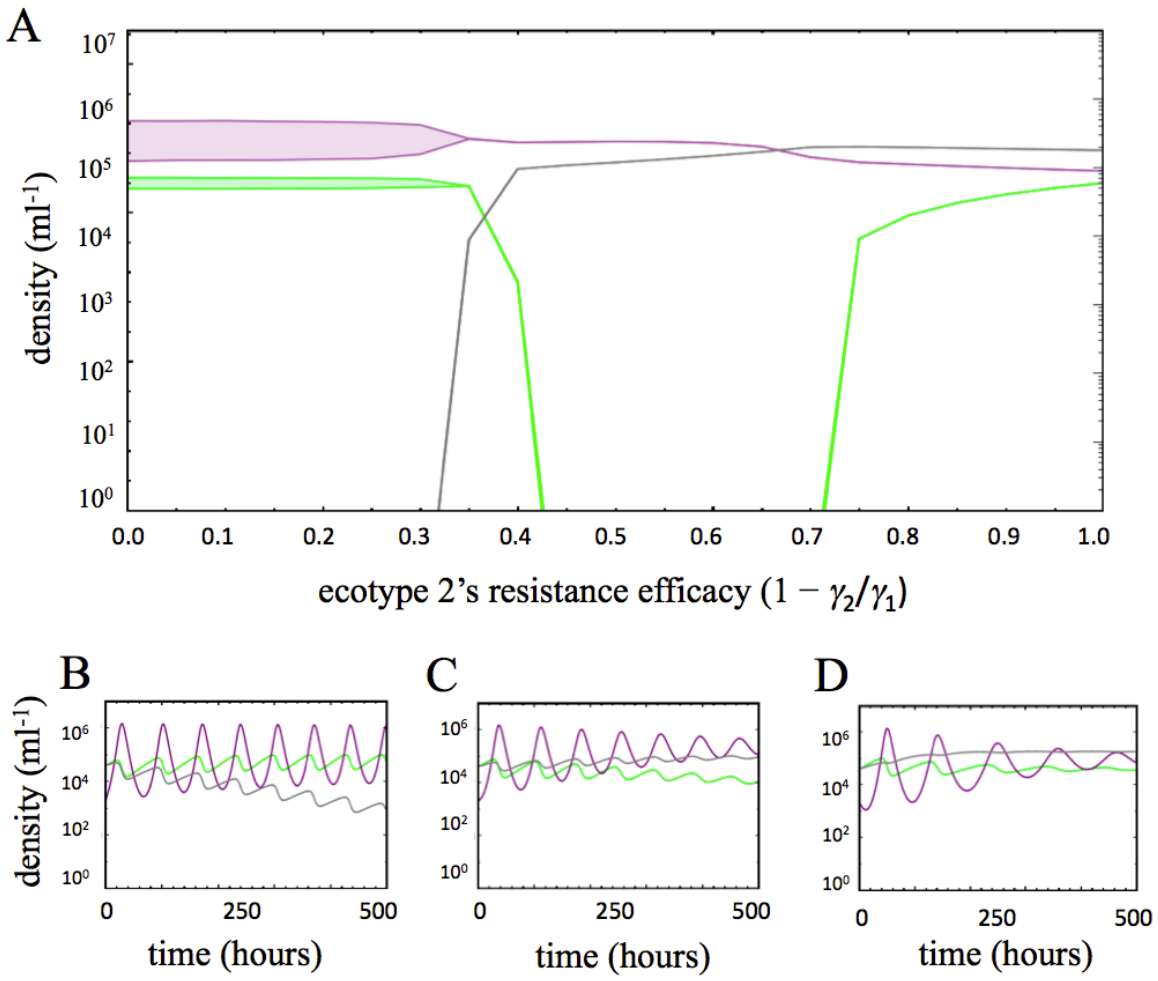

Partial Cytoplasmic Resistance: To model partial cytoplasmic resistance, we introduce a new parameter, α, that describes the probability that an infected cell blocks phage replication and thereby survives. Cytoplasmic resistance is complete (α = 0, i.e., 100% efficacy) if phage infections are never successful; it is partial ($1 > \alpha > 0$) if some infections are successful and others are not. The following set of equations describe the dynamics when cytoplasmic resistance may be either partial or complete:

$$\frac{dr}{dt} = \rho(c - r) - \frac{P_1 r}{Q_1 + r}(n_1 + m_1) - \frac{P_2 r}{Q_2 + r}(n_2 + m_2) \quad (4\text{-}1)$$

$$\frac{dn_1}{dt} = n_1 \frac{P_1 r}{Q_1 + r}/e_1 - \rho n_1 - \gamma_1 n_1 p \quad (4\text{-}2)$$

$$\frac{dn_2}{dt} = n_2 \frac{P_2 r}{Q_2 + r}/e_2 - \rho n_2 - \gamma_2 n_2 p + (1 - \alpha) m_2 \frac{P_2 r}{Q_2 + r}/e_2 \quad (4\text{-}2b)$$

$$\frac{dm_1}{dt} = \gamma_1 n_1 p - \rho m_1 - e^{-\rho l} \gamma_1 n_1' p' \quad (4\text{-}3)$$

$$\frac{dm_2}{dt} = \gamma_1 n_2 p - \rho m_2 - (\alpha) e^{-\rho l} \gamma_2 n_2' p' \quad (4\text{-}3b)$$

$$\frac{dp}{dt} = b_1 e^{-\rho l} \gamma_1 n_1' p' - \rho p - \gamma_1 (n_1 + m_1) p - \gamma_2 (n_2 + m_2) p + (\alpha) b_2 e^{-\rho l} \gamma_2 n_2' p' \quad (4\text{-}4)$$

Changing the form of bacterial defense against phage from envelope to cytoplasmic resistance changes the community structure. In particular, the phage-amplifying effect that can lead to the phenomenon of apparent competition with envelope resistance disappears in the case of cytoplasmic resistance (Fig. 3.4A vs. 5A). Instead, sensitive bacteria persist in the community across all levels of efficacy of cytoplasmic resistance. Similar to the special case of complete cytoplasmic resistance (Fig. 3.3), cells with partial cytoplasmic resistance also trap and remove phage, thereby providing protection to the more sensitive bacteria. Therefore, both the form and strength of bacterial resistance to phage can influence the dynamics and resulting structure of microbial communities.

Figure 3.5. Outcomes and dynamics of two-host model with partial cytoplasmic resistance. Panel A: The x-axis shows the resistance efficacy of bacterial ecotype 2, where 0 is as sensitive as ecotype 1 and 1 is completely resistant. The shaded regions depict the maximum and minimum densities for each population between 9800 and 10,000 hours of numerical simulation. Panels B, C, and D show dynamics at illustrative low, medium, and high resistance efficacies (B: 0.1, C: 0.5, and D: 0.9). Green: ecotype 1; gray: ecotype 2; purple: phage. Parameter values are the same as in Fig. 3.3 except $\gamma_1 = \gamma_2 = 1.24 \times 10^{-7}$.

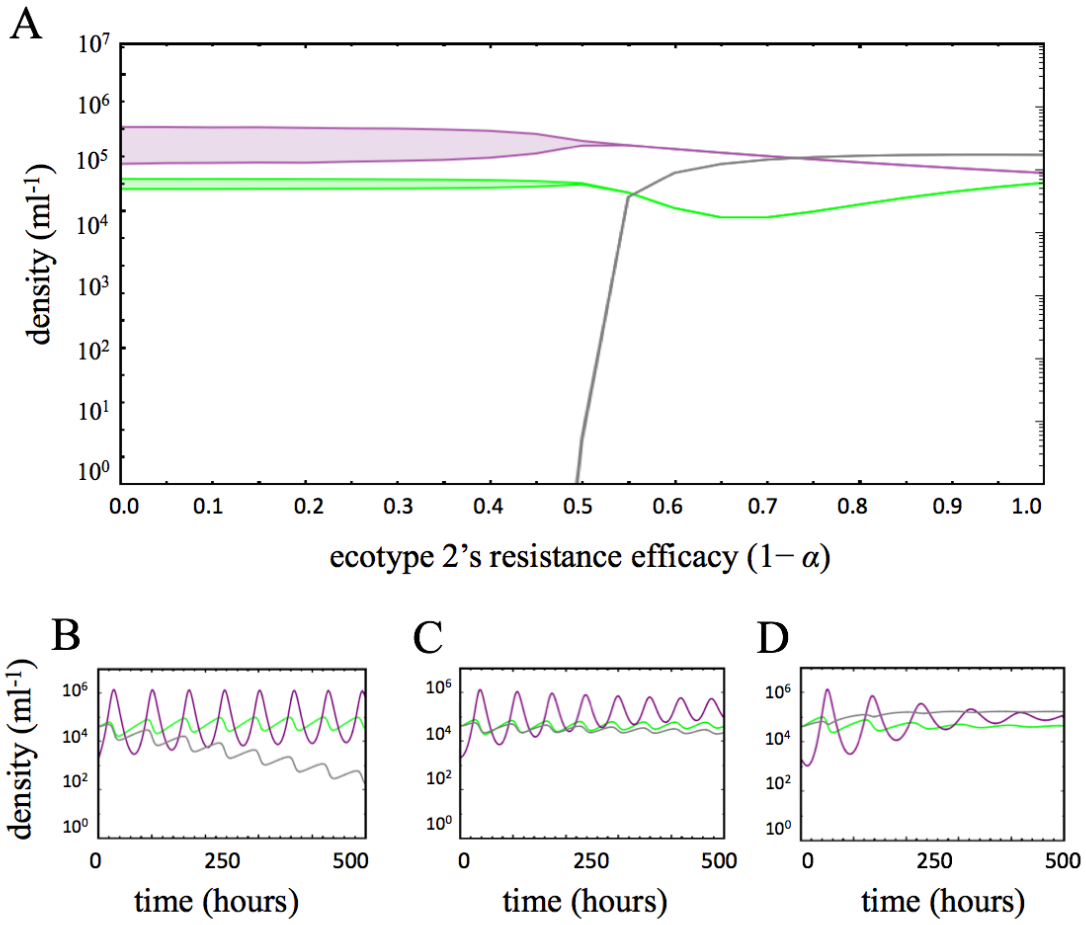

Discussion

We find it particularly interesting that cytoplasmic resistance, unlike envelope resistance, can protect and sustain populations of bacteria that are sensitive to phage. These internally resistant hosts can be said to trap (15) or dilute (16) the parasite population. This effect has also been dubbed "friendly competition" (17), in contradistinction to "apparent competition" (14) whereby partial envelope resistance can cause the extinction of a competitively superior sensitive ecotype (4, 7). Such friendly competition has been observed for sensitive strains of *Daphnia* that benefit from the presence of other strains that trap and remove parasitic fungal spores from the environment (17). The trap effects of bacteria with cytoplasmic resistance on phage and of *Daphnia* that remove fungal parasites are conceptually similar to effects in other antagonistic interactions, such as plants and herbivores. Grover et al. (18) presented theory in which inedible plants (analogous to bacteria with cytoplasmic resistance) may have detrimental effects on herbivore populations (analogous to phage), changing the structure and stability of ecological communities.

In contrast to the case of bacteria with cytoplasmic resistance (or other organisms that trap or otherwise harm parasites or predators), the presence of bacteria with partial envelope resistance can amplify the density of phage (or other parasites or predators), thereby harming the sensitive bacteria through the effect of apparent competition (14). Indeed, ecologists have debated—based on both theoretical and empirical grounds—whether increased diversity of hosts will tend to increase or reduce the level of parasitism, and the so-called "dilution effect" has therefore remained controversial. In part, the discussion has been hindered by overly general assertions, such as the idea that increasing

biodiversity necessarily increases the dilution effect, thereby reducing human disease. While some data appear to support this idea (19), other studies have found evidence of the opposite relation between diversity and disease (20).

Despite the uncertain implications for human disease and other areas of applied ecology, dilution effects may well be important in the ecology and evolution of natural communities. Models and experiments with tractable systems, such as bacteria and phages, offer the potential to clarify some complicated issues. Laboratory and mesocosm experiments have been useful for identifying dilution mechanisms and testing their effects in several systems. Of nine controlled studies across diverse host taxa (including amphibians, fish, zooplankton, and bacteria), eight found evidence for a dilution effect in which the parasite load was reduced by the presence of a diluting host (15, 17, 21-26). The one study that did not find evidence for a dilution effect instead found evidence that the parasite had evaded that effect (27). These studies together suggest that dilution effects may impact not only ecological communities but also the coevolutionary process that shapes the members' interactions. In the specific case of bacteria and lytic phage, our results show that the effect of increasing bacterial diversity on the persistence of sensitive populations will depend critically on the form, as well as the strength, of resistance. Natural microbial communities harbor many phage-resistant bacteria, with diverse forms of resistance, and some of them can be expected to trap phage and thereby remove them from the environment, thereby indirectly helping to maintain sensitive host populations.

Conclusion

We analyzed models with coupled differential equations to show that both the form and strength of bacterial resistance to phage can affect not only the population dynamics but also the structure of the resulting community. In particular, whether resistance is expressed at the cell envelope or within the cell cytoplasm affects whether partially resistant bacteria act as phage amplifiers or phage traps, which may either cause the sensitive bacteria to go extinct or allow them to coexist with their resistant counterparts, respectively. This work provides a theoretical framework for future experiments that may test these predictions and further investigate how different forms and strengths of resistance affect microbial population dynamics, community structure, and nutrient flows. Another possible direction for future research would extend these models to allow different modes of phage replication, including reversible adsorption and non-lethal parasitism.

Acknowledgments

We thank Gary Mittlebach, Elena Litchman, Bruce Levin, Paul Turner, Kenichi Okamoto, and Jory Schossau for useful discussions, and Caroline Turner, Michael Wiser, and Rohan Maddamsetti for comments on the manuscript. This work was supported in part by a National Science Foundation Graduate Research Fellowship (DGE-1424871) to ARB, by various units at Michigan State University, and by the BEACON Center for the Study of Evolution in Action (NSF Cooperative Agreement DBI-0939454). Any opinions, findings, conclusions, or recommendations expressed in this paper are those of the authors and do not necessarily reflect the views of the National Science Foundation.

REFERENCES

REFERENCES

1. **Hatfull GF**. 2015. Dark matter of the biosphere: the amazing world of bacteriophage diversity. Journal of Virology **89**:8107–8110.

2. **Lotka AJ**. 1920. Analytical note on certain rhythmic relations in organic systems. Proc Natl Acad Sci USA **6**:410–415.

3. **Volterra V**. 1926. Fluctuations in the abundance of a species considered mathematically. Nature **118**:558–560.

4. **Levin BR**, **Stewart FM**, **Chao L**. 1977. Resource-limited growth, competition, and predation: A model and experimental studies with bacteria and bacteriophage. American Naturalist **111**:3–24.

5. **Bohannan B**, **Lenski RE**. 2000. Linking genetic change to community evolution: insights from studies of bacteria and bacteriophage. Ecol Lett **3**:362–377.

6. **Lenski RE**, **Levin BR**. 1985. Constraints on the coevolution of bacteria and virulent phage: a model, some experiments, and predictions for natural communities. Am Nat **125**:585–602.

7. **Lenski RE**. 1988. Experimental studies of pleiotropy and epistasis in *Escherichia coli.* I. Variation in competitive fitness among mutants resistant to virus T4. Evolution **42**:425–432.

8. **Spanakis E**, **Horne MT**. 1987. Co-adaptation of *Escherichia coli* and coliphage λvir in continuous culture. J Gen Microbiol **133**:353–360.

9. **Meyer JR**, **Dobias DT**, **Weitz JS**, **Barrick JE**, **Quick RT**, **Lenski RE**. 2012. Repeatability and contingency in the evolution of a key innovation in phage Lambda. Science **335**:428–432.

10. **Burmeister AR**, **Lenski RE**, **Meyer JR**. 2016. Host coevolution alters the adaptive landscape of a virus. Proceedings of the Royal Society B: Biological Sciences **283**:20161528.

11. **Davies EV**, **James CE**, **Williams D**, **O'Brien S**, **Fothergill JL**, **Haldenby S**, **Paterson S**, **Winstanley C**, **Brockhurst MA**. 2016. Temperate phages both mediate and drive adaptive evolution in pathogen biofilms. Proc Natl Acad Sci USA **113**:8266–8271.

12. **Luria SE**, **Human ML**. 1952. A nonhereditary, host-induced variation of bacterial viruses. Journal of Bacteriology **64**:557–569.

13. **Barrangou R**, **Fremaux C**, **Deveau H**, **Richards M**, **Boyaval P**, **Moineau S**, **Romero DA**, **Horvath P**. 2007. CRISPR provides acquired resistance against

viruses in prokaryotes. Science **315**:1709–1712.

14. **Holt RD**. 1977. Predation, apparent competition, and the structure of prey communities. Theor Popul Biol **12**:197–129.

15. **Dennehy JJ**, **Friedenberg NA**, **Yang YW**, **Turner PE**. 2007. Virus population extinction via ecological traps. Ecol Lett **10**:230–240.

16. **Ostfeld RS**, **Keesing F**. 2000. Biodiversity and disease risk: the case of Lyme disease. Conservation Biology **14**:722–728.

17. **Hall SR**, **Becker CR**, **Simonis JL**, **Duffy MA**, **Tessier AJ**, **Cáceres CE**. 2009. Friendly competition: evidence for a dilution effect among competitors in a planktonic host-parasite system. Ecology **90**:791–801.

18. **Grover JP**. 1995. Competition, herbivory, and enrichment: nutrient-based models for edible and inedible plants. American Naturalist **145**:746–774.

19. **Keesing F**, **Holt RD**, **Ostfeld RS**. 2006. Effects of species diversity on disease risk. Ecology Letters **9**:485–498.

20. **Wood CL**, **Lafferty KD**, **DeLeo G**, **Young HS**, **Hudson PJ**, **Kuris AM**. 2014. Does biodiversity protect humans against infectious disease? Ecology **95**:817–832.

21. **Johnson PTJ**, **Hartson RB**, **Larson DJ**, **Sutherland DR**. 2008. Diversity and disease: community structure drives parasite transmission and host fitness. Ecology Letters **11**:1017–1026.

22. **Searle CL**, **Biga LM**, **Spatafora JW**, **Blaustein AR**. 2011. A dilution effect in the emerging amphibian pathogen *Batrachochytrium dendrobatidis*. Proc Natl Acad Sci USA **108**:16322–16326.

23. **Orlofske SA**, **Jadin RC**, **Preston DL**, **Johnson PTJ**. 2012. Parasite transmission in complex communities: predators and alternative hosts alter pathogenic infections in amphibians. Ecology **93**:1247–1253.

24. **Venesky MD**, **Liu X**, **Sauer EL**, **Rohr JR**. 2013. Linking manipulative experiments to field data to test the dilution effect. Journal of Animal Ecology **83**:557–565.

25. **Johnson PT**, **Preston DL**, **Hoverman JT**, **LaFonte BE**. 2013. Host and parasite diversity jointly control disease risk in complex communities. Proc Natl Acad Sci USA **110**:16916–16921.

26. **Dargent F**, **Torres-Dowdall J**, **Scott ME**, **Ramnarine I**, **Fussmann GF**. 2013. Can mixed-species groups reduce individual parasite load? A field test with two closely related poeciliid fishes (*Poecilia reticulata* and *Poecilia picta*). PLOS One **8**:e56789.

27. **King KC**, **Auld SKJR**, **Wilson PJ**, **James J**, **Little TJ**. 2012. The bacterial parasite *Pasteuria ramosais* not killed if it fails to infect: implications for coevolution. Ecol Evol **3**:197–203.

CHAPTER 4:

HOST COEVOLUTION ALTERS THE ADAPTIVE LANDSCAPE OF A VIRUS

Authors: Alita R. Burmeister, Richard E. Lenski, and Justin R. Meyer

This chapter was originally published in Proceedings of the Royal Society B: Biological Sciences, Burmeister AR, Lenski RE, Meyer JR. 283:20161528.

Abstract

The origin of new and complex structures and functions is fundamental for shaping the diversity of life. Such key innovations are rare because they require multiple interacting changes. We sought to understand how the adaptive landscape led to an innovation whereby bacteriophage λ evolved the new ability to exploit a receptor, OmpF, on *Escherichia coli* cells. Previous work showed that this ability evolved repeatedly, despite requiring four mutations in one virus gene. Here we examine how this innovation evolved by studying six intermediate genotypes of λ isolated during independent transitions to exploit OmpF and comparing them to their ancestor. All six intermediates showed large increases in their adsorption rates on the ancestral host. Improvements in adsorption were offset, in large part, by the evolution of host resistance, which occurred by reduced expression of LamB, the usual receptor for λ. As a consequence of host coevolution, the adaptive landscape of the virus changed such that selection favoring four of the six virus intermediates became stronger after the host evolved resistance, thereby accelerating virus populations along the path to using the new OmpF receptor. This dependency of viral fitness on host genotype thus shows an important role for coevolution in the origin of the new viral function.

Introduction

The diversity of complex structures and functions in the living world is striking. However, a detailed understanding of how species evolve key innovations is difficult because of limitations of both theory and data (1). One challenge is to understand how populations evolve traits that require multiple interacting changes, such as specific deformations in the reactive pocket of an enzyme (2) or the specialized modifications of an appendage (3). If each intermediate genotype leading to the new function is more fit than its immediate predecessor, then the new function can evolve readily, even if the fitness benefits do not accrue from the new function *per se* (4). By contrast, the evolution of a new function will be slower and more difficult – although not impossible (5) – if any of the requisite intermediates have lower fitness than their progenitors.

Evolution experiments provide a powerful way to study how mutations and the environment together can lead to key innovations. For example, the evolution of the new ability of *Escherichia coli* to consume citrate in an experimental population depended on its history, including the appearance of earlier potentiating mutations, as well as on the selective environment (6, 7). Experimental manipulation of environmental conditions can also provide information on factors involved in the evolution of novel functions. For example, Bono *et al*. showed that increasing competition led a virus to evolve the ability to infect a new host (8). In another study on viruses, Herfst *et al.* found that the genetic background of influenza influenced whether viral populations evolved the ability to spread via airborne transmission (9). Although genetic and environmental manipulations can reveal factors important for the evolution of new traits, the selective pressures that favor intermediate genotypes often remain elusive. One limitation to the study of innovations,

even in the laboratory, is their rare occurrence; therefore, having parallel histories leading to the same innovation would increase one's ability to analyze how and why new traits evolve. In the ideal scenario, the selective benefit or cost for each intermediate mutation along multiple independent paths leading to the same innovation could be described quantitatively, in terms of the resulting fitness, and qualitatively in terms of the phenotypic traits responsible. In this study, we use this framework to describe how replicate populations of the virus bacteriophage λ evolved a key innovation in parallel, and we specifically investigate how the host's coevolution changed the adaptive landscape for the virus, sometimes potentiating the key innovation.

Meyer *et al.* (10) previously reported the parallel evolution of a new function while studying populations of bacteriophage λ in the laboratory. They found that λ sometimes evolved to target a new receptor on the surface of its host, the bacterium *E. coli*, with the innovation occurring in 24 of 96 replicate populations. They further showed that these parallel innovations involved a common set of four mutations in the phage's host-specificity gene. The ancestral phage λ adsorbs to and infects through a porin protein called LamB; the evolved phage that acquired the key innovation can also use another porin called OmpF. This new function had not previously been observed, despite decades of intensive study of λ by virologists and molecular biologists. One reason this new function had not previously been observed was that it required four mutations in the *J* gene (10). *J* encodes the tail protein, J, which λ uses to recognize and attach to LamB receptor proteins on the surface of the host cell. Importantly, none of the phage genotypes examined by Meyer *et al.* (10) that had just three of the four required mutations had any capacity whatsoever to infect hosts that expressed only the OmpF receptor. It would be extremely unlikely to detect

a function that required four simultaneous mutations using traditional microbiological methods. However, Meyer *et al.* (10) observed the mutations accumulate over time as the phage and bacteria coevolved. In fact, the new function emerged repeatedly and quickly, arising in 24 of 96 populations after only 12 days on average. Here, we address the question as to how the phages evolved this new function, and so quickly, if the intermediate genotypes did not confer any ability to exploit the alternative receptor.

One compelling hint is the highly non-random pattern of substitutions observed among the independently derived *J* alleles. In particular, all of the phage that could infect through the OmpF receptor had mutations in four narrow regions of the *J* gene (10). We know that the four mutations did not arise simultaneously because alleles with subsets of these mutations were sampled at earlier time points (10). The genetic parallelism evident in the intermediate states strongly suggested that natural selection favored the intermediate *J* alleles, even though they did not allow the phage to use the OmpF receptor. Meyer *et al.* (10) also observed that the phage mutations accumulated while the hosts were evolving substantial, but not complete, resistance through reduced expression of the LamB receptor. This synchrony suggested that the reduction in the density of the LamB receptor increased the strength of selection on λ to improve its binding to LamB, thereby favoring certain mutations in *J* that, fortuitously, served as stepping stones on the way to the new capacity to use the OmpF receptor. Under this scenario, the arms race between the coevolving hosts and parasites changed the fitness landscape for the phage populations, thereby opening new – and uphill – paths to the innovation (11). Taken together, these observations and hypotheses lead to the predictions that we test here.

First, we test whether antagonistic coevolution caused alternate steps that increased host fitness at the expense of parasite fitness and vice versa (12). For the coevolved λ and *E. coli*, we expect adsorption rates to change with the phages' and hosts' coevolutionary steps. More specifically, we predict that: (i) the ancestor phage should adsorb faster to the ancestral cells than to the coevolved cells; (ii) the evolved phages should adsorb faster to the ancestral cells than to the coevolved cells; (iii) the evolved phages should adsorb faster than the ancestor phage to the ancestral cells; and (iv) the evolved phages should adsorb faster than the ancestor phage to the coevolved cells.

Second, we test the hypothesis that the coevolutionary arms race changed the phage's adaptive landscape, opening new and uphill paths to the key innovation. That is, we predict that the evolved intermediate phage genotypes should have a fitness advantage over the ancestral phage. More specifically, these intermediates should possess a greater advantage when competing for coevolved host cells than when competing for ancestral hosts; in the most extreme case, the intermediate phage types might have an advantage only on the coevolved host cells.

To test these two sets of predictions, we measured the adsorption rates of six independently evolved phage λ intermediates. We also measured the fitness of each intermediate in competition with the ancestral phage. To examine the effects of host coevolution, we conducted all of the assays using both the ancestral sensitive *E. coli* cells and resistant coevolved cells. The resulting data generate the phage genotype-by-host (GxH) reaction norm for phage fitness.

Materials and methods

Overview: In the coevolution experiments performed by Meyer *et al.* (10), strictly lytic phage λ strain cI26 and *E. coli* B strain REL606 (Table A4.1) were propagated together in 96 replicate communities by transferring 0.1 ml from each 10-ml culture into a new flask containing 9.9 ml of fresh medium every day for 20 days. Whenever possible, we performed our assays under the same conditions as those used in that earlier study; however, as discussed below, we sometimes had to alter certain conditions in order to obtain reliable measurements. Before each transfer, a separate 0.2-ml mixed-population sample (i.e., with phage and host together) was frozen; these samples provide viable representatives of the λ and *E. coli* populations that were used to understand their evolution. Meyer *et al.* found that the first mutations to reach high frequency in the bacterial populations were in *malT*, which encodes a positive regulator of *lamB*, which in turn encodes the native phage receptor protein LamB. These mutations reduced expression of LamB, thereby conferring substantial (but not complete) host resistance to the ancestral phage, and they reached near-fixation in all host populations by day 8 of the experiment. Also, one-quarter (24/96) of the phage populations evolved the new ability to infect the bacteria through the OmpF protein, which took 12 days on average (range: 9-18 days).

To study the adsorption rate and competitive fitness of the intermediate λ genotypes, we sampled a single phage isolate from six independently evolved populations exactly four days before the ability to use OmpF was first observed in that population; we confirmed that none of these phages had the ability to infect through OmpF. We chose the six populations haphazardly, except that we paid attention to choosing phage from replicates that had evolved distinct *J* alleles by the end of the original experiment. We sequenced the

J genes of the six intermediate genotypes to check that they had some, but not all, of the four mutations needed to exploit OmpF.

We measured phage adsorption rates because the J protein physically interacts with host receptors to initiate infections and mutations in the *J* gene affect adsorption to the host's LamB receptors (13, 14). Thus, changes in the adsorption rate would help elucidate the mechanism of phage adaptation. We also directly assayed relative fitness in a manner similar to that used in studies of *E. coli* evolution (15), where evolved genotypes compete head-to-head against a genetically marked ancestor. We performed all adsorption rate and fitness assays in two environments that differed only in the identity of the bacterial host. One environment used the sensitive ancestral host, REL606; the other used a partially resistant evolved strain, EcC4, that has a point mutation in *malT,* which generates a premature stop codon in the gene at amino-acid position 295.

Culture conditions: All *E. coli* cultures were inoculated from freezer stocks into Luria-Bertani (LB) broth (16), then grown overnight at 37°C while shaking at 120 rpm. Host cells were preconditioned for the phage competition experiments by growing them in the same medium and other conditions used in the coevolution experiments performed by Meyer *et al.* (10): 10 ml of modified M9 (M9 salts with 1 g/L magnesium sulfate, 1 g/L glucose, and 0.02% LB) for 24 h at 37°C and 120 rpm. Phage strains were isolated by plating diluted frozen samples on a lawn of REL606 cells suspended in soft agar (LB with 0.8% *w/v* agar) and spread on the surface of an LB plate (LB broth with 1.6% *w/v* agar). We then picked an individual plaque (a small clearing in the host lawn caused by the phage population expansion from a single infection) for each phage strain of interest. These isolates were immediately re-suspended in soft agar and the plaque-picking procedure was repeated to

ensure that only a single phage genotype was sampled. Next, the phage stocks were grown on ~10^8 cells of REL606 for ~16 h in the same modified M9 medium and other conditions as above. The phage were then harvested by chloroform preparation (17) and stored at 4°C. Samples of each isolated phage were also preserved at -80°C in 15% *v/v* glycerol.

Sequencing the J gene: We sequenced the *J* gene (host specificity gene, GenBank: NP_040600) from all six λ intermediates; previous work showed that the mutations responsible for the ability to use OmpF were in this gene (10). The sequences were obtained by the Michigan State University Research Technology Support Facility using an ABI 3730xl Sanger sequencing platform. PCR-amplified fragments of the *J* gene were sequenced after column-purification with the GE Illustra GFX kit; Table A4.1 shows the primers used for amplification and sequencing. Point mutations were automatically scored using the DNASTAR SeqMan SNP analysis tool and then manually confirmed.

Sequencing the cI gene: Phage λ cI26, the ancestral virus in this study, has a 1-bp deletion in *cI* (repressor gene, GenBank: NP_0040628.1), causing a frame shift that makes it obligately lytic. We sequenced the *cI* gene using the same general methods as for the *J* gene and the specific primers shown in Table A4.1.

Adsorption assays: We used a modified version of the 96-well filter plate method described by Shao and Wang (18) while keeping other conditions as close as feasible to the Meyer *et al.* (10) evolution experiment. In preliminary experiments, we found that measuring adsorption rates in these conditions required long periods, such that phage replication confounded the measurements. Therefore, we added chloramphenicol to inhibit cell growth and thereby prevent phage replication. We diluted each phage stock to 2 x 10^5 plaque-forming units per ml in modified M9, added 10 µl of a solution containing 15 µg/ml

chloramphenicol in ethanol, and then put 550 µl of each resulting phage mixture into one well of a ClavePak Racked Tubes block (Denville Scientific #B1251-S) for every replicate assay. The ClavePak block was then incubated for 20 min at 37°C and 120 rpm. Immediately before adding host cells (designated as T_0), we transferred 100 µl to a 96-well filter plate (Pall #8019) that was centrifuged for 2 min at 2000 rpm. Fifty µl of each host type or blank cell-free medium was then added to each well, the contents were gently mixed by pipetting, and the plate was incubated at 37°C and 120 rpm. The resulting phage concentration during the assay was 1.8×10^5 plaque-forming units per ml, and the host cell density was 8.6×10^7 colony-forming units per ml for each host type. After 67 min, we sampled and processed 100 µl from each well using the same procedures as at T_0. The background decay rate of each phage genotype was estimated as the rate at which free phage declined when the blank cell-free medium was added instead of host cells. The phage adsorption rate was estimated as the rate at which phage disappeared after subtracting the background decay rate, and then dividing by the density of cells during the adsorption-rate assay. The mean background decay rate was 0.29 h^{-1} (Fig. A4.1). This value is greater than one previously reported for phage λ (19), which may reflect different assay conditions, the specific phage genotypes tested, or both.

Phage fitness assays: We performed phage fitness assays by direct competitions between each of the six evolved λ isolates and a genetically marked ancestor phage that can be differentiated when grown on a lawn of *E. coli* cells. Some aspects of the assays had to be refined before reliable estimates could be obtained, as discussed in the Appendix. Here we provide the methods used in the final approach and some background on protocol development.

First, we modified the ancestral λ strain to make blue plaques on a lawn of *lacZα*$^{-}$ *E. coli* (strain DH5α) supplemented with X-gal (5-bromo-4-chloro-3-indolyl-β-D-galactopyranoside). When *E. coli* cells metabolize X-gal, they produce a blue compound; however, cells without a functional *lacZα* gene cannot metabolize X-gal. By inserting a functional *lacZα* gene into the phage genome, the phage complements the cell's capacity to metabolize X-gal and generates a blue spot where a plaque forms. To construct a marked version of phage λ strain cI26, we infected *E. coli* cells that contained a plasmid encoding the phage *R* gene fused to *lacZα* (18, 20). Phage λ has an efficient system for homologous recombination (21), allowing some of the resulting genomes to recombine with the *R-lacZα* fusion. The phage progeny were then plated on a lawn of DH5α hosts in the presence of X-gal, and a single blue plaque was chosen. Upon studying this marked strain, we found that the marker was not neutral but instead reduced phage fitness. To quantify the marker's fitness cost, we computed the mean ± 95% confidence intervals of the selection rate against the marker across several blocks of experiments on each host (ancestral host REL606: 0.120 h^{-1} ± 0.019 based on six blocks; evolved host EcC4: 0.039 h^{-1} ± 0.017 based on four blocks). The marker effect varied by host ($F_{1, 54} = 46.4$, $p < 0.001$) but not by block ($F_{5, 54} = 1.395$, $p = 0.241$), which we account for as described below in the sections on Statistical Analyses and Results. A fitness cost was also reported for this marker in a related λ strain when phage competed for *E. coli* K12 hosts (18).

The phage fitness assays were run in the same medium and other conditions as used in the coevolution experiments performed by Meyer *et al.* (10). For each of the six phage isolates tested, we grew one stock culture under the conditions described above. We used aliquots from that stock culture to run replicate assays on both the ancestral (REL606) and

evolved (EcC4) hosts. Competitions were done in sets of eight assays per host, except for phage B2, which was run with four assays per host; procedural errors led to occasional missing values. The assays were blocked such that all replicates for one phage genotype were assayed on both hosts on the same day. To initiate a competition, we added ~10^8 *E. coli* cells (REL606 or EcC4) acclimated to the culture conditions, ~10^5 of the marked ancestral phage λ_{lacZ}, and ~10^5 of a particular evolved λ genotype to each flask. The host density was chosen to match the start of the coevolution experiments performed by Meyer *et al.* (10); however, phage densities were almost 10-fold lower because we could not produce dense stocks of the evolved types, despite several attempts. (The lower density should reduce competition between the phage genotypes and thereby diminish our ability to detect fitness differences. Nonetheless, we measured significant fitness gains for the evolved phage, as shown in the Results.) The mixed cultures were incubated for 8 h, and the phage were sampled and enumerated at the beginning and end of that period. We chose a duration of 8 h for two reasons: (i) given the large fitness advantages of the evolved genotypes, they would drive the ancestral phage to very low relative frequency if the assays ran for 24 h (the period between transfers during the original evolution experiment), thereby compromising our ability to quantify the fitness difference; and (ii) resistant host mutants often arose and reached substantial frequency in 24 h, thereby altering the competitive environment of the phage. We discuss these time constraints more fully in the Appendix. Phage samples were diluted in TM (50 mM tris hydrochloride, pH 7.5 and 8 mM magnesium sulfate), and multiple dilutions were plated to find one where individual plaques could be counted. Plates used to count the phage contained DH5α host cells and

9.5 mg/ml X-gal in the top agar, and they were incubated at 37°C for two days to allow the blue plaques to develop full pigmentation.

We calculated fitness for the phage using the difference, not the ratio, of the two competitors' realized growth rates during the competition assay. This quantity, sometimes called the selection rate *r*, is related to, but distinct from, the more familiar ratio of the competitors' growth rates (i.e., relative fitness *W*). We used the difference here because it is more robust to large differences in growth rates between competitors, including those cases where one competitor declines and the other increases in abundance (22, 23), which we sometimes observed.

Statistical analyses: We tested the following four predictions based on the adsorption-rate assays: (i) the ancestor phage adsorbs faster to the ancestral cells, REL606, than to the coevolved cells, EcC4; (ii) the evolved phages adsorb faster to the ancestral cells than to the coevolved cells; (iii) the evolved phages adsorb faster than the ancestor phage to the ancestral cells; and (iv) the evolved phages adsorb faster than the ancestor phage to the coevolved cells. Given the predicted directional effects, we used one-tailed *t*-tests of the associated hypotheses.

For the competitive fitness assays, we expected the fitness of the evolved phage (expressed as a selection rate differential relative to the marked ancestral phage) to be greater on the coevolved host cells than on the ancestral cells. We also expected the realized growth rates of the evolved phage to be lower on the coevolved cells than on the ancestral cells. Therefore, we employed one-tailed *t*-tests of these hypotheses. (In those cases where the outcome was opposite to our expectation, we report the p-value as >0.5.) We tested

each hypothesis for six evolved phage genotypes, and so we performed Bonferroni corrections for multiple comparisons, resulting in an adjusted $\alpha = 0.05/6 = 0.0083$ per test.

We performed a two-way ANOVA to determine the effect of assay date (block) and host type (coevolved versus ancestral) on the fitness cost of the phage's *lacZα* marker. This analysis showed that the *lacZα* marker imposed a greater cost when competing for the ancestral cells than for the coevolved cells. Therefore, we also asked whether correcting for this effect would alter our interpretation of the differences in phage fitness on the two host types; the correction was a simple subtraction of the grand mean of the difference in the fitness cost of the marker between the two hosts. In fact, this correction did not affect our interpretation (Table A4.2).

All analyses were performed in R version 3.1.1 (24) using custom scripts.

Results and Discussion

Mutations in the J and cI genes of the evolved phage intermediates: The six independently derived λ genotypes that we studied had different subsets of the four *J* mutations needed to exploit the OmpF receptor (Table 4.1), indicating that they were intermediates; that is, each phage had some, but not all, of the mutations associated with that new function. In addition, all six phages had one or more other mutations in the *J* gene that were not required to use OmpF (Table 4.1).

Table 4.1. Mutations in the *J* gene of the evolved phage λ isolates in this study. Each virus was sampled from a different source population four days before phage that could use the OmpF receptor were first detected. Each mutation is identified by its ancestral DNA base, its position in the *J* gene, and the evolved base. Asterisks under "Line of Descent" indicate a mutation was present in the later phage able to use OmpF. Meyer et al. (10) found that phage λ requires four mutations—one or more in four specific regions of *J* to use OmpF: (A) one or more mutations between positions 2969 and 2999, (B) a mutation at 3320 or 3321, (C) the specific mutation G3319A, and (D) the specific mutation A3034G. The last column shows which, if any, of these categories each mutation satisfies.

Source Population	Day of Isolation	Set of *J* Mutations	Line of Descent	OmpF Category
A12	10	C599T	*	
		G2921A		
		T2991G	*	A
		C3033T		
		C3147A		
		T3380C	*	
A7	10	A2989G	*	A
		C2999T	*	A
		C3119T	*	
		G3319A	*	B
B2	13	C2969T	*	A
		C3119T	*	
		G3319A	*	B
D9	8	C2879T	*	
		T2991G	*	A
		C3119T	*	
		G3319A	*	B
E4	13	C2969T		A
		C3119T	*	
		G3319A	*	B
G9	11	A1747G	*	
		A2989G	*	A
		C2999T	*	A
		C3119T	*	
		G3319A	*	B

In four cases (A7, B2, D9, and G9), the additional mutations were also present in the eventual $OmpF^+$ phage (i.e., the phage with the new ability to use the OmpF receptor), indicating that these genotypes were on the evolutionary line of descent leading to that innovation. In two cases (A12 and E4), the other mutations were not present in the later

OmpF$^+$ isolates, implying that these genotypes were somewhat off the direct line of descent leading to the OmpF$^+$ phage. We also sequenced the *cI* repressor gene to ensure that the evolved phages did not contain *cI* reversions, which would allow them to undergo lysogeny and replicate while integrated into the host chromosome. Five of the evolved phages had no new mutations in that gene. Phage A12 had a point mutation (G170A) in the out-of-frame portion of the gene, where it should not affect the potential for lysogeny.

Phage evolution increases and host coevolution reduces adsorption rates: Phage λ uses its J protein to adsorb to the LamB receptors on the surface of host cells (25), and the mutations that distinguish the intermediate phage genotypes from their ancestor are in the gene that encodes that protein. Therefore, we hypothesize that adaptive evolution of the phage populations led to increased rates of adsorption to LamB prior to the emergence of the ability to exploit the alternative OmpF receptor, which would explain why the intermediates evolved even before they had acquired that new ability.

To understand how the mutations in the phage's *J* gene and in the host's *malT* gene affected their interaction, we quantified the rate at which the ancestor and evolved intermediate phage genotypes adsorbed to both the ancestor and coevolved hosts (Fig. 4.1). The evolved intermediate phages as a group had higher adsorption rates than the ancestor phage on both the ancestral host (paired *t*-test, $t_s = 18.893$, d.f. = 5, $p < 0.001$) and coevolved host (paired *t*-test, $t_s = 1.837$, d.f. = 5, $p = 0.063$), although the latter difference was only marginally significant. Also as expected, the evolved intermediate phages had significantly lower adsorption rates on the coevolved host than on the ancestral host (paired *t*-test, $t_s = 21.895$, d.f. = 5, $p < 0.001$). These results indicate that the parasite and host populations engaged in a coevolutionary tug-of-war over the rate at which the parasites

adsorb to and infect host cells. Mutations that increase the adsorption rate benefit the phage, and mutations that decrease the adsorption rate benefit the host. (We note that for some phage λ strains, the adsorption rate is influenced by a second gene, *stf*, that affects so-called side-tail fibers (26). However, the phage strain that we used, cI26, is stf^- and lacks side-tail fibers. The cI26 genotype was generated by a 5,996-bp deletion that includes the last 235 bp of the *stf* gene (10), so reversion to the stf^+ allele is not possible.)

These results indicate that the adsorption rate was under strong selection during the experimental evolution of the phage λ populations. However, we were unable to resolve a difference in adsorption rates for the ancestral phage between the two hosts, because those rates were so low that they were at or even below our limit of detection. (In fact, the observed difference was opposite in direction to our hypothesis, and so the result of the *t*-test is $p > 0.5$). This low resolution is similar to previous attempts to quantify the adsorption rate of stf^- phage λ to sensitive *E. coli* cells in a similar glucose environment, whereas phage λ adsorbs quite rapidly to cells grown on maltose, which induces LamB expression (18, 26). Under the glucose conditions used in our assays, the expression of LamB protein is under catabolite repression; these phage receptors are therefore scarce, and the absence of phage side-tail fibers also reduces the phage's adsorption rate. We observe that on the coevolved host, where LamB expression is further reduced by the host's *malT* mutation, adsorption is even more difficult to detect. Despite this limitation, our results demonstrate that all six evolved phage λ substantially improved their rate of adsorption to the scarce LamB molecules found on both the ancestral and coevolved hosts in the glucose environment (Fig. 4.1).

Figure 4.1. Virus and host coevolution alters adsorption rates. The evolved phages (A12, A7, B2, D9, E4, and G9), as a group, have increased adsorption rates relative to their ancestor (cI26) on both host types (see text for statistical analyses). The coevolved host lowers the adsorption rates of the evolved phages relative to the ancestral host. No difference between the two hosts was detected for the ancestral phage; however, a difference was evident based on the growth rates of that phage. N = 4 for each evolved phage-host combination and N = 24 for each ancestor phage-host combination. Error bars are 95% confidence intervals.

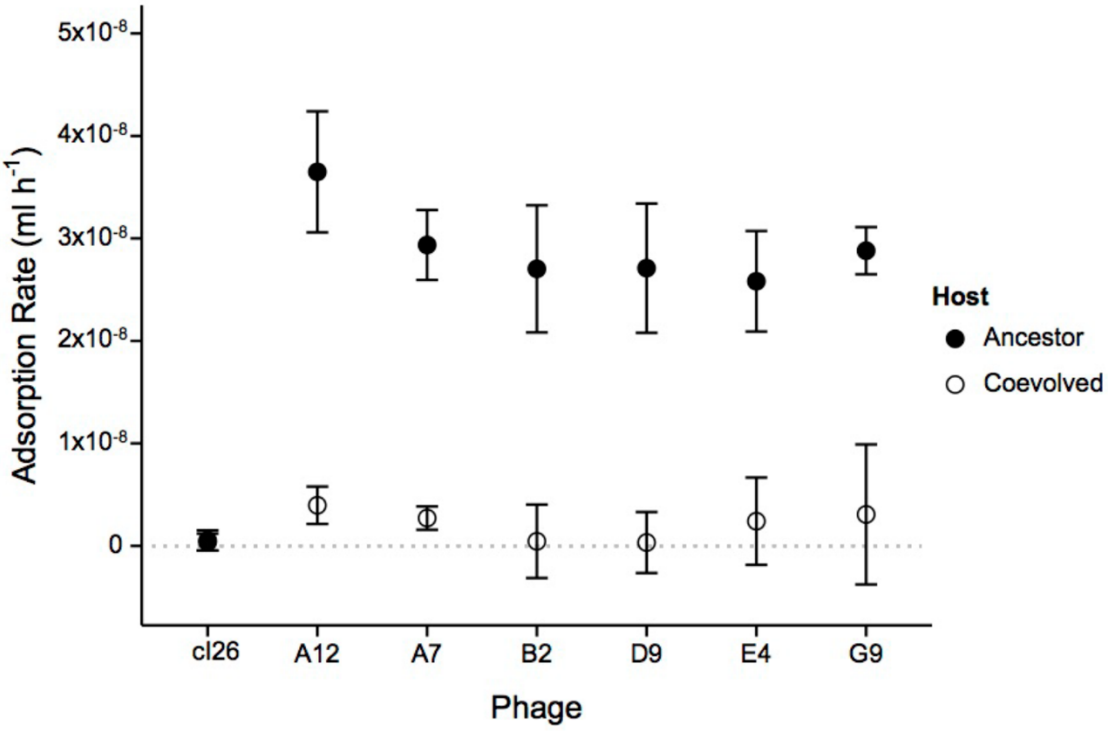

Mutations increase population growth rates of the intermediate phage genotypes: Selection has clearly favored increased adsorption rate in the phage populations, but these improvements could, in principle, have harmful pleiotropic effects on other phage traits. Therefore, to quantify the full effect of the *J* alleles on phage fitness, we calculated the population growth rates of the ancestral and same six evolved phages during direct competitions for both the ancestral and coevolved hosts. If competition for LamB receptors drove the evolution of the *J* gene, then we also expect the evolved phages, with their faster adsorption rates, to initiate infections more quickly and

have increased population growth rates and higher relative fitness. By performing the competitions on both cell types, we can also see how the host's coevolution affected selection on the phage.

All six evolved intermediate phage genotypes grew faster than their ancestor (Fig. 4.2A, solid versus dotted lines) during competitions for the ancestral host, the coevolved host, or both. Five of the six evolved phages (all except G9) grew more slowly on the coevolved *malT*$^{-}$ host than on the ancestral host. The ancestral phage population grew measurably on the ancestral host (despite the low adsorption rate discussed above), even in the presence of the evolved phage genotypes, but it did not grow to any measurable extent on the coevolved host during the competitions.

Figure 4.2. Effects of coevolution on the growth rates and fitness of phage λ. **Panel A:** Realized growth rates of ancestral (dashed lines) and evolved phage (solid lines) during direct competition for the ancestral and coevolved *E. coli* hosts. Phage genotypes A12, A7, B2, D9, and E4 grew faster on the ancestral than the evolved host (one-tailed *t*-tests, $p < 0.05$ after Bonferroni correction); G9 appeared to grow faster on the coevolved host, contrary to our expectation. **Panel B:** Selection rates, which provide a measure of the fitness of an evolved phage relative to the ancestral phage, on the ancestral and coevolved hosts. Selection rates are calculated as the difference in the growth rates of the evolved and ancestral phage using the data shown in Panel A. Four of the six evolved phage (A12, A7, D9, and G9) were significantly more fit than their ancestor on the ancestral host; all six were significantly more fit than their ancestor on the coevolved host. Also, four phage (A12, B2, E4, and G9) had significantly higher selection rates on the coevolved host than on the ancestral host (Table A4.2). The genetic marker used to distinguish phage competitors imposed a small fitness cost on the phage, and that cost differed between the two hosts; the black dashed lines show the 95% confidence intervals for the selection rate when the unmarked and marked ancestral phages competed.

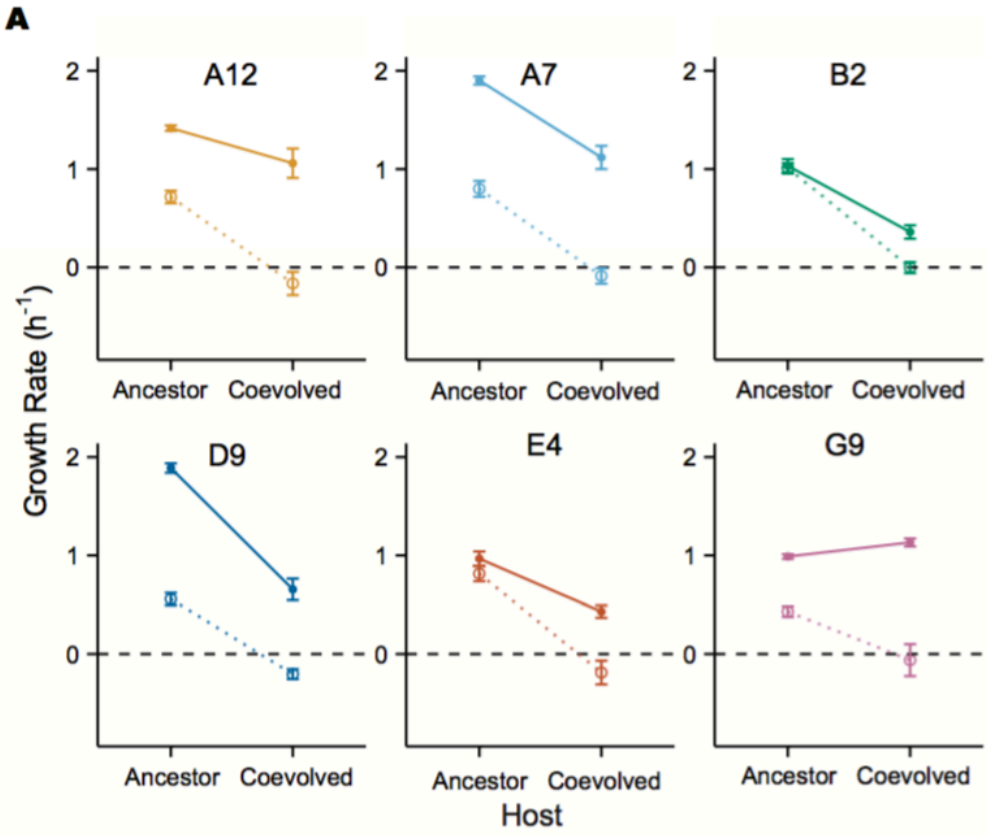

Figure 4.2 (cont'd)

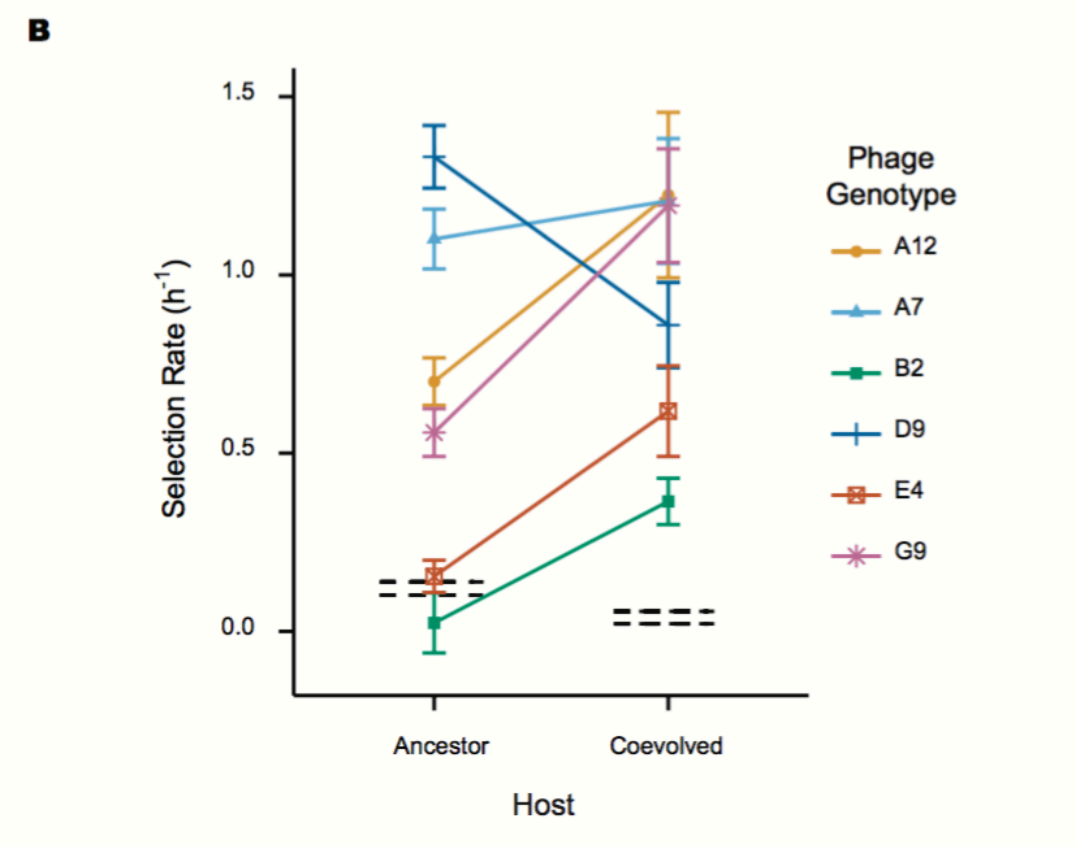

Mutations improve relative fitness of the intermediate phage genotypes: The competitions between the evolved and ancestral phage genotypes allow us not only to calculate growth rates but also to quantify their relative fitness. As noted in the Methods, we express relative fitness using selection rates calculated as the *difference* in realized growth rates of the evolved and ancestral phage, rather than as the *ratio* of their growth rates. We do so because the ancestral phage grows so poorly, if at all, on the coevolved host (Fig. 4.2A) that the ratio becomes noisy and even pathological (e.g., producing a negative value). The difference in growth rates, by contrast, is no more sensitive to errors in measuring the ancestor phage's growth rate than it is to errors in measuring the evolved genotype's growth rate.

By considering the growth rates of the evolved intermediate and ancestral phages together, we can assess whether the host evolution at the *malT* locus increased or reduced the strength of selection for the phage intermediates. Such data, in turn, offer insights into whether the host's coevolution promoted or impeded the evolution of the phage's ability to use the alternative OmpF receptor. Four of the six evolved intermediate phage genotypes (A12, A7, D9, and G9) were significantly more fit than their common ancestor on the ancestral host cells (Fig. 4.2B, Ancestor Host). All six evolved phage types were more fit than their ancestor when competing for the coevolved host cells (Fig. 4.2B, Coevolved Host). These data demonstrate that all six of the independently evolved phage genotypes had selective advantages, even *before* their descendants had gained the ability to use the OmpF receptor. Such benefits were previously hypothesized because, without them, it was difficult to understand how the first few mutations required for phage λ to evolve the ability to exploit the OmpF receptor had accumulated so quickly and repeatedly across many replicate populations (10). Our results show that at least some of the intermediate steps that led to this new function increased the phage's adsorption rate and relative fitness. These mutations were thus favored by selection, which helps to explain how the phage quickly and repeatedly achieved their innovation.

Host coevolution alters the adaptive landscape for the phage: In addition to showing that the intermediate phage genotypes were favored by selection, the competition assays also reveal a parasite genotype by host genotype interaction. That is, the fitness of most of the tested phage genotypes (all except A7) relative to their ancestor depends significantly on the host genotype (Fig. 4.2B).

In four cases (A12, B2, E4, and G9) the selective advantages of the evolved phages were significantly greater during competition for the coevolved host cells (Fig. 4.2B). Selection

favoring the evolved phage types was stronger on the coevolved host genotype despite the fact that phage growth was significantly slower on that host in three of these four cases (all except G9: Fig. 4.2A). Thus, in these four cases, host coevolution accelerated the evolution of phage lineages that were on the path leading to the new ability to use the OmpF receptor (Fig. 4.2B). By contrast, evolved phage D9 had a significantly greater advantage on the ancestral host, and phage A7 was approximately equally fit on the ancestral and coevolved hosts (Fig. 4.2B).

Taken together, our results reveal important similarities and substantial variation among the six intermediate phage types examined here. Most importantly, and consistent with the general hypothesis that the intermediates reached high frequencies because the mutations they carried conferred selective advantages, all six phage were significantly more fit than their ancestor when competing for the ancestral host, the coevolved host, or both. The results also tend to support, though not in every case, the specific hypothesis that *host* coevolution pushed the evolving phage populations along paths that accelerated the rise of the intermediate types and hence the subsequent emergence of phage with the novel ability to exploit the OmpF receptor. This latter trend is consistent with theory that predicts coevolution can drive innovation by altering the shape of fitness landscapes in ways that favor new phenotypes (27-29).

Several other studies also support the hypothesis that coevolution can promote innovation. Populations of phage ϕ2 explored genomic space more broadly when they adapted to coevolving hosts than when they adapted to a static host (30). When phage M1 was sequentially presented with hosts expressing potential receptors that were increasingly different from its usual receptor, the phage evolved the ability to use a protein not

previously known to have that capacity (31). Also, experiments with digital hosts and parasites, analogous in some respects to bacteria and phage, showed that coevolution generated negative frequency-dependent selection, which deformed fitness landscapes in ways that favored the evolution of new, more complex traits (32). Together with these studies, our results show that the adaptive landscape of a virus or other parasite can be reshaped by the coevolution of its hosts.

Relationships between adsorption, growth, and selection rates: In general, the increased adsorption rates of the evolved phages (Fig. 4.1) resulted in faster population growth (Fig. 4.2A) and higher fitness (Fig. 4.2B) relative to the ancestral phage on one or both host genotypes. However, there are some apparent discrepancies between the various performance measures. The most striking cases are B2 and E4; both have much higher adsorption rates than their ancestor on the ancestral host, but they have little or no growth or fitness advantage on that host. There are several potential explanations for these differences. First, there could be tradeoffs between adsorption rate and other phage life-history traits (19, 33). For example, some mutations might cause phage particles to be less stable and decay more rapidly. We measured decay rates in cell-free media in assays performed alongside the adsorption-rate assays, subtracting the decay rate from the overall rate of phage loss in the presence of host cells, and then dividing by the host-cell density, to obtain the adsorption rates reported in Figure 4.1. The decay rates were generally small (more than an order of magnitude lower than the overall rate of phage loss by adsorption to the ancestral host for the six evolved phage), and there were no large differences among the phage genotypes in their decay rates (Fig. A4.1). However, decay rates might also depend on the density of receptors in the cell debris that is generated as phage replicate and

lyse their hosts, which would not be reflected in decay rates measured in cell-free media. Second, trophic interactions, including those between phage and bacteria, can generate feedbacks that may complicate interpretation of the dynamics. For example, a faster-growing phage population kills more host cells, which would otherwise replicate and provide more prey, than does a slower-growing phage population. Third, the competition protocol might produce some complications. In particular, using the *lacZ* marker system for the phage required removal of the host cells (which are $lacZ^{+}$) from the samples prior to counting the phage competitors. (If the cells were not removed, they would form a blue lawn on the plates, preventing differentiation of the evolved and marked ancestral phage.) The removal of host cells also removes phages that have initiated but not yet completed infections, which might lead to underestimating the growth rate and fitness of phage with high adsorption rates. Despite these and perhaps other complications, however, the adsorption, growth, and selection rates collectively show that the evolving phage populations were under intense selection to improve their adsorption to the LamB receptor both before and after their hosts evolved reduced expression of that protein.

Implications of ecological interactions for predicting evolution: It is important to account for the effects of ecological interactions on the relative fitness of different genotypes if one is to understand and even predict evolutionary changes (34, 35). In this study, we examined how the tug-of-war over a virus's adsorption rate mediated the coevolutionary arms race between a phage and its bacterial host. Additionally, we demonstrated how the host's coevolution led to varied – and sometimes even opposite – effects on the relative fitness of different virus genotypes (Fig. 4.2B). Predicting viral evolution may therefore depend on knowing the genetic states of both the host and parasite populations and understanding how

those states affect fitness. Scaling this understanding to more diverse and complex ecosystems is challenging (36), but it may well be necessary to predict such phenomena as disease emergence. It is not difficult to imagine that coevolution might sometimes *block* certain adaptive paths. However, our results show that coevolution can produce dynamic fitness landscapes in which populations are *more* evolvable than they would otherwise be. As a consequence, coevolutionary dynamics may promote some key innovations and other hard-to-reach adaptations.

Acknowledgments

We thank Neerja Hajela and Rachel Sullivan for assistance in the laboratory, and Mike Wiser, Caroline Turner, Rohan Maddamsetti, Ben Kerr, Jenna Gallie, and Kayla Miller for comments on previous versions of this paper. This paper is based upon work supported by the National Science Foundation Graduate Research Fellowship (DGE-1424871) to A.R.B., the BEACON Center for the Study of Evolution in Action (NSF Cooperative Agreement DBI-0939454), and the John Hannah endowment from Michigan State University. Any opinions, findings, and conclusions or recommendations expressed in this paper are those of the authors and do not necessarily reflect the views of the National Science Foundation.

APPENDIX

Supplementary Materials and Methods

Duration of fitness assays

The derived phage λ genotypes used in this study evolved in serial batch culture with daily transfers [10]. In principle, we would have preferred to measure fitness over the same 24-h period in the competitive fitness assays. However, preliminary experiments indicated that the fitness advantages of the evolved genotypes were often so great that they overwhelmed the ancestral phage over the 24-h transfer cycle, making it difficult to detect the ancestral type in the final plate counts. We tried plating higher concentrations of phage, and that allowed us to detect some ancestral plaques, but these plates were then too crowded to count reliably. We also tried (i) increasing the initial frequency of the ancestor and (ii) reducing the duration of the competitions to 4 h, before settling on the 8-h assays as the most reliable.

A second obstacle that arose during 24-h phage competitions was that Mal^- phage-resistant mutant hosts often evolved from the Mal^+ ancestral strain, REL606, and reached high frequencies over that period. This rapid host evolution would therefore confound the comparisons of phage fitness values measured on the ancestral and coevolved hosts. We monitored the frequency of Mal^- bacteria in all phage competitions on the ancestral host to ensure that these mutants did not interfere with our estimates. To do so, we plated cells at the end of each replicate competition onto tetrazolium maltose indicator agar; Mal^- and Mal^+ cells produce red and white colonies, respectively, on that medium [10]. We found that the frequency of Mal^- cells remained <5% in most 8-h competitions, whereas their frequency rose to >50% in most preliminary competitions that ran for 24 h.

Table A4.1. Bacterial strains, phage strains, and PCR primer sequences used in this study.

Bacterial strains

Strain	Source	Relevant Characteristics
REL606	Ancestor host	λ susceptible, *lamB*$^+$, *ompF*$^+$, *lac*$^+$
EcC4	Evolved from REL606	Partial λ resistance, *malT*$^-$, *lamB*$^+$, *ompF*$^+$, *lac*$^+$
DH5α	Unrelated plating host	Used for plating marked ancestor λ, *lacZα*$^-$

Phage strains

Strain	Source	Relevant Characteristics
cI26	Ancestor phage λ	Strictly lytic (frameshift mutation in *cI*), Δ*stf*, no mutations in *J* gene
λ_{lacZ}	Marked ancestor phage λ	Derivative of cI26 carrying *lacZα* gene
A12	Population A12, day 10	6 *J* mutations, 1 of 4 required for infection via OmpF
A7	Population A7, day 10	4 *J* mutations, 2 of 4 required for infection via OmpF
B2	Population B2, day 13	3 *J* mutations, 2 of 4 required for infection via OmpF
D9	Population D9, day 8	4 *J* mutations, 2 of 4 required for infection via OmpF
E4	Population E4, day 13	3 *J* mutations, 2 of 4 required for infection via OmpF
G9	Population G9, day 11	5 *J* mutations, 2 of 4 required for infection via OmpF

PCR primer sequences

Primer	Location	Sequence
RL0932	Upstream of λ *J* gene	Forward, 5’ CTGCGGGCGGTTTTGTCATT 3’
RL0933	Downstream of λ *J* gene	Reverse, 5’ ACGTATCCTCCCCGGTCATCACT 3’
RL1031	Internal to λ *J* gene	Reverse, 5’ GACGCCGGACAGCACCACAGACC 3’
RL1032	Internal to λ *J* gene	Reverse, 5’ CGCCCTGAAGGACCGCCATAAT 3’
RL1033	Internal to λ *J* gene	Reverse, 5’ CAGCATGTGCCGGAAAAAGAGG 3’
RL1034	Internal to λ *J* gene	Reverse, 5’ CTTTTATATCCGCAGTGTGAAC 3’
RL1035	Internal to λ *J* gene	Reverse, 5’ ATAGCTGAAAACTGTACGATAAAC 3’
cI rev	In *cro* upstream of cI	Reverse, 5’GCGGGGTTATTTATGCTGTTGTT 3’
cI for	In *rexA* downstream of cI	Forward, 5’AGCGCTTATCTTTCCCTTTATTTT 3’

Table A4.2. Calculated *p*-values for two methods used to determine whether the fitness of the evolved phage genotypes depended on the host genotype. Values in the first column were not corrected for the fitness effects of the *lacZ* marker, which differed between the two host types, whereas those in the second column were adjusted by subtracting the average marker effect on each host before determining significance. Adjusting for the marker effect changed the *p*-values slightly, but it did not affect the overall interpretation of the results. The asterisk indicates that the observed difference went in the opposite direction to that hypothesized.

Genotype	Uncorrected	Corrected
A12	< 0.001	< 0.001
A7	0.107	0.019
B2	< 0.001	< 0.001
D9	> 0.5*	> 0.5*
E4	< 0.001	< 0.001
G9	< 0.001	< 0.001

Figure A4.1. Decay rates of six evolved phage genotypes and their ancestor, cI26, in media without any host cells. These decay rates were subtracted from the rates of phage loss in the presence of host cells to obtain the adsorption rates shown in Figure 4.1.

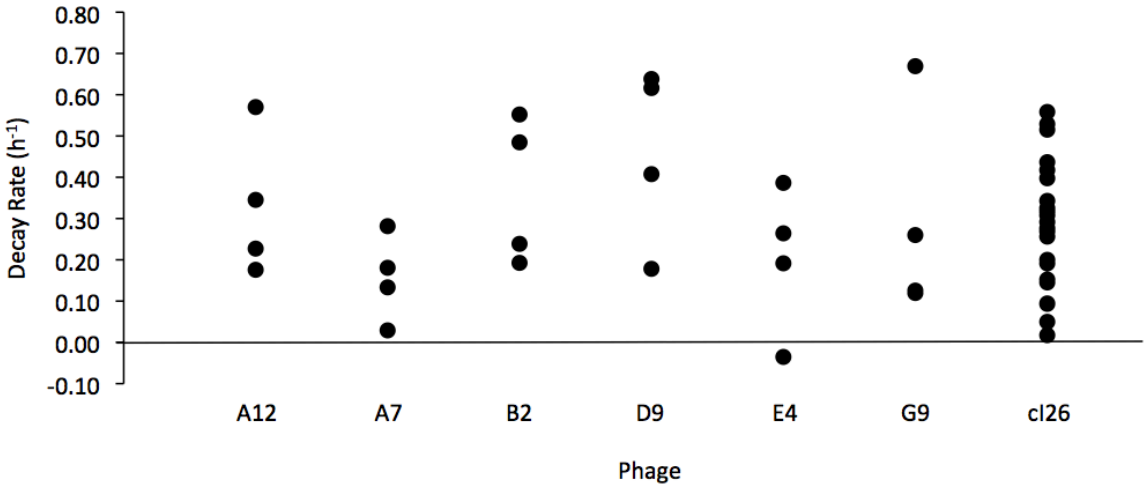

REFERENCES

REFERENCES

1. **Gavrilets S**. 2010. High-dimensional fitness landscapes and speciation. Evolution: the extended synthesis. Cambridge, MA: MIT Press p 45–79.

2. **Voordeckers K**, **Brown CA**, **Vanneste K**, **van der Zande E**, **Voet A**, **Maere S**, **Verstrepen KJ**. 2012. Reconstruction of ancestral metabolic enzymes reveals molecular mechanisms underlying evolutionary innovation through gene duplication. PLOS Biol **10**:e1001446.

3. **Moczek AP**, **Rose DJ**. 2009. Differential recruitment of limb patterning genes during development and diversification of beetle horns. Proc Natl Acad Sci USA **106**:8992–8997.

4. **Lenski RE**, **Ofria C**, **Pennock RT**, **Adami C**. 2003. The evolutionary origin of complex features. Nature **423**:139–144.

5. **Covert AW**, **Lenski RE**, **Wilke CO**, **Ofria C**. 2013. Experiments on the role of deleterious mutations as stepping stones in adaptive evolution. Proc Natl Acad Sci USA **110**:E3171–8.

6. **Blount ZD**, **Barrick JE**, **Davidson CJ**, **Lenski RE**. 2013. Genomic analysis of a key innovation in an experimental *Escherichia coli* population. Nature **488**:513–518.

7. **Quandt EM**, **Gollihar J**, **Blount ZD**, **Ellington AD**, **Georgiou G**, **Barrick JE**. 2015. Fine-tuning citrate synthase flux potentiates and refines metabolic innovation in the Lenski evolution experiment. eLife **4**.

8. **Bono LM**, **Gensel CL**, **Pfennig DW**, **Burch CL**. 2012. Competition and the origins of novelty: Experimental evolution of niche-width expansion in a virus. Biol Lett rsbl20120616.

9. **Herfst S**, **Schrauwen EJA**, **Linster M**, **Chutinimitkul S**, **de Wit E**, **Munster VJ**, **Sorrell EM**, **Bestebroer TM**, **Burke DF**, **Smith DJ**, **Rimmelzwaan GF**, **Osterhaus ADME**, **Fouchier RAM**. 2012. Airborne transmission of influenza A/H5N1 virus between ferrets. Science **336**:1534–1541.

10. **Meyer JR**, **Dobias DT**, **Weitz JS**, **Barrick JE**, **Quick RT**, **Lenski RE**. 2012. Repeatability and contingency in the evolution of a key innovation in phage Lambda. Science **335**:428–432.

11. **Thompson JN**. 2012. The role of coevolution. Science **335**:410–411.

12. **Van Valen L**. 1973. A new evolutionary law. Evolutionary theory **1**:1–30.

13. **Shaw JE**, **Bingham H**, **Fuerst CR**, **Pearson ML**. 1977. The multisite character of host-range mutations in bacteriophage lambda. Virology **83**:180–194.

14. **Werts C**, **Michel V**, **Hofnung M**, **Charbit A**. 1994. Adsorption of bacteriophage lambda on the LamB protein of *Escherichia coli* K-12: Point mutations in gene *J* of lambda responsible for extended host range. J Bacteriol **176**:941–947.

15. **Wiser MJ**, **Ribeck N**, **Lenski RE**. 2013. Long-term dynamics of adaptation in asexual populations. Science **342**:1364–1367.

16. **Sambrook J**, **Russell DW**. 2001. Molecular Cloning: A Laboratory Manual, 3rd ed. Cold Spring Harbor Laboratory.

17. **Adams MH**. 1959. Bacteriophages. New York: Interscience Publishers.

18. **Shao Y**, **Wang IN**. 2008. Bacteriophage adsorption rate and optimal lysis time. Genetics **180**:471–482.

19. **De Paepe M**, **Taddei F**. 2006. Viruses' life history: Towards a mechanistic basis of a trade-off between survival and reproduction among phages. PLOS Biol **4**:e193.

20. **Wang IN**, **Deaton J**, **Young R**. 2003. Sizing the holin lesion with an endolysin-galactosidase fusion. J Bacteriol **185**:779–787.

21. **Ellis HM**, **Yu D**, **DiTizio T**, **Court DL**. 2001. High efficiency mutagenesis, repair, and engineering of chromosomal DNA using single-stranded oligonucleotides. Proc Natl Acad Sci USA **98**:6742–6746.

22. **Lenski RE**, **Rose MR**, **Simpson SC**, **Tadler SC**. 1991. Long-term experimental evolution in *Escherichia coli.* I. Adaptation and divergence during 2,000 generations. Am Nat 1315–1341.

23. **Travisano M**, **Vasi F**, **Lenski RE**. 1995. Long-term experimental evolution in *Escherichia coli*. III. Variation among replicate populations in correlated responses to novel environments. Evolution **49**:189-200

24. **R Development Core Team**. 2011. R: A language and environment for statistical computing. R Foundation for Statistical Computing, Vienna, Austria.

25. **Gurnev PA**, **Oppenheim AB**, **Winterhalter M**, **Bezrukov SM**. 2006. Docking of a single phage lambda to its membrane receptor maltoporin as a time-resolved event. J Mol Biol **359**:1447–1455.

26. **Hendrix RW**, **Duda RL**. 1992. Bacteriophage lambda PaPa: Not the mother of all lambda phages. Science **258**:1145–1148.

27. **Rosenzweig ML**, **Brown JS**, **Vincent TL**. 1987. Red Queens and ESS: The coevolution of evolutionary rates. Evol Ecol **1**:59–94.

28. **Weitz JS**, **Hartman H**, **Levin SA**. 2005. Coevolutionary arms races between bacteria and bacteriophage. Proc Natl Acad Sci USA **102**:9535–9540.

29. **Williams HTP**. 2013. Phage-induced diversification improves host evolvability. BMC Evol Biol **13**:17.

30. **Paterson S**, **Vogwill T**, **Buckling A**, **Benmayor R**, **Spiers AJ**, **Thomson NR**, **Quail M**, **Smith F**, **Walker D**, **Ben Libberton**, **Fenton A**, **Hall N**, **Brockhurst MA**. 2010. Antagonistic coevolution accelerates molecular evolution. Nature **464**:275–278.

31. **Hashemolhosseini S**, **Holmes Z**, **Mutschler B**, **Henning U**. 1994. Alterations of receptor specificities of coliphages of the T2 family. J Mol Biol **240**:105–110.

32. **Zaman L**, **Meyer JR**, **Devangam S**, **Bryson DM**, **Lenski RE**, **Ofria C**. 2014. Coevolution drives the emergence of complex traits and promotes evolvability. PLOS Biol **12**:e1002023.

33. **Goldhill DH**, **Turner PE**. 2014. The evolution of life history trade-offs in viruses. Curr Opin Virol **8**:79–84.

34. **Bohannan B**, **Lenski RE**. 2000. Linking genetic change to community evolution: insights from studies of bacteria and bacteriophage. Ecol Lett **3**:362–377.

35. **Meyer JR**, **Kassen R**. 2007. The effects of competition and predation on diversification in a model adaptive radiation. Nature **446**:432–435.

36. **Telfer S**, **Lambin X**, **Birtles R**, **Beldomenico P**, **Burthe S**, **Paterson S**, **Begon M**. 2016. Species interactions in a parasite community drive infection risk in a wildlife population. Science **330**:20161528.